Mars: the interaction cross-section of positive and negative muons

Hamdan, M. A.

MARS - The Interaction Cross-Section of Positive and Negative Muons

by

M. A. Hamdan, B.Sc., M.Sc.

A Thesis submitted to the

University of Durham

for the

Degree of Doctor of Philosophy

July, 1972

M.A.R.S.

THE DURHAM MAGNETIC AUTOMATED

RESEARCH SPECTROGRAPH

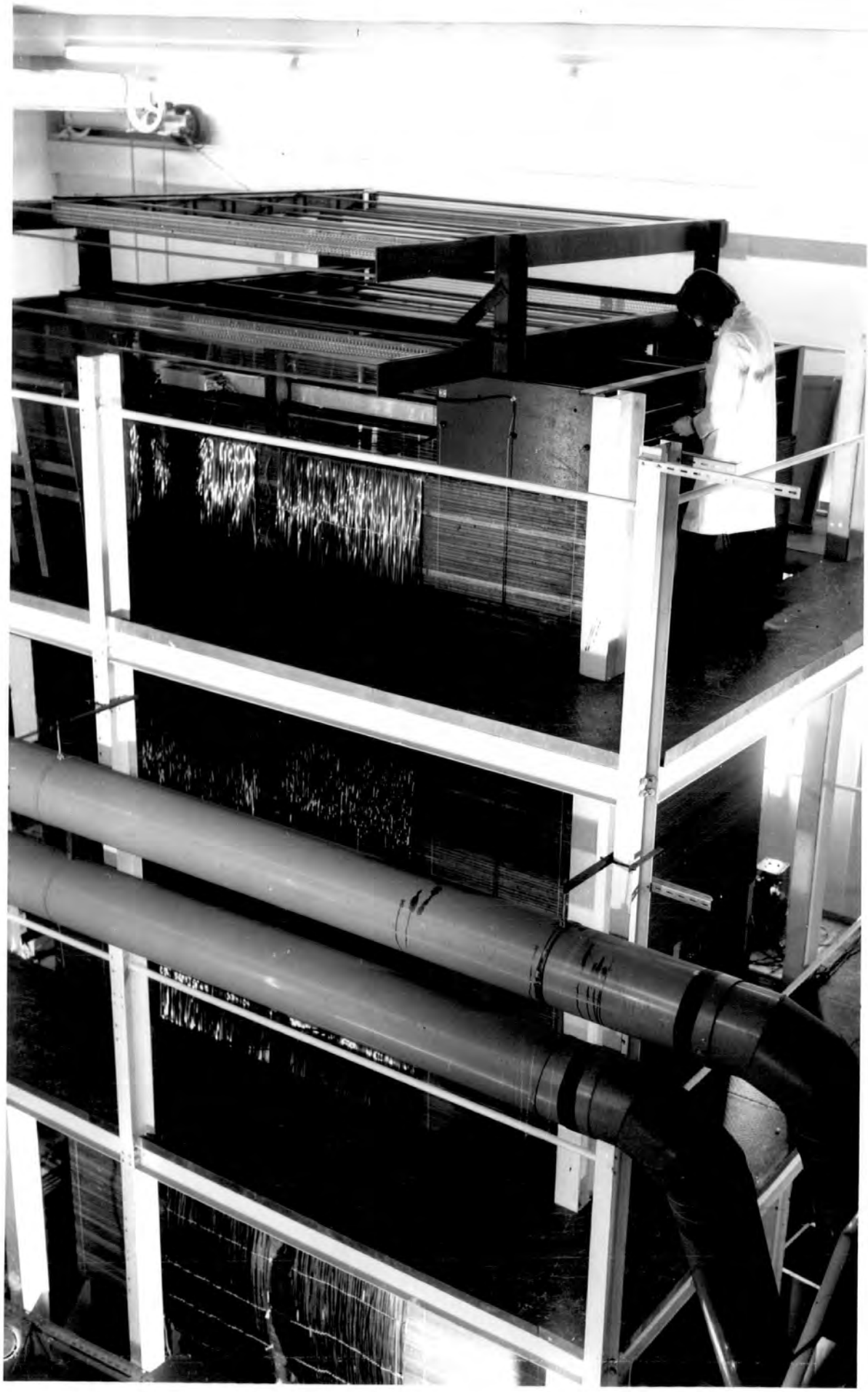

ABSTRACT

The Durham spectrograph MARS, has been used to study the electromagnetic interactions of cosmic ray muons in iron in the range 6 - 200 GeV. Single electrons and electron bursts of various sizes from the knock-on, direct pair production and bremsstrahlung processes were observed.

The possible asymmetry in the interaction of positive and negative muons as a function of muon energy and energy transfer was investigated. Also investigated was the absolute value of the interaction probability for single electrons and electron bursts of different sizes as a function of muon energy. Experimental burst spectra for burst sizes up to 80 particles were established and compared with prediction.

The results on the interaction asymmetry suggest no asymmetry for single electron production and give an asymmetry value of $1{\cdot}08 \pm 0{\cdot}055$ for production of two or more secondaries. The results on the absolute values of the interaction probability are in good agreement with expectation. Thus, it is concluded that there is satisfactory agreement with theory.

PREFACE

The work presented in this thesis was carried out in the period 1969-1972 while the author was a research student under the supervision of Professor A. W. Wolfendale and Dr. M. G. Thompson in the Cosmic Ray Group of the Physics Department of the University of Durham.

The work describes a study of the interaction probability for positive and negative muons and also a determination of the absolute value of the total interaction probability using the Durham cosmic ray spectrograph MARS.

The author played a part in constructing the spectrograph and was solely responsible for running the 'red side' of the instrument for interaction studies. He was responsible for introducing the modifications to the scintillation counters and the selection system used in interaction experiment II. He was also solely responsible for the collection of all data, and much of its analysis and interpretation. Assistance was however received during the analysis from Dr. C. Grupen and Dr. E.C.M. Young. The investigation of the interaction asymmetry in the data of the Durham Mk II horizontal spectrograph was carried out by the author.

The theoretical probabilities of the direct pair production process were derived by Dr. M. G. Thompson and they have been used in this thesis.

The results given in this thesis have been reported in three papers: Ayre et al. (1971), Grupen et al. (1972 I) and Grupen et al. (1972 II).

CONTENTS

CHAPTER 1

INTRODUCTION

1.1 Summarised features of cosmic rays

The hint for the existence of a penetrating radiation coming from outside the atmosphere was supplied at the end of the last century by measurements on the conductivity of gases. Soon afterwards a number of workers flew ionisation chambers in balloons to study the variation of conductivity with height. In order to interpret their results, Hess (1912) put forward the hypothesis of the existence of an extremely penetrating radiation, coming from outer space and not of solar origin. This penetrating radiation soon came to be known as the 'cosmic radiation'.

The search for the origin of the cosmic radiation has been started ever since the radiation was discovered and up to now the source is not known with certainty. However, it seems to be generally accepted that the sun is, at least partly, responsible for low energy radiation, whereas the more energetic primaries are of galactic origin and it may well be that at very high energies their origin is outside the galaxy. The complete solution of the problem of the origin of cosmic rays must await further study.

At energies below about 10 GeV, the primary radiation is composed of $\sim 85\%$ protons, $\sim 10\%$ α-particles and 1 - 2% nuclei with $Z > 2$. As for the intensity of electrons in the primary radiation, this is thought to be very low $\sim 1\%$, under normal conditions. The intensities of γ-rays and neutrons are even lower than that of the electrons.

On entering the earth's atmosphere the primary radiation interacts with the nuclei of the atmosphere where on average the primary particle loses $\sim 50\%$ of its energy in each collision. In these interactions a variety of particles are produced, such as pions, kaons, nucleon-anti nucleon pairs and other baryons. The primary particles carry on with residual energy to undergo

further nuclear interactions in which more and more secondaries are produced. The secondary particles either decay or interact and in either case more and different secondaries are produced. At low primary energies, the emitted particles would probably have such low energies that none would reach sea level. However, at much higher energy very many particles would be produced and would arrive at sea level.

The charged pions ($\pi^{\pm}$) produced in a nuclear interaction of the primaries, will either decay or interact. Those decaying produce positive and negative muons and neutrinos. A high energy pion has a higher probability for interaction than decay and the product of these interactions will be more pions of lower energy which in turn by decay will produce more muons. Muons are also produced directly from the decay of kaons in the $k^{\pm}_{\mu_2}$, $k^{\pm}_{\mu_3}$ modes and indirectly from the decay of pions produced by the decay of kaons. Photons and electrons are produced from the decay of the neutral pions and also from the decay of low energy muons.

Starting from the top of the atmosphere, the abundance of the primary particles would decrease rapidly with increasing depth due to the absorption in the atmosphere. The average absorption length is $\sim$120 gm/cm^2. The intensity of the muons rises rapidly with depth, goes through a maximum and then falls off. The reduction occurs because of the loss of low energy muons by decay into electrons which are not balanced by the production of more muons from the decay of pions and kaons because of the low intensity of protons. The fall off in the intensity of the muons is relatively slow compared with that of the protons due to their very weak interaction with nuclei.

The mean lifetime of muons is 2·198 μsec is longer by about two orders of magnitude than the life times of pions and kaons. Moreover, since the muons are weakly interacting particles, the muons survive and penetrate a large thickness of atmosphere, whereas pions and kaons decay or are absorbed,

near the point at which they are produced. As a result of the various processes, the charged component of the cosmic radiation at sea level consists of ~70% muons, 30% electrons, 1% protons and smaller percentages of other strongly interacting particles. The muons and protons represent the so-called hard component of cosmic radiation whereas the electrons and photons represent the soft component. The latter is almost entirely absorbed by 10 cm of lead.

An interesting feature of the muon component is an appreciable excess of positively charged particles. This positive excess, characterized by the ratio $\frac{N_{\mu^+}}{N_{\mu^-}}$, is significantly greater than unity over practically the entire muon momentum range examined to date. The existence of the positive excess is due to the fact that the primary radiation is positively charged. Owing to charge conservation, this excess is transmitted from pions generated during interactions between primaries and atmospheric nuclei to muons produced in their decay.

1.2 Electromagnetic interactions of muons

Electromagnetic interactions of the muons, and of all charged particles, with matter can be classified according to the proximity to the nucleus of the position at which the interaction occurs. If the 'impact parameter' is large compared with the atomic radius, the atom reacts as a whole to the variable field set up by the passing particle. The result is excitation or ionisation of the atom.

If the impact parameter is of order of the atomic dimensions, the interaction no longer involves the passing particles and the atom as a whole, but rather the passing particle and one of the atomic electrons. And if the energy transfer to the electrons is large compared with its ionisation potential, then the process may be considered as being between the incident particle and a free electron. In this case the electron is ejected from the atom with considerable energy. This interaction has become known as knock-on process.

On further reduction of impact parameter to distances smaller than the atomic radius, the deflection of the trajectory of the passing particle in the electric field of the nucleus becomes the most important. The deflection will be accompanied by the emission of photons whose total energy is usually a small fraction of the energy of the incident particle. However, there is a definite probability that the incident particle will radiate a photon of considerable energy and this process is known as bremsstrahlung.

A process that is similar to bremsstrahlung except that when the muon is deflected in the electromagnetic field of the nucleus it produces an electron-positron pair rather than emitting a photon, is known as direct pair production. It is interpreted as an interaction between the electromagnetic field of the nucleus and a photon of the virtual photon flux of the incident particle.

Another process for the muon to undergo in interacting with matter is what is known as nuclear interaction. The interaction is regarded as being between photons of the virtual photon cloud accompanying the muon, and the nucleus, which results in pion production. The cross section for this process is small compared with the others.

Muons produced in the atmosphere lose energy during their propagation to sea level by undergoing the above mentioned interaction processes. The dominant process of energy loss is the ionisation process, but at higher energy transfers and higher muon energies the other processes become also important. Electrons suffer more energy loss than muons due to the fact that bremsstrahlung for the electron is more important. This results in few very energetic electrons at sea level.

In propagation underground, electrons lose energy rapidly by bremsstrahlung and protons lose energy by nuclear interactions. Thus, at depths below $\sim$10 meters all electrons and protons present at sea level have been effectively absorbed and only muons are left. The muons do produce a small flux of secondary electrons by the knock-on process as they pass through, but this

only amounts to ~5% of the muon flux. Thus the cosmic ray flux deep underground consists mainly of muons and many experiments have been made there to take advantage of the nearly pure beam.

1.3 Importance of the study of the electromagnetic interactions of the muons

The study of the electromagnetic interaction of muons is of importance because it tests interaction theory and also because it may throw some light on the existence of the muon by perhaps distinguishing it from a heavy electron. It is also important in view of the fact that the magnitude of the energy loss of the muon and hence the important range-energy relation is derived from a knowledge of the interaction theory. Precise information about the range-energy relation is necessary for both sea level and underground measurements.

Besides all the above reasons the present work was strongly motivated by the striking results from previous cosmic ray experiments. Two recent experiments with cosmic ray muons reported a totally unexpected result, that is they observed a different interaction probability for differently charged muons. At the present time this is perhaps the most important reason to study the electromagnetic interaction of the muons.

1.4 Present work

This thesis describes two experiments which were undertaken to study the electromagnetic interactions of high energy cosmic ray muons arriving at sea level in a vertical direction using the new Durham cosmic ray spectrograph MARS . In particular two experimental questions were put:

1. Are the interactions probabilities for positive and negative muons equal, or might there exist a charge asymmetry in muon interactions?
2. What are the absolute interaction probabilities of the muon?

Chapter 2 gives a brief review of the recent experimental developments concerning muon interactions. Chapter 3 gives a description of 'MARS'

as far as the present work is concerned. The two experiments on the interaction asymmetry are fully described, together with analysis and results in Chapters 4 and 5. Chapter 6 gives a direct comparison of the results of the interaction experiments of the present work and more details of the experiments mentioned in Chapter 2, together with a comparison between the results from all the experiments on the interaction asymmetry. Chapter 7 gives the analysis and the results for the absolute interaction probability of the muon from the present work and also a comparison with results from previous experiments. Finally, Chapter 8 contains the conclusions that can be drawn from the present work.

CHAPTER 2

PREVIOUS STUDIES OF ELECTROMAGNETIC INTERACTIONS

2.1 Introduction

In the past few years a number of experiments have been performed with cosmic rays to measure the probability of production of bursts (due mainly to knock-on electrons) by muons traversing absorbers. The results are summarised in figure 2.1 where the ratio of the measured to the observed probabilities are plotted against the energy transferred to the electron. A feature of these data is a large deviation in the region of energy transfer 1 - 10 GeV in some experiments. This possible deviation from the accepted theory has contributed considerably to the interest in investigating the dependence of the knock-on, and burst-probabilities on muon energy and also on muon sign.

Kotzer and Neddermeyer (1965) investigated the knock-on probabilities possible charge asymmetry in muon interactions using cosmic ray muons. Their work was followed by that of the Keil group (Allkofer et al., 1971) and later by the Durham group (Ayre et al., 1971, to be described in this thesis).

This chapter will be devoted to giving a brief description of the above-mentioned experiments with particular reference to the results on the possible charge asymmetry in cosmic ray muons interactions. Moreover, results from accelerator experiments will also be mentioned.

2.2 Previous Experiments on Knock-on Electrons

2.2.1 Neddermeyer and associates

Deery and Neddermeyer (1961) and Kotzer and Neddermeyer (1965) used cloud chambers to study the production probabilities of knock-on electrons, with energies > 100 MeV , from carbon and paraffin targets for cosmic ray muons of energy in the range 5 - 50 GeV. Their instrument was essentially a vertical array of three cloud chambers placed in a magnetic field of 11 K gauss.

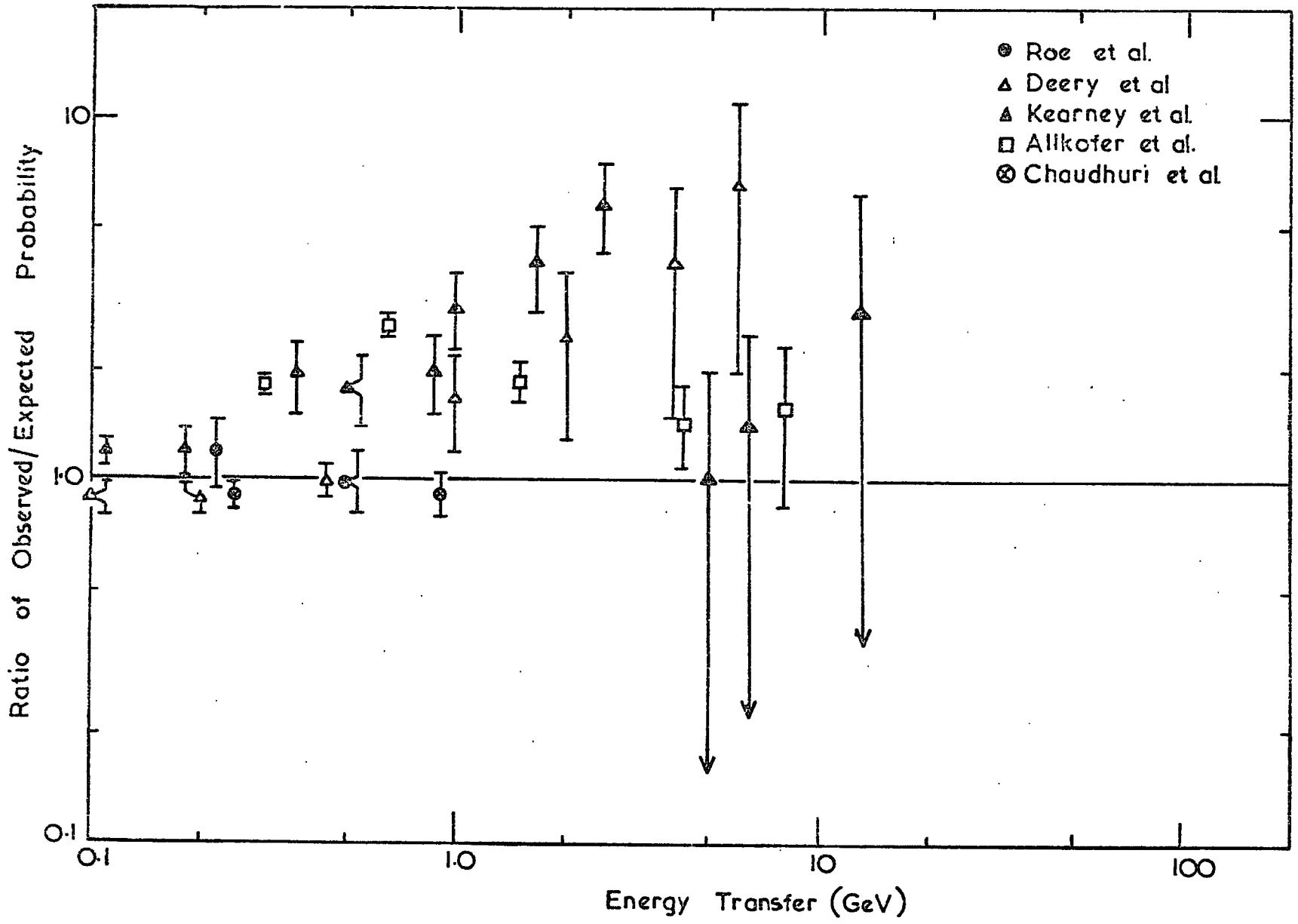

Figure 2.1 Results on knock-on production by cosmic ray muons

The target was placed on top of the upper cloud chamber. Events were selected by a fourfold coincidence between two trays of Geiger counters, one above the target and the other under 14" of lead below the chamber, and two proportional counters, the first being placed between the target and top of the upper chamber while the second was placed on top of the second cloud chamber.

The proportional counters were designed to permit efficient selection of electromagnetic interaction processes of high energy transfer. Electron energies were determined from their ranges using the range-energy relation or from their shower production in $\frac{1}{2}$"and 1" lead plates at the bottom of the upper and the top of the lower cloud chamber respectively.

Their results show an excess of events with energy transfer in greater than 1 GeV (Figure 1). When they examined their data in terms of the sign of the muon which produced the event, they found that whereas negative muons exhibit a behaviour agreeing with expectation, the positive muons persisted in showing upward deviations. If we define N^+ and N^- as the number of interaction events produced by equal numbers of positive and negative muons, respectively, then according to this experiment $\eta = N^+/N^- = 1{\cdot}60 \pm 0{\cdot}30$. This is to be compared with an expected value of one. Such a result can be characterised as an asymmetry in the interaction of two differently charged muons with electrons.

2.2.2 Allkofer et al (1971)

Allkofer et al. (1971) have used the Keil spectrograph to study the possible charge asymmetry in muon-electron interactions.

The Keil spectrograph consists of a solid iron magnet placed symmetrically between six double gap spark chambers and four scintillation counters. The spectrograph is situated at a zenith angle of 83° in order to take advantage of the higher intensity of high energy muons. The momentum range determined

by the spectrograph is 7 - 1000 GeV/c. Operated in coincidence with the spectrograph is an interaction calorimeter which consists of multiplate spark chambers (Fe-type and Aℓ-type). The momentum and the sign of each muon entering the calorimeter is determined from the spectrograph data. The muons traversing the calorimeter have a mean energy of about 27 GeV and their passages through the spectrograph and the calorimeter are photographed.

When an interaction takes place in the calorimeter with energy transfer exceeding 0·2 GeV, an electromagnetic shower is developed and its entire section can be observed. In this case the energy transfer in the calorimeter is determined by shower calculations. Thus, for every interaction event it is possible to determine the muon energy, muon sign and the transferred energy. The results reported by Allkofer et al. (1971) show an overall asymmetry favouring positive muons, the asymmetry quoted being $1{\cdot}20 \pm 0{\cdot}11$. (The equipment is currently being improved prior to a further study of this problem).

2.2.3 The Durham MkII horizontal spectrograph

Ashton et al. (1965) studied the electromagnetic interactions of cosmic ray muons in iron using the Durham MkII horizontal spectrograph.

This spectrograph consisted of six trays of Geiger counters, five trays of flash tubes and two identical solid iron magnets. The spectrograph was inclined at a mean zenith angle of 87°. Muons were selected by the Geiger counters trays, four of which were placed vertically in order to define the trajectory. The remaining two trays of counters were placed symmetrically over the instrument and connected in anticoincidence to the others so as to reduce the frequency of extensive air showers triggering the system. The maximum detectable momentum (m.d.m.) of the spectrograph was about 1000 GeV/c and the mean muon momentum selected by the spectrograph was about 30 GeV/c. An interaction in either magnet could be observed in the

flash tube tray placed behind each magnet. The data on interactions from the spectrograph have been reanalysed in 1971, by the present author with particular emphasis on the sign of the muon producing the event. The results emerging from the data suggest no asymmetry greater than about 11%, The integral asymmetry value for shower production being 0·97 ± 0·11.

2.3 Experiments giving the total interaction probabilities

Many experiments have been carried out which relate to total probabilities. A useful summary has been given recently by Allkofer et al. (1971) and a figure from this paper is reproduced in Figure 2.2 It can be seen that there is a widespread of values about the expected result and no systematic trend is apparent.

2.4 Experiments with Machine muons

Interaction probabilities of muons have also been studied using machine-accelerated particles. Backenstoss et al. (1963) carried out an experiment with a beam of negative muons arising from particles generated by the CERN proton synchrotron. Muons with momenta peaking at 8·5 GeV/c were caused to pass through an iron-scintillation sandwich counter. Their results in the region of energy transfer of 1·6 to 7 GeV show a normal behaviour for the negative muons with no deviation greater than 3% from their predicted value. They stated that the small differences that were observed were probably due primarily to uncertainty in their effective target thickness.

Kirk and Neddermeyer (1968) used beams of positive and negative muons with momenta peaked at 5·5 and 10·5 GeV/c respectively to compare the interaction probability for both signs of the muon. Their results show no asymmetry greater than 10% in the region of energy transfer from 0·1 to 6 GeV. The absolute probabilities agree with theory to within ± 30%.

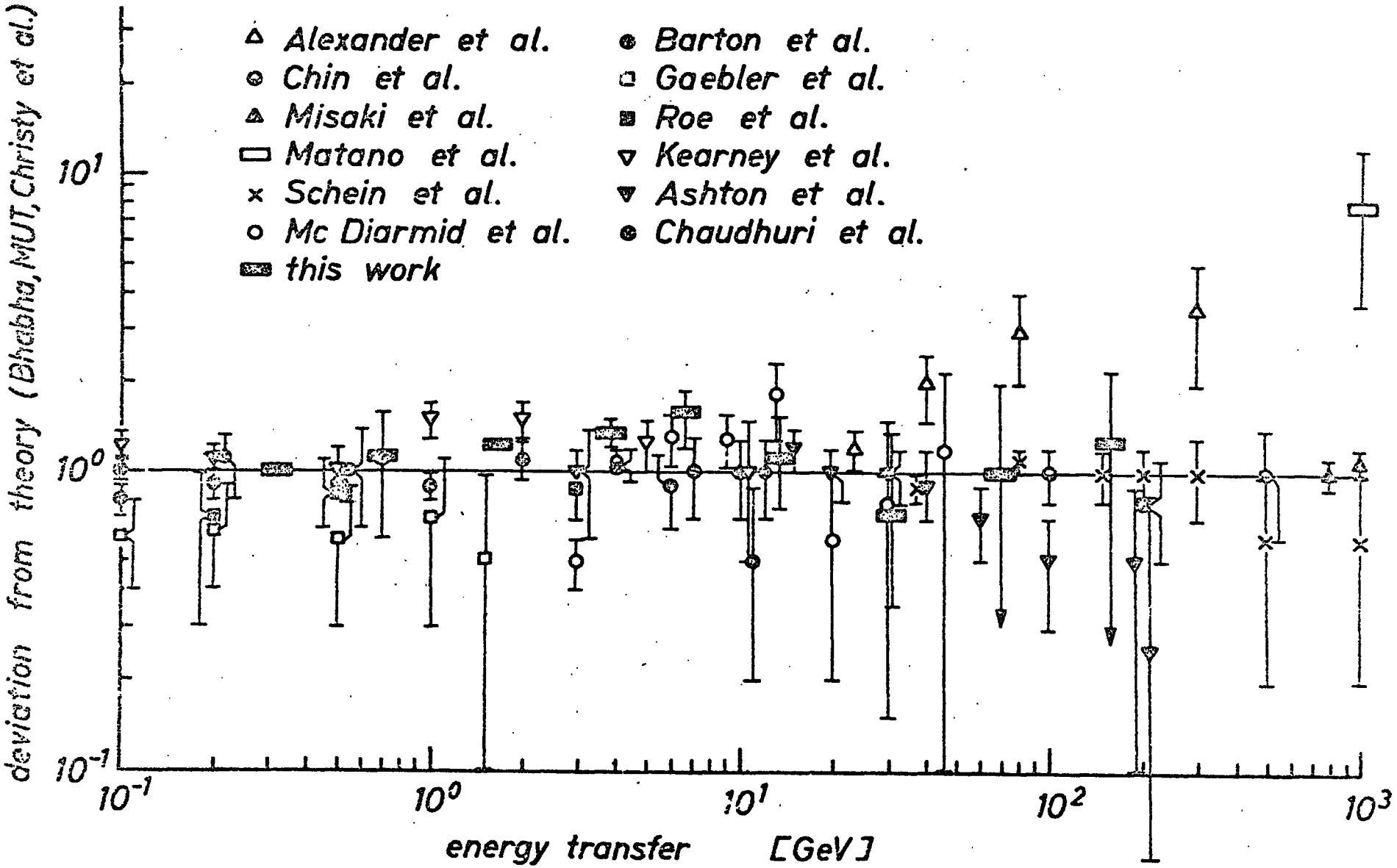

Figure 2.2 Comparison between experiment and theory for the total interaction cross section of muons as a function of energy transfer, after Allkofer et al. (1971)

Jain et al. (1970) studied the elastic muon-electron scattering in emulsions using beams of 10·1 and 5 - 14·5 GeV/c positive and negative muons respectively. Excellent agreement with theory was claimed for both negative and positive muons for transferred energies up to 1·4 and 3 GeV respectively (although on examining their results it appears that an asymmetry as high as 20% could be present).

2.5 Discussion

Three experiments were made using cosmic rays to investigate the possible charge asymmetry in muon interactions. Those experiments were carried out in different ways with different zenith angle and muon mean energies. The first and the second experiments suggested a generally larger burst probability for positive than for negative muons for energy transfer above 1 GeV, yet the third experiment (Ashton et al.) showed no asymmetry > 11%. Experiments with machine muons show no deviation from the normal behaviour. Cosmic ray results, which are in contradiction to accelerator data, are most unexpected and if substantiated (the statistical precision is not great) cannot be explained by the normal behaviour of the muons. It is important to stress that the deviation from the normal behaviour appears to take place in the region of energy transfer >1 GeV where knock-on production is the dominant process of energy loss. If there is in fact such a deviation from normal behaviour, which has not been observed with machine muons, then serious consequences will follow for many parameters in cosmic rays. An interpretation which immediately arises is that the so-called cosmic ray 'muons' contain a significant fraction of non-muons which behave in a different manner (e.g. an excess of positive, more strongly interacting particles). Before such a conclusion can be drawn it is of course necessary to put the phenomenon of charge asymmetry on a much stronger experimental basis.

Detailed discussion and extended comparison between the various experiments on charge asymmetry will be given in Chapters 6 and 8, and details about burst frequencies will be given in Chapter 7.

CHAPTER 3

MARS: CHARACTERISTICS OF THE INSTRUMENT

3.1 Introduction

The Durham magnetic automated research spectrograph, MARS, consists essentially of four solid iron magnet blocks, A, B, C and D. A scale diagram of the spectrograph together with its approximate dimensions is presented in figure 3.1. Each magnet block has dimensions 1·24m x 2·13m x 3·66m and weighs 71 tons. A magnetic field of approximately 16 K gauss is produced in each block by an electric current of about 50 A passing through the energising coils. Scintillation counters and trays of neon flash tubes are placed between the blocks. The scintillation counters determine the acceptance and are used to trigger the spectrograph. The flash tube trays are used to determine the trajectory of each of the triggering particles.

In addition to the flash tube trays placed between the magnet blocks, two more trays of flash tubes are placed on top of the spectrograph (azimuth trays). The flash tubes in the azimuth trays are placed in the transverse direction with respect to the flash tubes in the remaining trays. This enables an estimate to be made of the entry angle of each particle in the back plane of the spectrograph to within $\pm 0{\cdot}5^{\circ}$.

The spectrograph is symmetric about a vertical plane through its centre which divides the spectrograph into two similar sides. For simplicity the two sides of the spectrograph are called the 'red' and the 'blue' sides and they are the western and eastern sides of the spectrograph respectively. The main characteristics of the instrument are listed in Table 3.1. In its final form MARS will be fully automated, however, the work described in this thesis is concerned with running the red side of the spectrograph only and the method of photography is used to record the data.

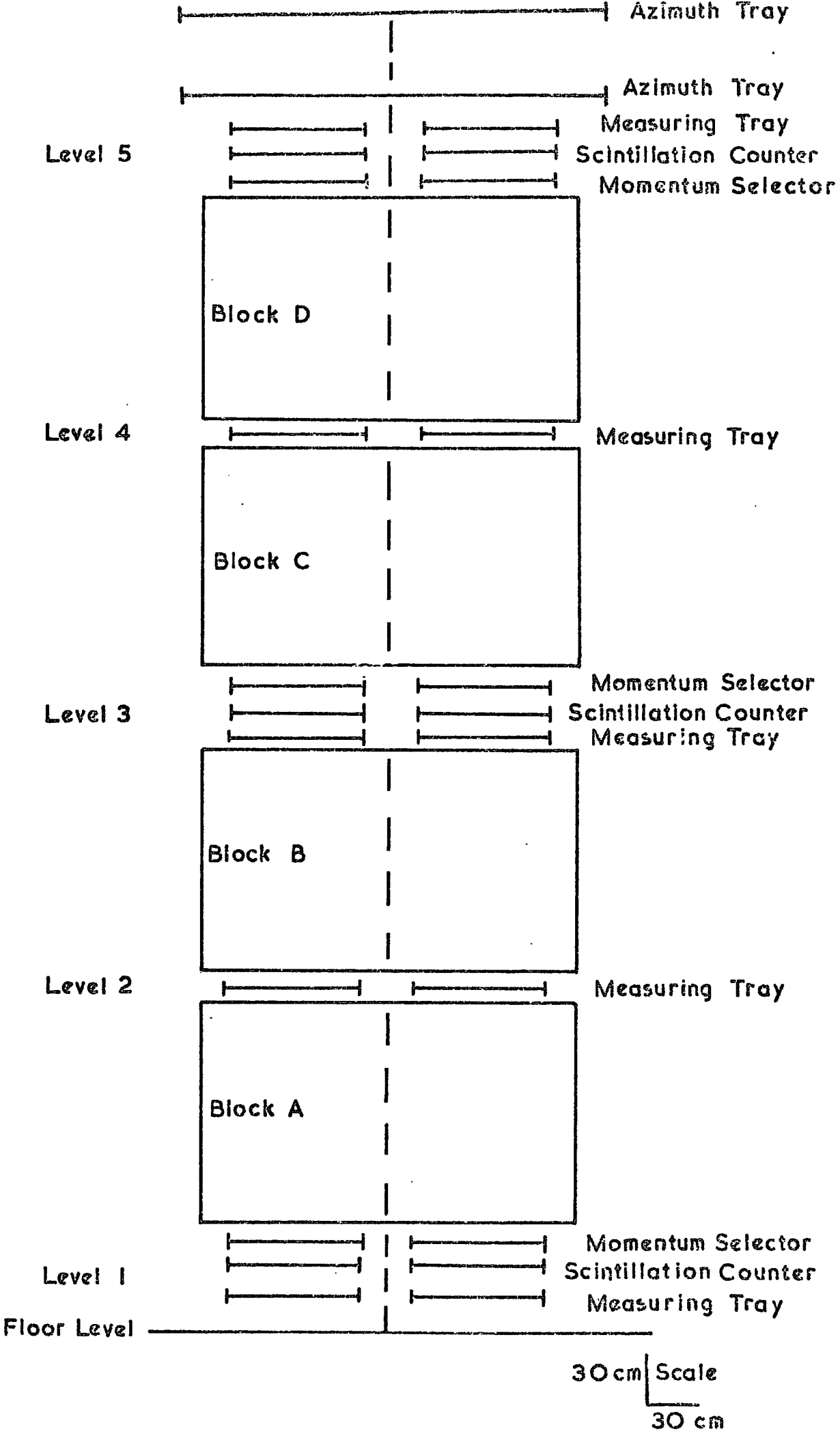

Figure 3.1 Front view of MARS

TABLE 3.1

M.A.R.S. : The Main Characteristics of the Instrument

Dimensions of a Magnet Block	3·66m x 2·13m x 1·24m
Weight of a Magnet Block	71 tons
Overall Height	7·62m
Acceptance of each side at infinite momentum	420 cm^2 ster.
Angular Range (neglecting magnetic deflection and multiple scattering)	
(i) Deflection Plane	$\pm$ 7°
(ii) Rear Plane	$\pm$ 15·5°
Magnetic Induction	16·3 $\pm$ 0·1 : K gauss
$\int Bd\ell$	8·09 x 10^6 gauss cm
$\frac{\langle\theta\rangle \text{ scatt}}{\phi \text{ mag}}$	$\sim$ 0·12
Minimum Detectable Momentum (Zero Field)	6·9 GeV/c
Minimum Detectable Momentum (Maximum Field)	7·5 GeV/c
Maximum Detectable Momentum	$\sim$ 6000 GeV/c
Zero field rate (no paralysis)	28·0 $\pm$ 1·0 min^{-1}

Expected rates through each side of the Spectrograph using Integral Spectrum of Hayman and Wolfendale (1962), (Magnetic Induction = 16·3 k gauss, no paralysis)

Momentum (GeV/c)	Rate
> 7·5	1200 hr^{-1}
> 50	63·6 hr^{-1}
> 100	14·8 hr^{-1}
> 200	3·1 hr^{-1}
> 500	7·8 day^{-1}
> 1000	1·3 day^{-1}

3.2 The Magnets

There are four identical magnet blocks (A, B, C and D) in MARS spectrograph as shown in figure 3.1. The magnets are in the shape of large rectangular transformers, each of deflecting length 125 cm. Each magnet block is made from 78 steel plates, each plate having a thickness 1·6 cm and weighing about 1 ton.

In order to measure the uniformity of the magnetic field in each block, search coils were placed between the plates in several places during assembly of the blocks. The energising coils for each magnet consist of 92 turns of 4 SWG copper wire. The coils are held in position by wooden formers at the block edges. The total resistance of each coil is 1 Ω. The coils on block A are joined in series with those on block C, so are the coils on block B and D. The two sets of coils are connected in parallel through a reversing switch across 100 V x 100 A D.C. rectifier unit. When all the coils are connected to the rectifier a current of 50 A flows through each coil. With this current a mean magnetic field of 16·3 ± 0·1 K gauss can be produced over the sensitive region of the magnet. The field in each magnet block is uniform over the volume of the magnet used for deflecting a traversing particle to within ± 2%.

3.3 The scintillation counters

The scintillation counters used to trigger the spectrograph each consist of a rectangular slab of plastic scintillator, Ne 102 A of approximate area 177 cm x 75 cm and thickness 5 cm. Four photomultipliers (Mullard type 53 AVP) are fixed on to perspex light guides on the ends of the scintillators by means of optical cement (N.E. 580 manufactured by Nuclear Interprises Limited). The same optical cement is used to join the light guides to the scintillators. Figure 3.2(a) shows the form of the scintillation counters and the positions of the photomultipliers.

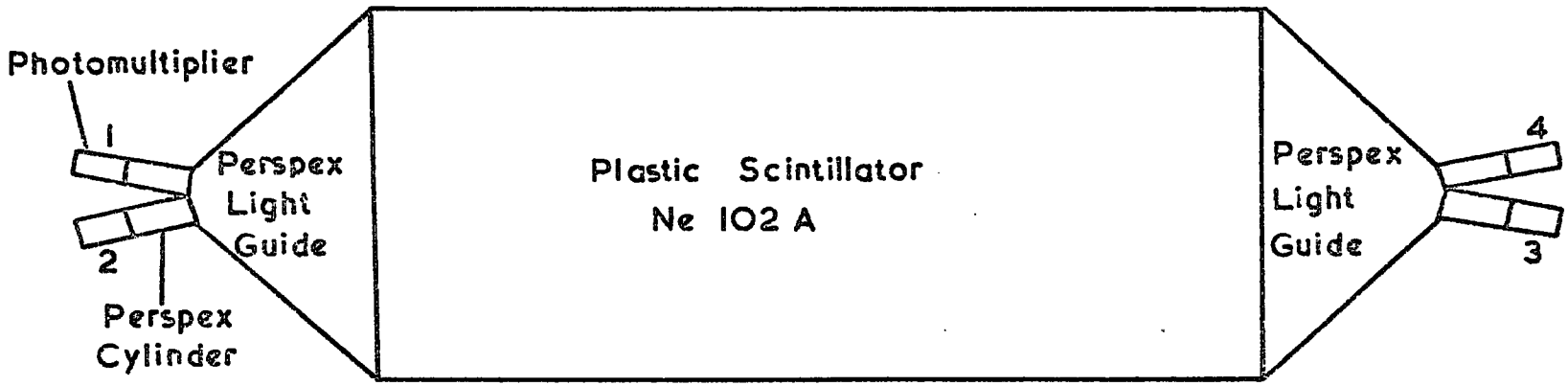

Figure 3.2(a) MARS scintillation counter

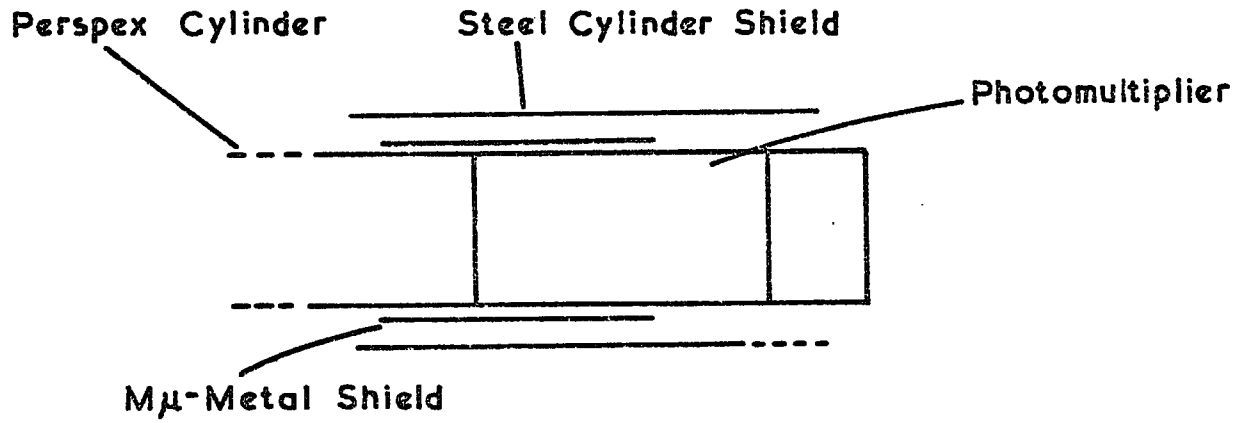

Figure 3.2(b) The shielding arrangement on a photomultiplier

The scintillator and the light guides are enclosed in thin aluminium foil in order to reduce the light lost from the outer surfaces. Sheets of black plastic are used to cover the aluminium foil sheets to prevent any external light from entering the system. The whole scintillation counter is placed in a light tight box.

The gain of a photomultiplier is affected by the presence of a magnetic field. Since the scintillation counters in MARS are situated in the vicinity of a magnetic field, it is necessary to shield all photomultipliers attached to the scintillation counters from the stray field of the magnets. The magnetic shields used for each photomultiplier consist of mu-metal and steel cylinders. The most effective disposition of the two shields in order to minimise the effect of the magnetic field was developed experimentally and is shown in figure 3.2(b).

The voltage (EHT) on each photomultiplier was adjusted so that all photomultipliers had the same gain. This was achieved with the aid of two small scintillator telescopes. One scintillator telescope was placed above and the other below the scintillation counter such as to select only particles traversing the central region of the counter. The output of each telescope was passed through a discriminator. The discriminated outputs for the telescopes were fed to a coincidence unit. The output from the coincidence unit was used to gate the 400 channel pulse height analyser (P.H.A.). The output pulses from each photomultiplier were fed into the P.H.A. and the EHT on each photomultiplier was adjusted so that peak of the pulse height distribution recorded on the P.H.A., was the same for each photomultiplier. The peak of the distribution on the P.H.A. represents the most probable pulse height when a particle traversing the central region of the counter. A block diagram showing the method used in matching the gain of the photomultipliers is given in figure 3.3.

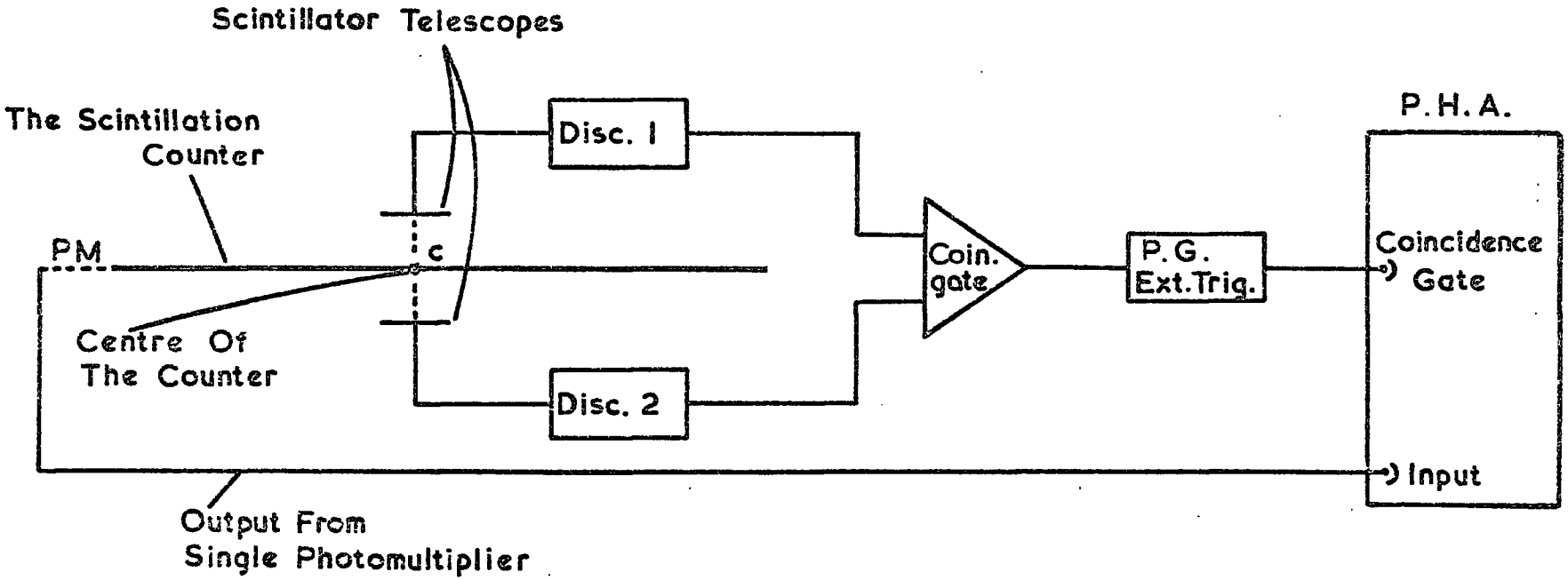

Figure 3.3 Block diagram of the method used in matching the gain of the photomultipliers

To obtain a uniform response over the scintillator the pulses from a diagonal pair of photomultipliers are added. The uniformity of the counter along its central axis was measured for the added pair and for single photomultiplier with the aid of the two scintillator telescopes. The scintillator telescopes were used to select a small region of the counter and the pulse height distribution was measured as a function of the position of a particle traversing the counter along its central axis. The result on the uniformity of the counter is given in figure 3.4. It can be seen from figure 3.4 that the uniformity of the counter is significantly improved by adding the pulses for each diagonal pair. The coefficient of variation (i.e. standard deviation divided by the mean) in the uniformity of the counter is 15%, to be compared with 46% obtained with a single photomultiplier. There is no significant variation in the uniformity across the counter.

The output pulse from the two paired photomultipliers, after passing through a head amplifier and the pulse adding circuit, is amplified and fed by coaxial cable to a discriminator and pulse shaper. The same procedure is followed for the second pair of photomultipliers. The outputs from the two discriminators are fed into a two fold coincidence circuit. A block diagram of the scintillation counter electronics is shown in figure 3.5. An output from the coincidence circuit is usually only obtained when at least one particle passed through the counter. The resolving time for each counter is 0·7 μsec. and the efficiency of each counter is $(99{\cdot}4 \pm 0{\cdot}4)\%$.

3.4 The flash tube trays

The positions of the flash tube trays in MARS are illustrated in figure 3.1. Each side of the spectrograph consists of eight trays of tubes, three of which contain large diameter tubes and are identified as the 'momentum selector' trays. The other five trays of flash tubes use

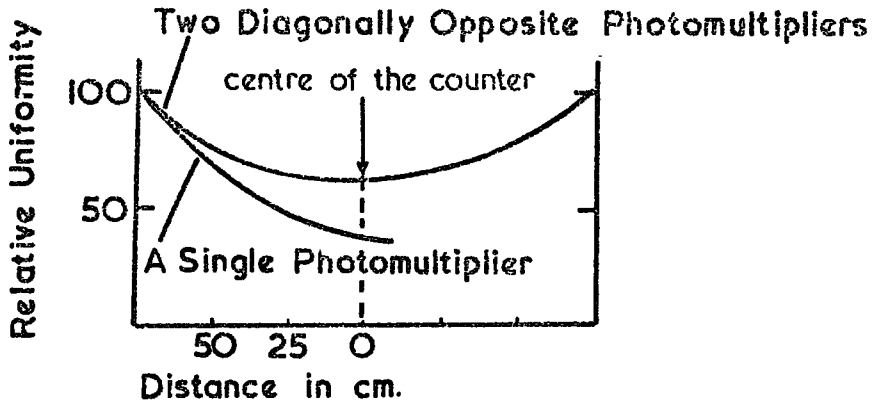

Figure 3.4 The uniformity of the scintillation counter

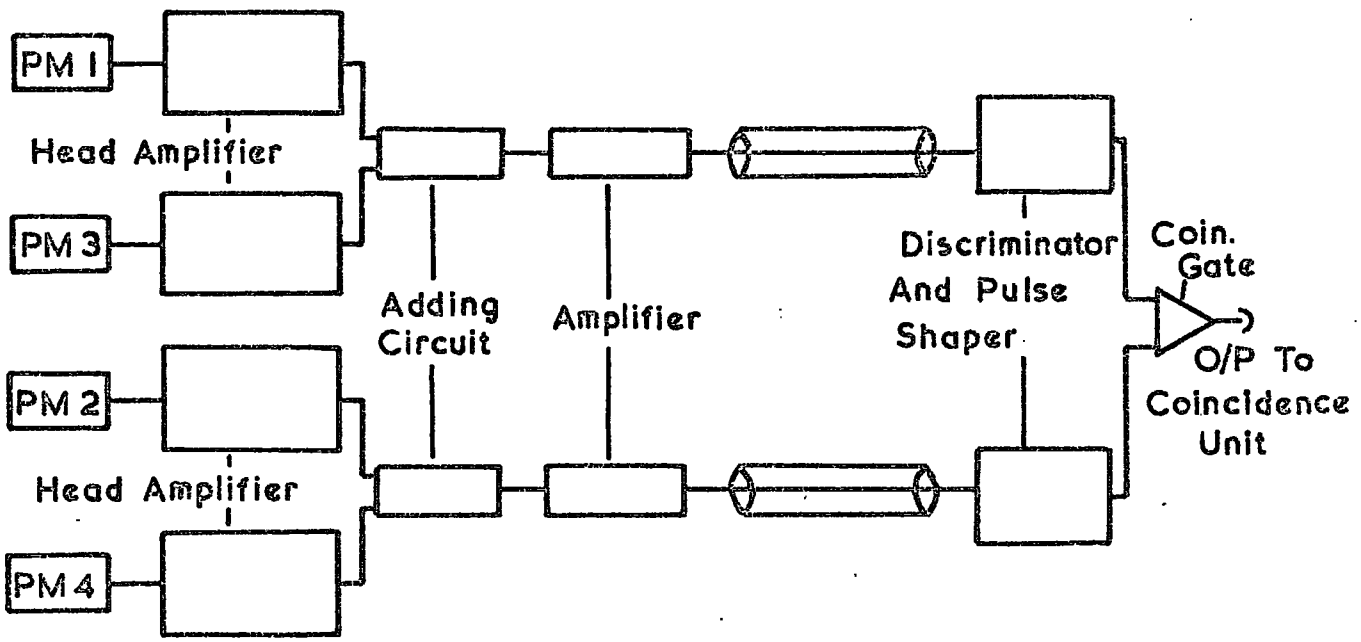

Figure 3.5 Block diagram of the electronics for the scintillation counter

small diameter flash tubes and are termed the 'measuring trays'. The work described in this thesis makes use of the measuring trays on the red side of MARS and therefore they will be described in this section. The momentum selector trays are described elsewhere (Ayre et al., 1972).

The measuring trays comprise eight layers of small diameter flash tubes with eighty-nine tubes per layer. The tubes are filled with commercial neon gas to a pressure of 2·4 atmospheres. The dimensions of the glass envelopes are: O.D., 7·5 - 8·0 mm; I.D., 5·2 - 5·8 mm, length 2 m. The tubes are painted black to prevent one flash tube setting off adjacent tubes when it discharges.

Each measuring tray contains nine 1·2 mm aluminium sheets as electrodes, connected alternately in the usual manner with the outer electrodes in each tray being earthed for safety. The sensitive area of each tray is defined by the overlap of the electrode and is $\sim$ 76·5 cm x 180·3 cm. The tubes are located at both ends of a tray in holes drilled in a 3 mm thick brass plate. The tubes are kept parallel along their length by suitably positioned Tufnol spacers. The pattern of the tubes in each measuring tray is shown in figure 3.6.

The high voltage pulse for the flash tube tray is obtained by discharging a delay line through a resistor by means of a spark gap. A square negative pulse is obtained across the resistor, which is applied to the flash tube trays. The spark gap is triggered by discharging a condenser of capacity 0·05 μf through the primary of a transformer using a thyristor, type BTX 64. The circuit for the spark gap is triggered by the pulse obtained when an accepted particle passes through the spectrograph. The high voltage pulse, which has a width of 1·8 μsec and rise time of 1 μsec, is applied to the flash tube tray 1·5 μsec after the passage of the triggering particle.

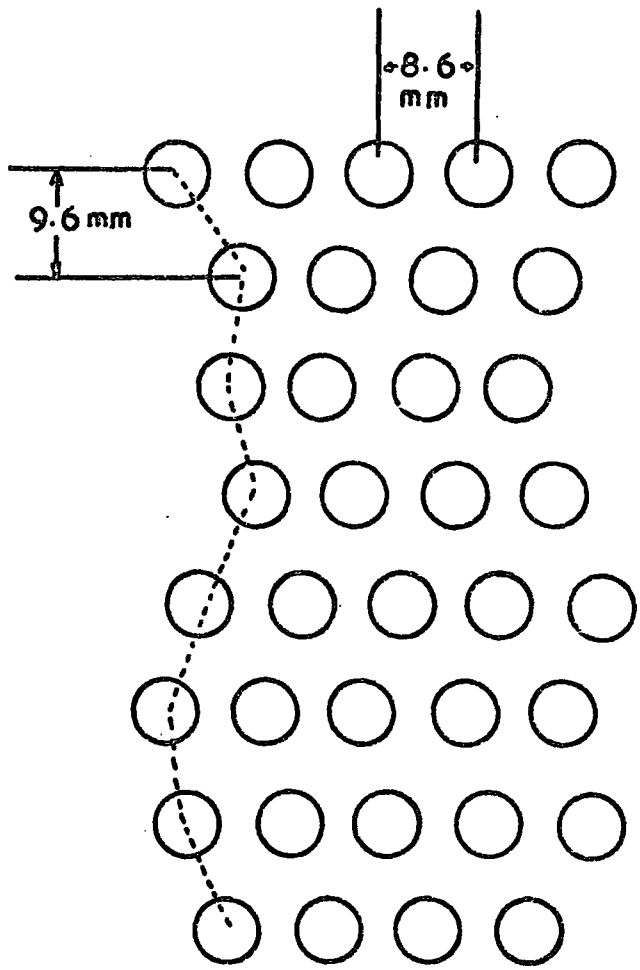

Figure 3.6 The pattern of flash tubes in the measuring tray

Efficiency measurements on the flash tubes were carried out using a single particle traversing the spectrograph. A high voltage pulse was applied to the flash tube trays after the occurrence of an event and the flashes were recorded photographically. About 500 events were recorded for each of several values of the high voltage pulse. The layer efficiency was calculated by noting the number of flashes in each tray for every single track. The layer efficiency was then converted into internal tube efficiency by correcting for the glass thickness and for gaps between tubes. The chosen value for the high voltage pulse was 13 KV. The corresponding internal tube efficiency is 92%.

3.5 The acceptance of the spectrograph

The acceptance of MARS is particle collection power of the spectrograph (i.e. area x solid angle). In the presence of the magnetic field in the spectrograph, the acceptance is a function of incident momentum. For a given incident momentum it depends on both the magnetic deflection and the energy loss in the spectrograph. Figure 3.7 shows the variation of the acceptance with incident momentum for the red side, if the incident particle is required to pass through the scintillation counters and the five measuring trays. It was calculated by simulating particles through the spectrograph of given momentum with different incident angles. The acceptance of such particle as a function of angle was evaluated considering the effect of energy loss and magnetic deflection in a field of 16·3 K gauss. The effect of multiple scattering was neglected. Integration over all angles then gives the acceptance for a given incident momentum. As can be seen from figure 3.5, the acceptance of MARS spectrograph is zero for particles with momentum below 7·5 GeV/c. However, it increases very rapidly with increasing momentum and reaches saturation value at a momentum of about 60 GeV/c. The mean muon momentum traversing the red side of the

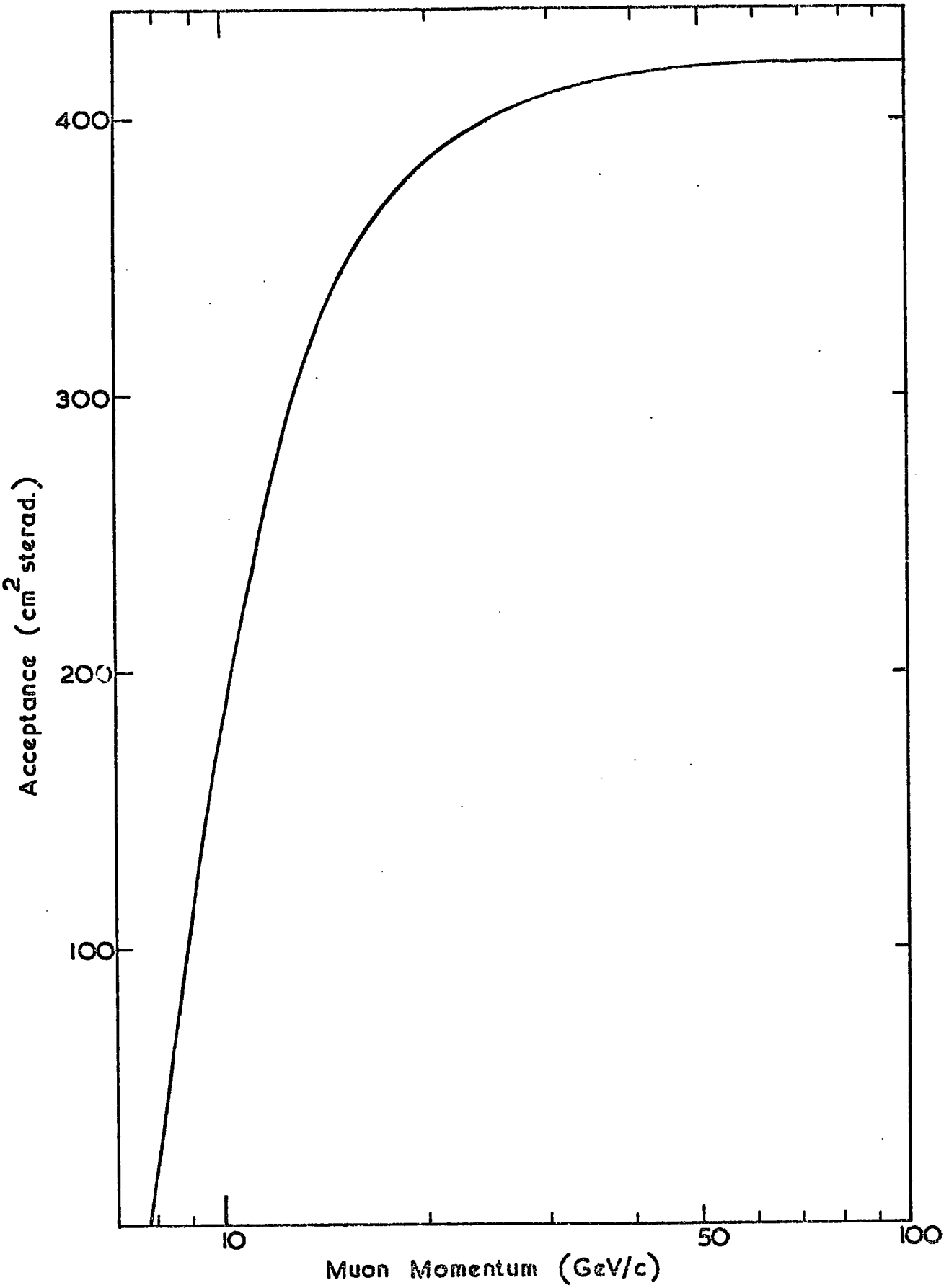

Figure 3.7 The acceptance of the red side of MARS

spectrograph, calculated by folding the acceptance function into the sea level muon momentum spectrum, is 16 GeV/c.

3.6 The maximum detectable momentum of MARS

The maximum detectable momentum (m.d.m.) of MARS is defined as the momentum of a particle whose deflection is equal to the standard deviation of the error in the deflection. The value of the m.d.m. shows a dependence on the combinations of measuring trays used in the parabola fit to determine the momentum of the traversing particle. The maximum value for the m.d.m. is obtained when information from all five measuring trays is used in the process of momentum determination. The m.d.m. of the spectrograph is a minimum when information from only half of the spectrograph is used for determining the momentum (by half is meant either the top or the bottom three measuring trays). The m.d.m. for various combinations of measuring trays is given in Table 3.2.

3.7 Triggering mode

The triggering elements of MARS are its three scintillation counters. The scintillation counters are placed on top (S5), middle (S3) and bottom (S1) of the spectrograph. The output pulses from the coincidence circuit of each scintillation counter are fed into a coincidence unit. When a threefold coincidence is obtained from the scintillation counters (S1 S3 S5) an output pulse fed to a high voltage trigger unit is used to apply a high voltage pulse to the five measuring trays of flash tubes. As already remarked, this pulse is applied 1·5 μsec after the passage of the triggering muon.

Another output pulse is fed to a cycling system used to illuminate a clock, flash two fiducial bulbs on each measuring tray and illuminate an information board on which is displayed the series number of the film,

TABLE 3.2

The m.d.m. of the spectrograph, for various combinations of measuring tray data (theoretical values assuming a location error of ± 0·3 mm at each level).

Trays Utilised	m.d.m. (Gev/c)
12345	5856
1345 or 1235	5560
1245	4655
1234 or 2345	3210
123 or 345	1280
234	1365
135	5140
134, 245, 235 or 124	2575

the field direction and the date of the run. All of these are recorded on the same frame of the events through a system of plane mirrors. The cycling system also winds on the film in the camera after the occurrence of the event. The system can be paralysed, if required, after the occurrence of each event by a series of switches placed on the front panel of the coincidence unit. The length of the paralysis time can be varied from 1 to 13 sec. After the end of the paralysis time the system is ready to accept the next event.

The rate of single muons traversing the spectrograph depends on the length of the paralysis time and on whether or not the magnetic field is on. With no paralysis the rate of the muons with zero field is 28·0 ± 1·0 min^{-1}. For a magnetic field of 16·3 K gauss the rate differs from that of zero field by 31 ± 2%. The expected decrease based upon the Hayman and

Wolfendale spectrum is 36 ± 2%.

The expected rate of traversal of each side of the spectrograph by particles of various momenta, in the presence of the field, calculated using the integral spectrum of Hayman and Wolfendale is given in Table 3.1.

3.8 Possible use for Interaction studies

MARS is designed to be eventually full automated. However, it is only possible at present to use photographic recording on the red side and it is with data from this side that the present thesis is concerned. When a triggering particle passes through the red side the five measuring trays in the spectrograph discharge to indicate the trajectory of the traversing particle. The track in each measuring tray is photographed, together with other relevant information by a single camera. The momentum and the sign of the particle are determined from its bending in the magnetic field. If the triggering particle interacts in its passage through the spectrograph, then this can be recognised from the pattern of the flashes in the measuring trays. The fact that there are several magnetized iron blocks in MARS increases the chance of interactions in the spectrograph and also makes it possible to determine the momentum for particles undergoing multiple interactions in traversing the spectrograph. Therefore, information regarding the sign and momentum of muons undergoing interactions in the spectrograph can be obtained. An estimated number of secondary particles can be obtained from the pattern of the flashes in the measuring trays. Thus, it is possible to use MARS in order to investigate the interaction properties of the muon in traversing magnetised iron. We will see in Chapter 5 how the scintillation counters of MARS were modified to select only events associated with bursts in the measuring trays of levels 1 and 3.

CHAPTER 4

INTERACTION EXPERIMENT I

4.1 Introduction

The situation with the electromagnetic interaction of the muons is rather confused and uncertain. Results from some cosmic rays experiment shows a possible deviation from the accepted theories and go to the extent of suggesting an asymmetry in the interaction of two differently charged muons. On the other hand results from experiments with machine muons are in quite good agreement with the theoretical predictions of the standard quantum electrodynamics (Q.E.D.).

The cosmic ray results, if confirmed, do not necessarily imply a breakdown in Q.E.D. For instance the 'muons' in cosmic rays may differ from machine muons and there may be a new process which cosmic ray muons undergo when interacting with matter, a process which contributes independently of the normal electromagnetic interaction. This would be a very exciting possibility for neither the electron nor the muon has ever been observed to have other than electromagnetic and weak interactions. It is therefore highly desirable to run a new experiment to investigate the interaction of cosmic ray muons with particular emphasis on the sign of the interacting muon, hoping to understand the inconsistency with accelerator results. It was for this reason that the first interaction experiment using MARS was undertaken. This chapter will present the details of the experimental run, data analysis and the results.

4.2 Experimental conditions

4.2.1 Alignment of the Spectrograph

Before running the red side of MARS to study the electromagnetic interaction of cosmic rays, that side of the spectrograph was aligned. The flash tube trays and the scintillation counters in the spectrograph rest on $\frac{1}{2}$" steel rollers, which fit into bearings fixed in the magnet block support.

This facilitates ease of movement of the various components to the required position. There are two plumb lines for each side of the instrument, one at each end of the flash tubes in the trays. The fixed end of each is fastened to a bracket near the top of the spectrograph while the free end is dipped in oil, contained in a beaker, in order to prevent oscillations. The plumb lines on each side of the spectrograph are used as reference vertical lines to which all horizontal measurements are referred.

The positions of the five measuring trays, on the red side, were adjusted so that each tray was as nearly as possible in the middle of its gap and also all five trays were as close as possible for being underneath each other. This was achieved by measuring two perpendicular horizontal distances for each end of the tray from the plumb line close to it, using a ruler supplied with a spirit level. The trays were moved across and along their lengths in order to achieve the required position. This method of alignment gives the position of each tray to within ± 1 mm. The same method is used in aligning the three scintillation counters.

4.2.2 Running the experiment

For more accurate location of the measuring tray positions, a zero field run was carried out. The magnetic field in the spectrograph was brought down to zero. The spectrograph was then triggered on single muons traversing its red side. Every event was photographed. Because of the high rate of single muons passing through the spectrograph, a paralysis time of 4 sec was used after the occurrence of an event. This paralysis time gave a chance for the camera to wind on the frames of the photographed events and also reduced the probability of spurious flashes in the trays. It is important to have as few spurious flashes as possible to ease the finding of the muon track in the flash tube trays and also to enable a correct estimate to be made of the number of secondaries when interactions took place in the spectrograph.

The rate of single muons triggering the red side under the conditions of zero field and with 4 sec paralysis was measured and found to be 10·1/min ± 1%. A total of 3000 events were photographed with zero field corresponding to a running time of about 5 hours.

After the zero field run, the field was increased to its maximum value of 16·3 K gauss. The instrument was triggered with the same requirements used in the zero field run. However, the rate of trigger was less in this case. This is due to the inability of some particles to pass through all three scintillation counters in view of their large bending in the magnetic field. This loss is confined to the low energy muons traversing the spectrograph. The rate of triggers in the presence of the field and with 4 sec paralysis was found to 8·59/min ± 1%.

The field direction was reversed every 24 hours in order to eliminate any systematic bias for one sign of the muon. Equal running time was obtained for each field direction. The total number of events photographed was about 10,000.

4.3 Data analysis

4.3.1 Introduction

The photographs have been analysed by film scanning. The events on the film are projected on a board on which are placed diagrams of the five measuring trays of flash tubes. Each diagram gives the positions of the flash tubes and the fiducial bulbs for the tray it represents. The size of the diagrams is such as to match the magnification of the projection system (i.e. the two fiducials of each tray on the film fall exactly on the corresponding ones on the board).

The flash tubes in the diagram for each tray are divided into blocks. The first block in each tray consists of four columns of flash tubes while every other block in the tray consists of five columns. Each column has

eight layers of tubes. The first column in each block has its number marked near to it. The position of the track in each tray was recorded for analysis in the following manner: the fiducials on the diagram of the tray were aligned. The first column number of the block of flash tubes within which the track falls is read off and is fed onto paper tape together with the pattern of the flash tubes that have been discharged in their positions with respect to the first column. Also fed in are the tray number and the time of the event. This procedure is carried out for at least three trays in every accepted event.

4.3.2 Classification of events

The events observed during the single muon run can be classified as follows:

(1) Single muon

An event is considered as being due to a single muon traversing the spectrograph when one and only one track is observed in eash measuring tray. A muon track in a tray is defined as at least three flashes in different layers such that they can be associated with each other and with the tracks in the remaining trays. From the efficiency measurements of the trays, the average number of flashes for a single track in a tray is 5.

A single muon event has five clear tracks, all of which can be used for analysis. Such events are useful in determining the positions of the trays in the zero field run and for determining the momentum spectrum and the charge ratio of the muons in the magnetic field runs.

(2) Knock-on production event

If in addition to the muon track in each measuring tray, there is one additional track in one of the trays, apart from the tray in level 5, the event is considered as a knock-on event. The reason for excluding

tray 5 is because this tray is placed on top of the spectrograph (no absorber on top of it), and we are interested only in knock-on electrons produced in the iron. In what follows when interactions observed in the trays are discussed, tray 5 is excluded.

The knock-on events observed can be divided into two types. The first type consists of knock-ons within the flash tube trays. The second type comprises knock-on events in the magnet block on top of the tray. The event is classified as a knock-on in the tray if the extra track observed in the tray appears to originate in it. On the other hand the event is classified as knock-on in the magnet if the extra track observed in the tray appears to originate in the magnet. However, in analysing the data, only knock-on events in the magnets were considered. In order to accept a track in a tray as a knock-on in the magnet it must consist of at least two flashes if they are in the top two layers of the tray, otherwise it must consist of at least three flashes. In any case the flashes must appear associated with each other and form an apparent track. In the event where no distinct tracks are observed, the event is classified as a knock-on event if the number of flashes seen in the tray is < 15.

(3) Burst production event

An event is classified as a burst event if one of the measuring trays contains two or more tracks in addition to that of the muon. The requirements for the extra tracks are the same as for knock-on tracks. In the case where only a cluster of flashes is observed, the event is considered as a burst if there are ≥ 15 flashes.

(4) Vertical and oblique air showers

If more than two tracks are observed in tray 5 the event is classified as an extensive air shower (EAS). Oblique showers are those events with single tracks in tray 5, no track in tray 4 and a large shower in some of the remaining trays. These events are of no use to the present experiment and

therefore rejected. The rate of these events in MARS is $\sim 1\%$.

For illustration of the classification of events, a typical set is presented in plates 4.1 and 4.5.

4.3.3 Handling of zero field run data

As mentioned earlier, about 3000 events were photographed in the zero field run to enable more accurate location of the measuring trays positions. The photographs were scanned and about 600 single muon events were punched on the paper tape for analysis. These events were fed to the computer with a program developed to do the following:-

(1) Find each tray and its track. Considering the trays in turn, the program finds the best straight line to fit the pattern of the flashes for each track.

(2) After finding the best line for the track in the tray, the program chooses the point on the line which is in the middle of the tray as a best representation for the position of the track in that tray.

(3) Using the information about the measured positions of trays 1 and 5 (section 4.2.1), the position of the track in each of them relative to the plumb line is calculated. A straight line is then drawn between the position of the track in 1 and 5. For an ideal traversal the tracks in all trays will fall on the line. However, because of multiple scattering suffered by the traversing particle, this is rarely the case. Therefore, considering the trays 2, 3 and 4 in turn, the program calculates the distance between the track in the tray and the straight line. From knowing this distance, the position of the track in the tray and the position of the track in tray 5 (or tray 1) relative to the plumb line, it is easy to calculate the apparent distance (d) of a reference point on the tray from the plumb line, ignoring scattering, for each event.

By repeating the process for several hundred events a distribution

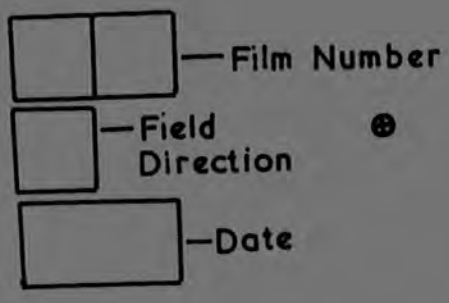

Plate 4.1

A single Muon Event

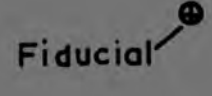

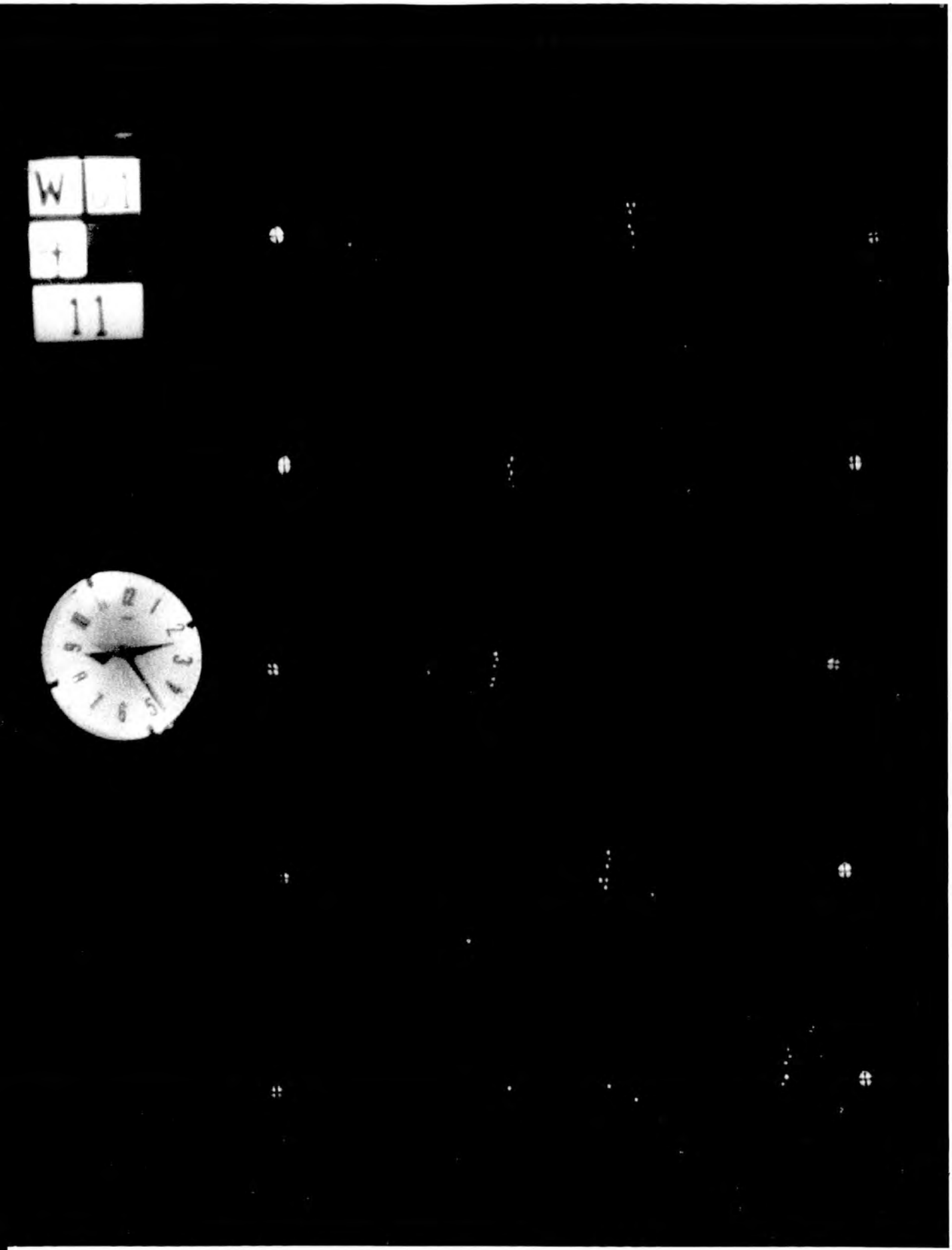
W
11

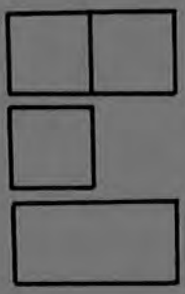

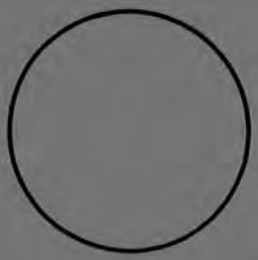

Plate 4.2

A single Knock-on
Electron Event in Level 3

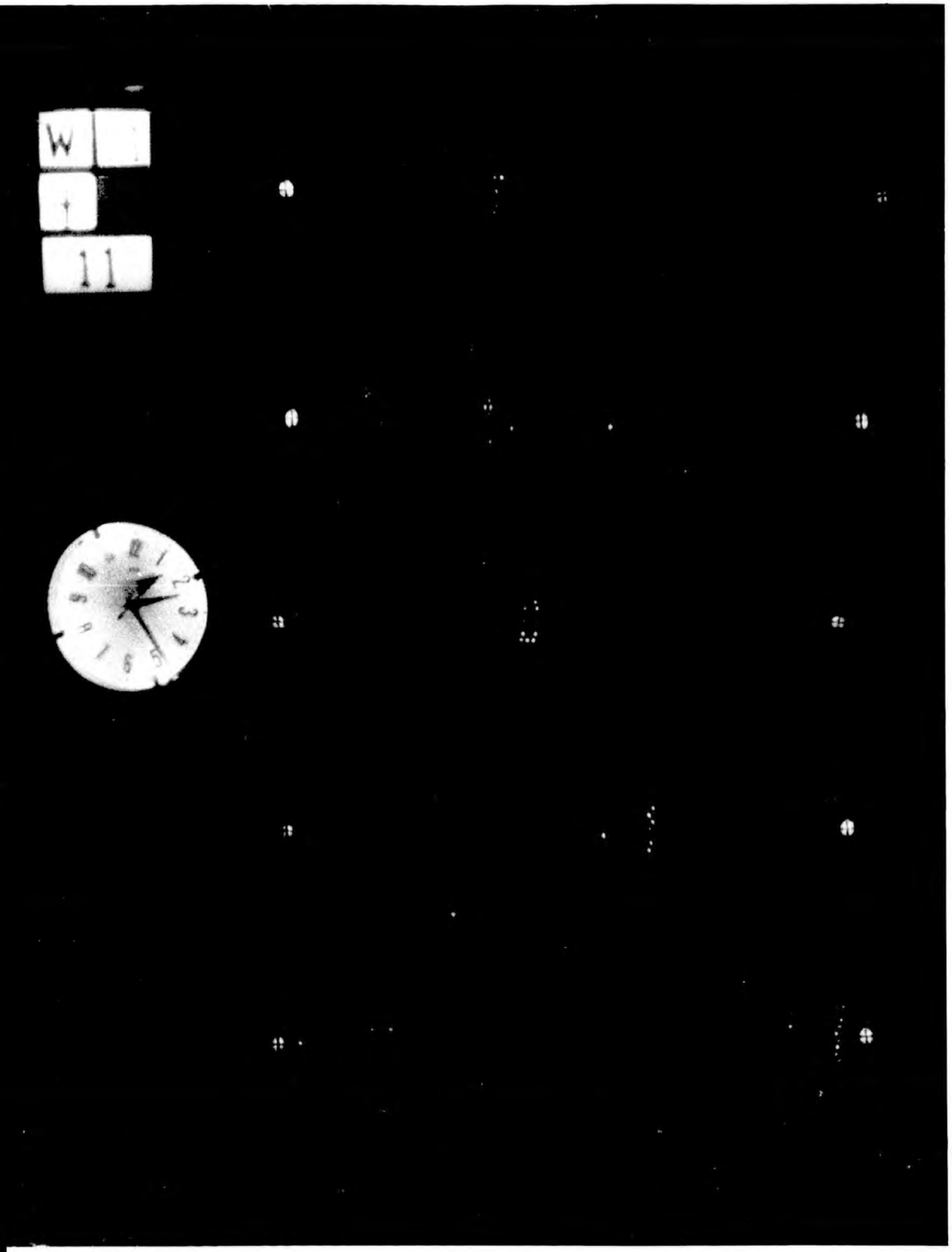
W
11

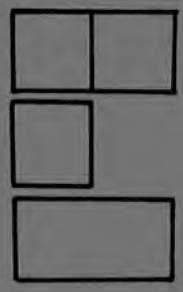

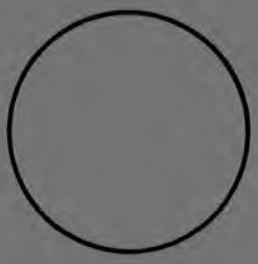

Plate 4.3

A single Knock-on Electron

in the Flash Tube Tray of Level 4

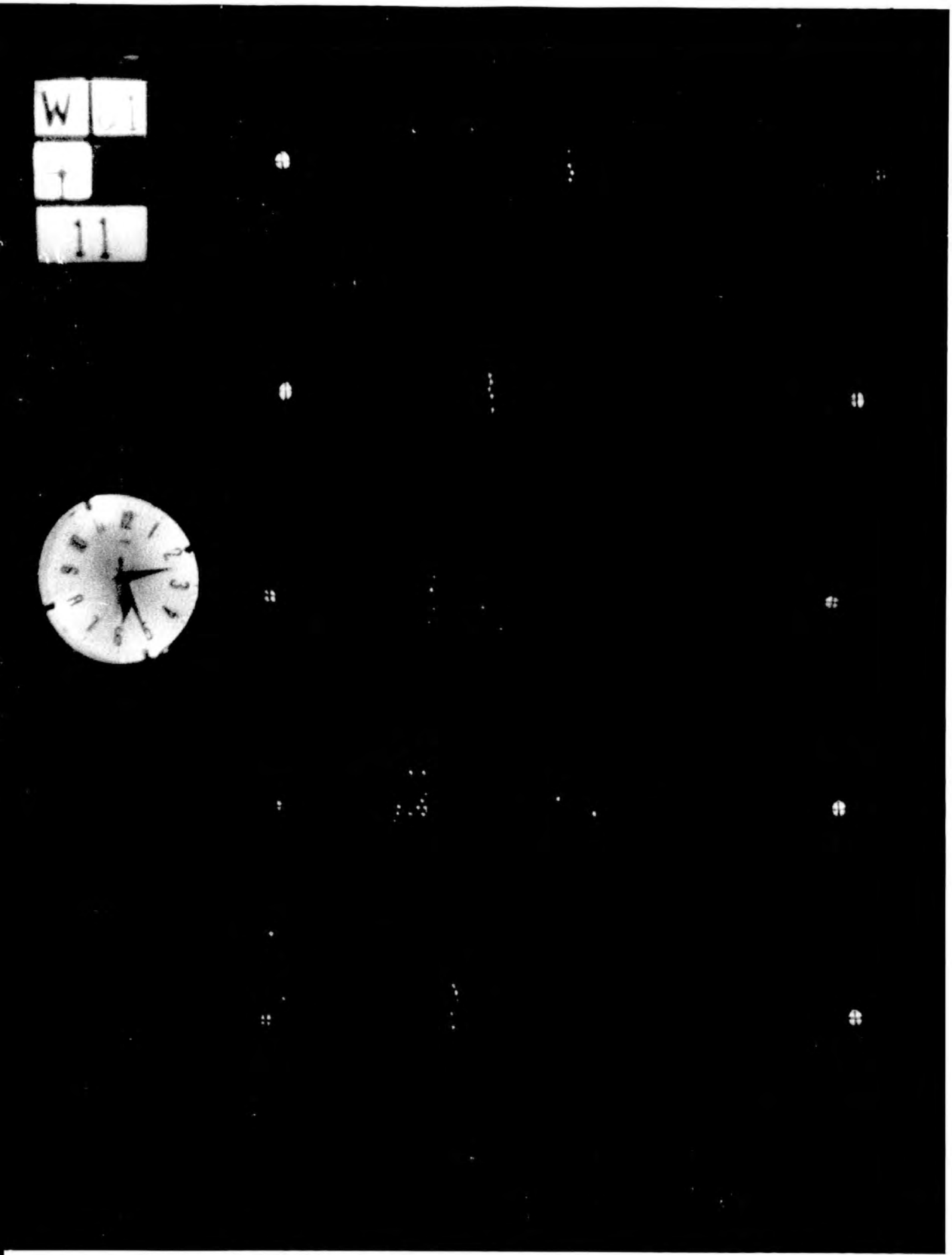
W
11

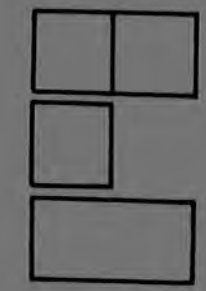

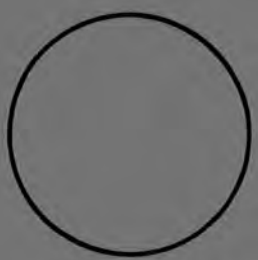

Plate 4.4

A burst Event in Level 3

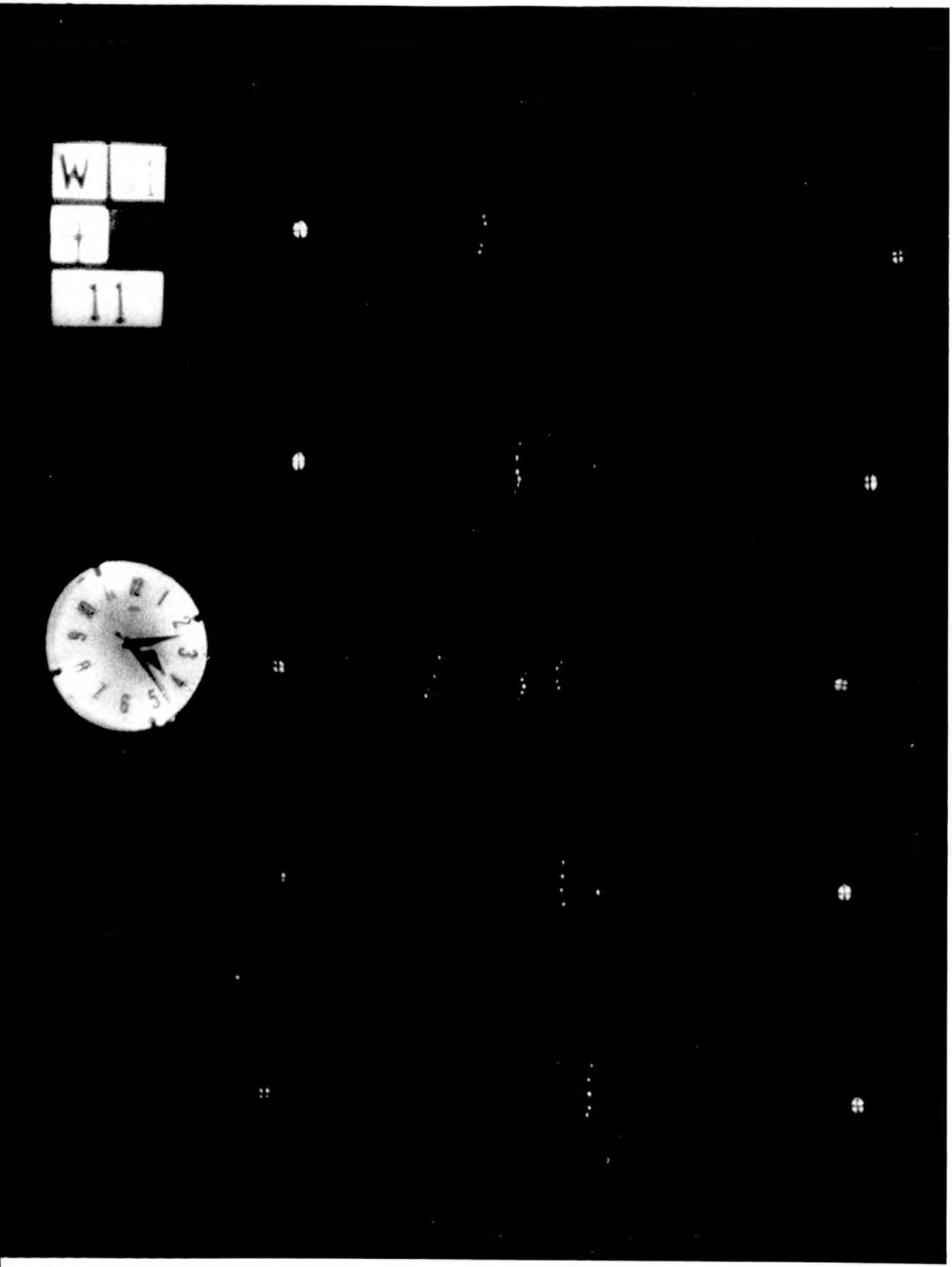
W
11

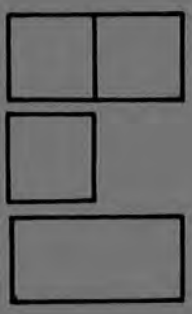

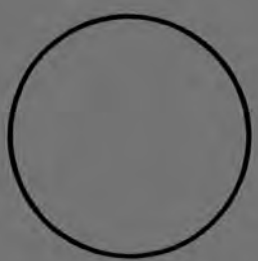

Plate 4.5

An Extensive Air Shower Event

of values for (d) for each tray (2,3 and 4) is obtained. The mean value of d then gives the position of the tray with respect to the plumb line. The standard error, defined as $\sigma/\sqrt{n}$, where σ is the standard deviation of the distribution and n is the number of events analysed, is considered as the accuracy in knowing the tray position. the values of the standard error obtained for trays 2, 3 and 4 are 0·070, 0·071 and 0·063 cm respectively. A typical standard deviation is 1·7 cm.

4.3.4 Handling of field run data

(A) Selection criteria

For an event to be accepted during film scanning, in the study of electromagnetic interactions of cosmic ray muons, it must satisfy the following:-

(1) There is a track in each measuring tray. An accepted track consists of two or more flashes which are roughly in the right place and direction with respect to the tracks in the remaining trays.

(2) Out of the five tracks for the event (one in each measuring tray) there must be at least three measureable tracks. A track in the tray is defined as a measureable track if it consists of at least three flashes in different layers in the tray which look to be associated with one another and with the tracks in the remaining trays.

(3) The event must be an interaction event i.e. knock-on or burst event.

If the scanned event satisfies the above requirements then the time, the coordinate and pattern of the measureable track and the tray number are fed on the paper tape for all measureable tracks in the event. The tray (or trays) which shows the interaction is excluded from the measurements, but the pattern of flashes is drawn. Thus, unless the event is a knock-on event, where the muon track can be recognised, data from a maximum of four trays are fed on to the paper tape for each event.

In a separate, but identical, scanning the single muon events are analysed for determining the charge ratio of the muons triggering the spectrograph. This charge ratio is used in investigating the charge asymmetry in muon interactions.

(B) Momentum and sign determination for the muons

In this section, a description is given of the method used to determine the momentum and the sign of the events punched on the paper tape. The paper tape is fed to the computer and in the same method as that mentioned in section 4.3.3, the track in each tray is represented by a single point. At least three points are obtained on the trajectory of the muon traversing the spectrograph. From these points the momentum and the sign of the muon can be found using the method of least squares to fit a parabola to the points.

The equation of the parabola used in the fitting technique is given by:

$$y = ax^2 + bx + c \qquad \text{.....(4.1)}$$

Where a, b and c are parameters whose value is determined by the fitting process. The important parameter, so far as the momentum and sign of the particle is concerned, is 'a'. It can be shown that a is related to the radius of curvature ρ of the particle trajectory by the equation

$$a = \frac{1}{2\rho} \qquad \text{.....(4.2)}$$

A particle of momentum P eV/c moving in a uniform magnetic field B Gauss, has a radius of curvature ρ cm given by the equation

$$P = 300\ B\rho \qquad \text{.....(4.3)}$$

Substituting for ρ in equation 4.3 give

$$P = \frac{150B}{a} \qquad \text{.....(4.4)}$$

The sign of the parameter a obtained from the parabola fit, together with the field direction, determine the sign of the muon traversing the spectrograph. Equation 4.1 assumes a continuous trajectory for the particle.

This is of course not true due to the gaps between the magnet blocks. Allowance for this reduces the momentum given by equation 4.4 by 20%. Therefore, for a field of 16·3 K gauss in the spectrograph the momentum of the particle is given by

$$P = \frac{0\cdot196}{a} \text{ GeV/c} \qquad \text{.....(4.5)}$$

a is measured in m^{-1}.

Consider Figure 4.1. The coordinates of the muon tracks in three measuring trays are given (any three or four measuring trays can be chosen) in the cartesian coordinates. The trajectory $y = ax^2 + bx + c$ is also shown. It is required to find the parameter a using the method of least square. Consider the i_{th} measuring tray:

$$\Delta_i = y_i - ax_i^2 - bx_i - c$$

The method of least square requires that the sum of Δ_i^2 for all measureable tracks is a minimum, i.e.

$$\Sigma\ \Delta_i^2 = \Sigma\ (y_i - ax_i^2 - bx_i - c) = Q = \text{minimum}$$

This implies

$$\frac{\partial Q}{\partial a} = \frac{\partial Q}{\partial b} = \frac{\partial Q}{\partial c} = 0 \qquad \text{.....(4.6)}$$

By solving equation 4.6, the values of a, b and c can be determined.

(C) <u>The m.d.m. of the instrument in the present experiment</u>

A definition for the m.d.m. of MARS, together with its ultimate values for various combinations of measuring trays is given in section 3.6. In the present section an estimate is given for the minimum value of the m.d.m. of the instrument when being used for interaction studies. The actual value for the m.d.m. depends on the combination of measuring trays used in the parabola fit and therefore differs from one event to another.

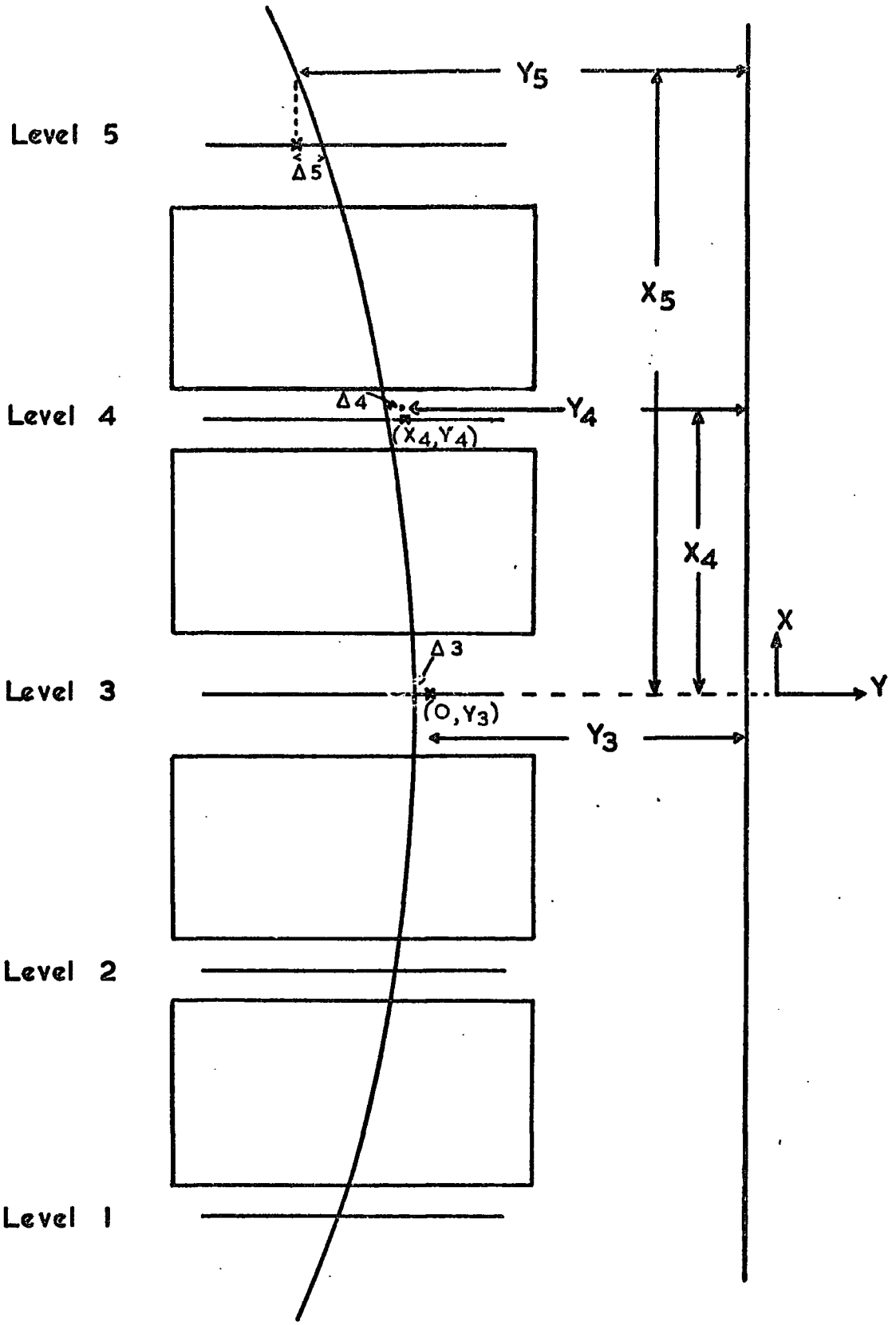

Figure 4.1 Typical trajectory of traversing particle in MARS.

Because of interactions in the spectrograph only three or four measuring trays are used for momentum determination. Three is the minimum number of measuring trays that can be used. In the ultimate accuracy in the track location in each level (0.3 mm) the minimum m.d.m. 1280 GeV/c, is obtained when only three measuring trays in the top or bottom half of the spectrograph are used. In the present experiment, however, the accuracy of track location is 0·7 mm (section 4.3.3), which in turn implies a lower value for the m.d.m.

Consider the definition of the m.d.m. given in section 3.6 and equation 4.5. They would imply

$$P_{mdm} = \frac{0{\cdot}196}{\sigma_a} \quad \text{GeV/c} \qquad \ldots\ldots\ldots\ldots\ldots\ldots\ldots(4.7)$$

where $\sigma_a(m^{-1})$ is the standard deviation of the coefficient a, which can be expressed in terms of the standard deviation in track location σ_y as

$$\sigma_a = \sigma_y / K \qquad \ldots\ldots\ldots\ldots\ldots\ldots\ldots(4.8)$$

K is determined by the number and the coordinates of the trays used. Substituting for σ_a in equation 4.7 give

$$P_{mdm} = \frac{0{\cdot}196}{\sigma_y} \; K \quad \text{GeV/c} \qquad \ldots\ldots\ldots\ldots\ldots\ldots\ldots(4.9)$$

Let us compare equation 4.9 for two values of the m.d.m., one is 1280 GeV/c for which σ_y = 0·3 mm, the other has value P_{mdm} and accuracy in track location σ_y mm. This results in

$$P_{mdm} = \frac{0{\cdot}3}{\sigma_y} \times 1280 \quad \text{GeV/c} \qquad \ldots\ldots\ldots\ldots\ldots\ldots\ldots(4.10)$$

For the present experiment (σ_y = 0·7 mm) and the lowest m.d.m. is thus

$$P_{mdm} = 548 \quad \text{GeV/c} \qquad \ldots\ldots\ldots\ldots\ldots\ldots\ldots(4.11)$$

(D) Estimation of burst size

In MARS there is no direct means of determining the energy transferred in the iron block for each interaction event. This is because it is not possible to observe the development of the electromagnetic shower in the magnet, only one section of the shower is observed in the flash tube tray. However, it is possible to estimate the number of secondaries, which in turn is a measure of the energy transferred, from the pattern of the flashes observed in the tray. In some cases the tracks of the secondaries in the tray are well separated, in which case the number of secondaries can be simply counted. However, in the cases where clusters of flashes are observed a statistical method is adopted to determine their number. This method, which is described by Rogers (1965), is based on Poisson statistics for the flash tubes fired due to the passage of the shower particles. A uniform shower density is assumed over the whole area of the shower. This assumption is incorrect since it is known that the particle density is higher near the shower axis and corrections are necessary to account for the non-uniform density distribution. This method of determining the burst size is thought to be accurate within $\pm$ 30%.

Since the average number of flashes for a single particle traversing the flash tube tray is 5, the number of flashes divided by 5 give a rough estimate to the number of particles in the tray. This method becomes inaccurate as the number of flashes increases because of the increased possibility of more than one particle passed through the same flash tube. One should also take into account that some secondary particles stop in the tray and therefore produce less than 5 flashes.

All the above mentioned methods were applied to each interaction event. By comparison between their results an estimate was made of the size of the burst observed.

4.4 Charge asymmetry in muon interactions

4.4.1 Introduction

As mentioned in the introduction to this chapter, the prime reason behind this experiment was to investigate the charge dependence of the electromagnetic interaction cross section. Therefore, the rest of the chapter will be devoted to such investigations. A study of the electromagnetic interaction process will be given in chapter 7.

In the present experiment (unbiased run) the total number of interaction events scanned and analysed is about 3000. The energy transfer involved in producing these events is mainly less than 5 GeV. This is because the experiment was carried out using single muon triggering and the events involved in the analysis were mainly due to the knock-on production process. In other words, they were either single knock-on electron or knock-on shower events. Consequently the results from this experiment can only examine the knock-on process.

In analysing the data to study the charge dependence of muon interactions, it is highly desirable to use an objective method of estimating the energy transfer for each event. Only then can one get the correct dependence of charge asymmetry on energy transfer. It is thought that the method described by Rogers (1965) is somewhat subjective and thus can give unreliable answers for events with low numbers of flashes (i.e. events with 1, 2 and 3 electrons, which is equivalent to energy transfers $\sim$ 1 GeV). If the asymmetry is confined to low energy transfers (i.e. 1 GeV or so) as suggested by Kotzer et al. (1965), and Allkofer et al. (1971), then great care must be taken when analysing the data for this region of transferred energy. Consequently in analysing the data for the asymmetry the Rogers method was not used. This method was used only in producing an overall burst spectrum, where no discrimination between positive and negative muons is considered.

The objective method used in classifying the events according to

their energy transfer, is the number of flashes associated with each event. It is believed that this method is a good one and introduces no bias favouring one sign of the muon on the other.

4.4.2 Results

About 75% of the events analysed are single knock-on electron events, the remaining 25% being burst events. The method used in classifying the events has been mentioned in section 4.3.2. In the asymmetry analysis, the events were divided according to the sign of the muon which produced the event. If N^+ is the number of interaction events produced by positive muons (μ^+) under a given condition and N^- is the corresponding number of interaction events produced by negative muon (μ^-) under identical conditions, then we define the asymmetry η as $N^+/(N^- \times R)$, where R is the charge ratio of the muons triggering the instrument. The value of R used in the analysis is that obtained from scanning of about 6000 single muon events ($R = 1{\cdot}30 \pm 0{\cdot}03$).

By comparing the total number of events (knock-on + burst) produced by μ^+ with the corresponding number produced by μ^- corrected for the charge ratio, an overall value for the asymmetry is obtained. The value given by this experiment is $\eta = 1{\cdot}05 \pm 0{\cdot}04$. This value is to be compared with the expected value of unity on the basis of quantum electrodynamics. Although the measured value is not inconsistent with unity, it is better to separate the knock-on events from burst events and evaluate the integral value of the asymmetry for each process. This will indicate whether there is a significant asymmetry for one of the processes. By doing so in our data, the integral values of the asymmetry are $1{\cdot}03 \pm 0{\cdot}053$ and $1{\cdot}12 \pm 0{\cdot}12$ for knock-ons and bursts respectively. There is clearly no possibility of a significant asymmetry for knock-on events but, although η is not significantly different from unity for bursts, an excess as high as 10 or 20% can not be ruled out. The reason for

mentioning the possibility of η being as high as 1·1 or 1·2 is the observations from other laboratories mentioned previously and indeed preliminary analysis of the present work (Ayre et al., 1971) gave $\eta = 1{\cdot}34 \pm 0{\cdot}10$. The reason for the high value is now understood as due to the difficulty in discriminating between single and double electron events when using Rogers' method. It so happened that the charge ratio of the misplaced events is very high (presumably because of a statistical fluctuation) which in turn causes a high asymmetry for burst production. This explains why we insist on using an objective criteria when investigating the asymmetry.

From what has been mentioned it is desirable to investigate the dependence of the asymmetry on energy transfer. Therefore the interaction events for μ^+ and μ^- are divided among themselves into cells of number of flashes, N_f, observed in the flash tube tray. The asymmetry is calculated for each cell and is presented as a differential spectrum in figure 4.2. It can be seen that the statistical accuracy is not sufficient to draw any firm conclusion about the dependence of the asymmetry on energy transfer. There seems to be no asymmetry (above 10%) for events with low numbers of flashes, $\bar{N}_f = 10$. These events correspond to single knock-ons. On the other hand, quite a big asymmetry can not be ruled out for events with $\bar{N}_f = 18$. These events correspond to small bursts (i.e. 2 or 3 electrons) with energy transfer around 1 GeV. At higher values of $\bar{N}_f$ the data are poor but there is no evidence against (or for) an asymmetry which increases with increasing energy transfer.

The next step is to investigate the dependence of the asymmetry for burst events on muon energy. The burst events due to μ^+ and μ^- have been divided amongst themselves into muon energy cells and each cell represented by its mean energy. The results are shown in figure 4.3. Within the statistics of the data there is no dramatic change of the asymmetry with muon energy. It should be noted that although none of the asymmetries are inconsistent with unity the measured values are all above unity.

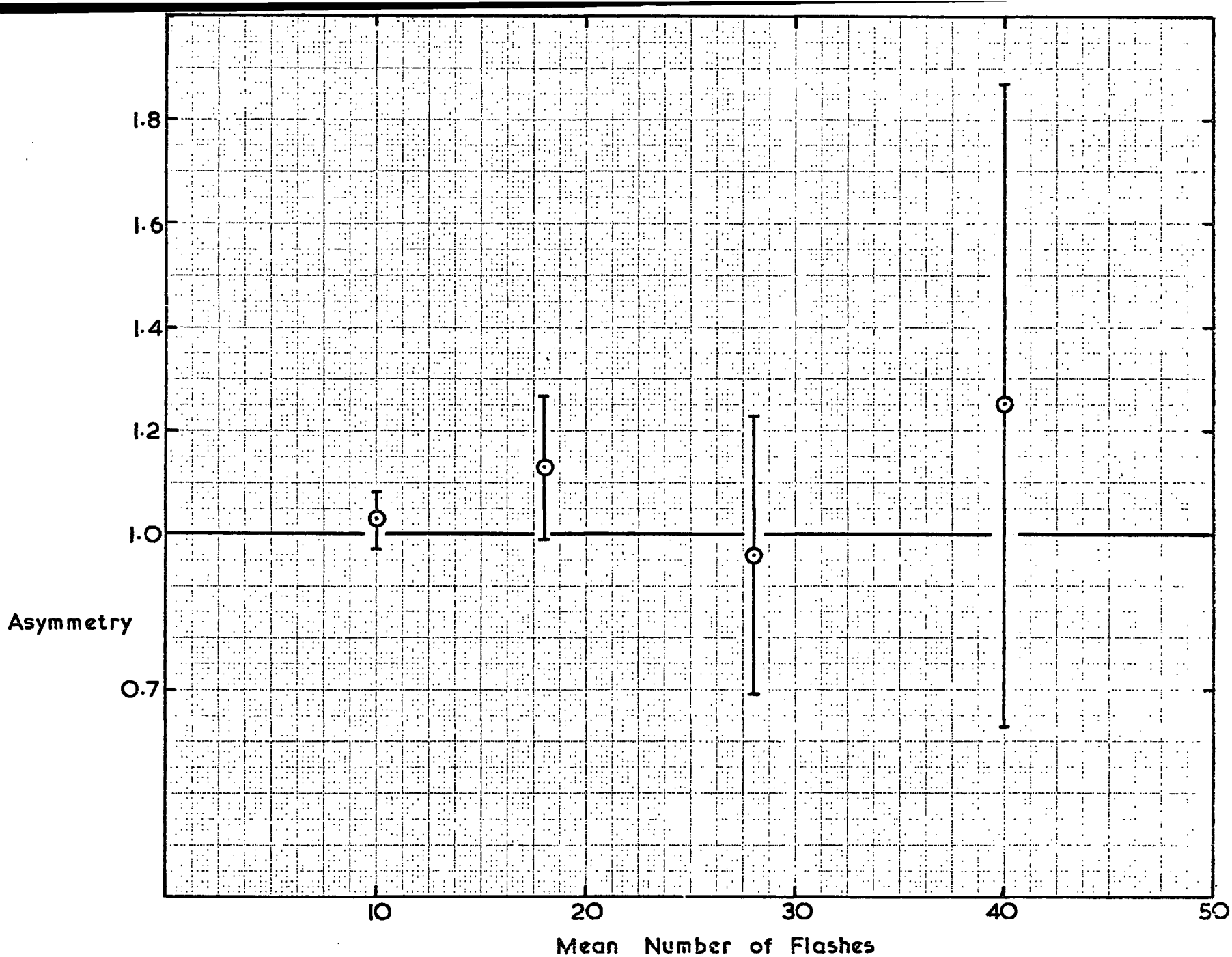

Figure 4.2 The differential spectrum of the asymmetry as a function of number of flashes

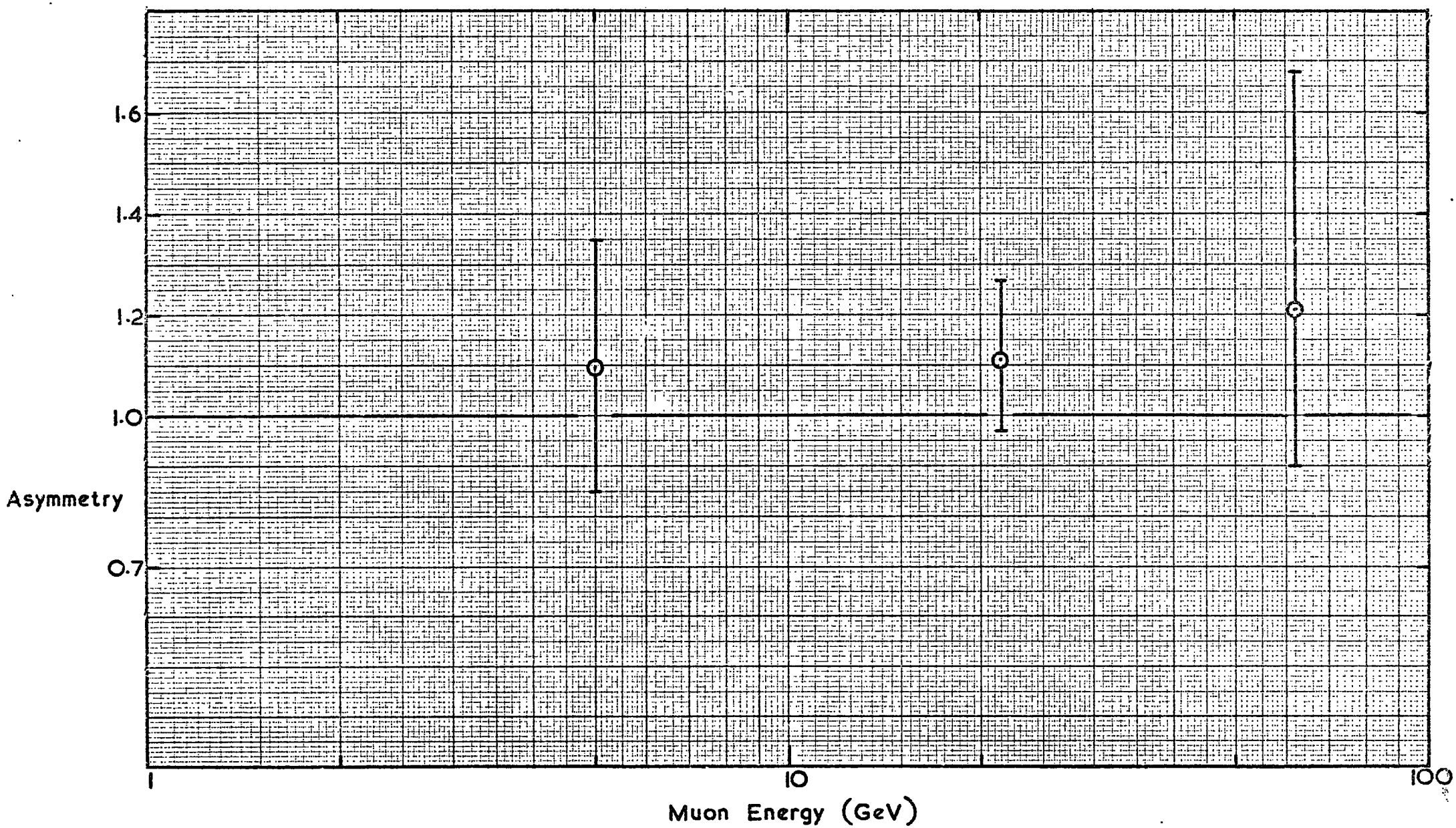

Figure 4.3 Asymmetry as a function of muon energy at interaction

4.5 Conclusions

Although the statistical accuracy on the asymmetry results obtained in this experiment is the best reported so far, they are by no means conclusive about the existence of an asymmetry. Within the statistical error a disagreement with expectation of Q.E.D. can not be claimed neither can an asymmetry of as much as 10% be ruled out. The most certain feature is that there is no appreciable asymmetry in single knock-on production. However, it is of great importance to improve the statistics for burst events because the results leave open the possibility of a significant asymmetry for these events.

CHAPTER 5

INTERACTION EXPERIMENT II

5.1 Introduction

In the previous chapter the results from interaction experiment I about the asymmetry in muon interactions were given. They suggest the possibility of a 10 to 20% asymmetry, favouring positive muons, in burst production with energy transfer in the region of 1 GeV. However, the statistical accuracy is not sufficiently great and the possibility of statistical fluctuations cannot be ruled out.

If the asymmetry is real then, since it is only observed with cosmic ray muons and not with accelerator muons, some difference must exist between the respective muons. Kotzer and Neddermeyer (1967) have suggested that muons from kaons may behave differently from muons which come from the decay of pions. The charge ratio of kaons in cosmic rays is probably in the region of 4:1 which favours the positive muons. Accelerator experiments, however, use predominantly muons from the decay of pions.

This interaction experiment has been undertaken for two main reasons. The first is to check the reproducibility of the results on the asymmetry obtained in experiment I. The second reason is to improve the statistical accuracy for the value of the asymmetry obtained for burst events. This chapter will give the details of the experimental run and the analysis of the results.

5.2 The scintillation counters

5.2.1 Modification of the counters

In order to increase the rate of bursts amongst the events triggering the instrument it is required to introduce an appropriate selection system. This has been achieved by modifying the scintillation counters in the spectrograph. The modifications were to fix two extra photomultipliers to

each scintillation counter. The pulses from these photomultipliers were then used to trigger the spectrograph only when a burst traversed the counter.

The modifications were applied only to the scintillation counters S1 and S3. The type of extra photomultipliers used is Mullard 56 AVP. This type is preferred because of its fast resolution and wider range of linearity. The dynode resistor chain connected to the base of each photomultiplier together with the head amplifier circuit is shown in figure 5.1. The E.H.T. to each photomultiplier can be varied by means of an arrangement of resistors, which is also shown in figure 5.1, connected to a stabilised high voltage power supply. Before fixing the photomultipliers to the counters the gain and the linearity of response of each tube was checked. This was achieved by placing them in turn in a light tight box and viewing the light pulses emitted by a light source, XP21 (this is a miniature gallium phosphide alloyed junction device which emits visible light with a fast rise and fall time, and is manufactured by Ferranti). First of all the focussing and the deflecting electrodes for the photomultiplier were adjusted such that maximum output pulse was observed for a given intensity of light incident on the photocathode. The photomultiplier in this case is in its optimum efficiency in collecting the photoelectrons emitted by the photocathode. The variation of the gain as a function of E.H.T. was measured by varying the E.H.T. on the photomultiplier and recording the corresponding pulse height observed on the oscilloscope. Figures 5.2 and 5.3 give the variation of the response with E.H.T. on the photomultipliers belonging to S1 and S3 respectively.

Although the dynode resistor chain used for each photomultiplier is that recommended by the manufacturer to give a good linearity in response to the variations in the intensity of light incident on the photocathode, the linearity of response of each photomultiplier was checked. Each photomultiplier was placed in the light tight box and run at its normal operating voltage. Variations in the intensity of light were obtained by putting

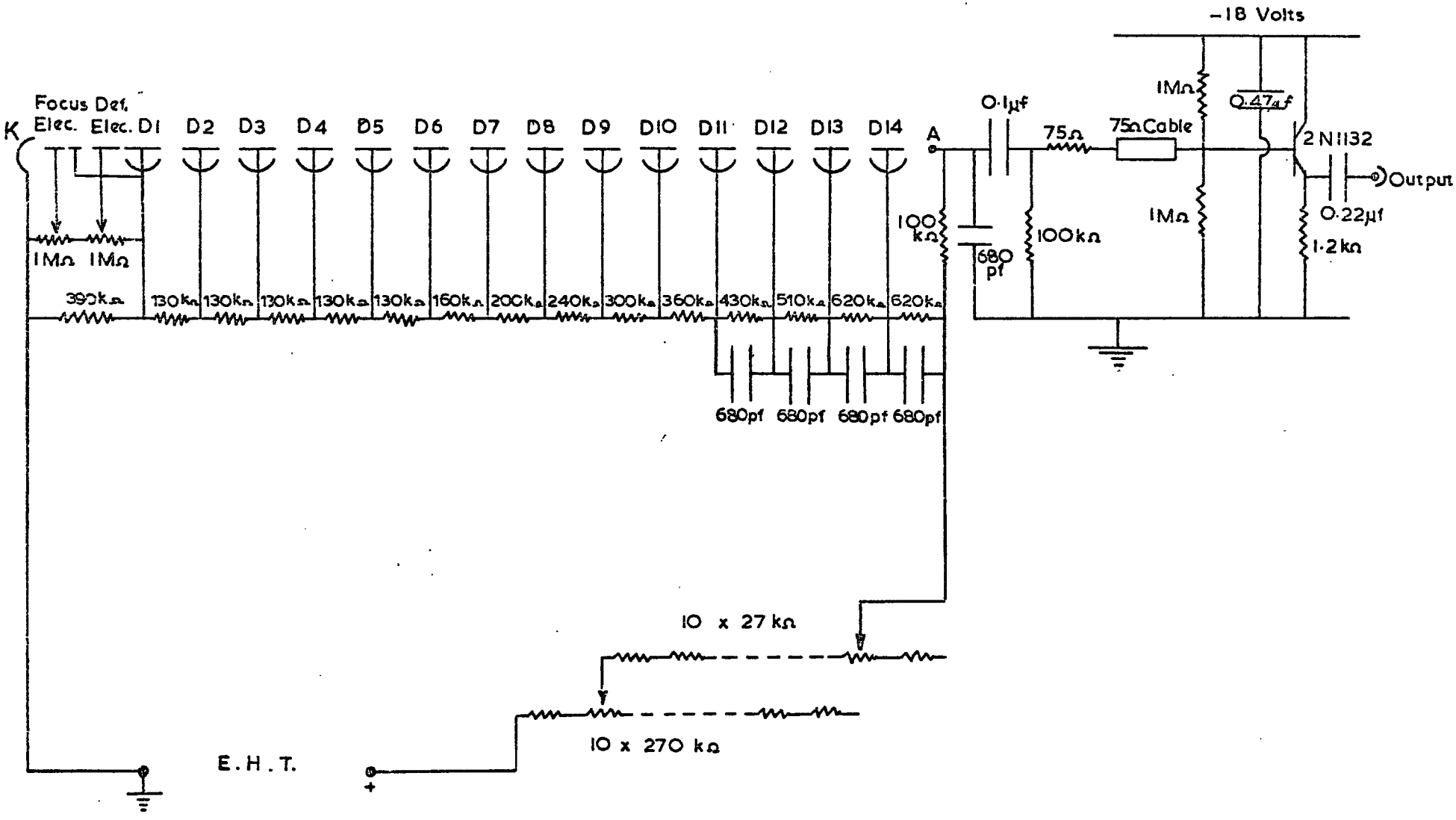

Figure 5.1 The dynode resistance chain for the photomultiplier base

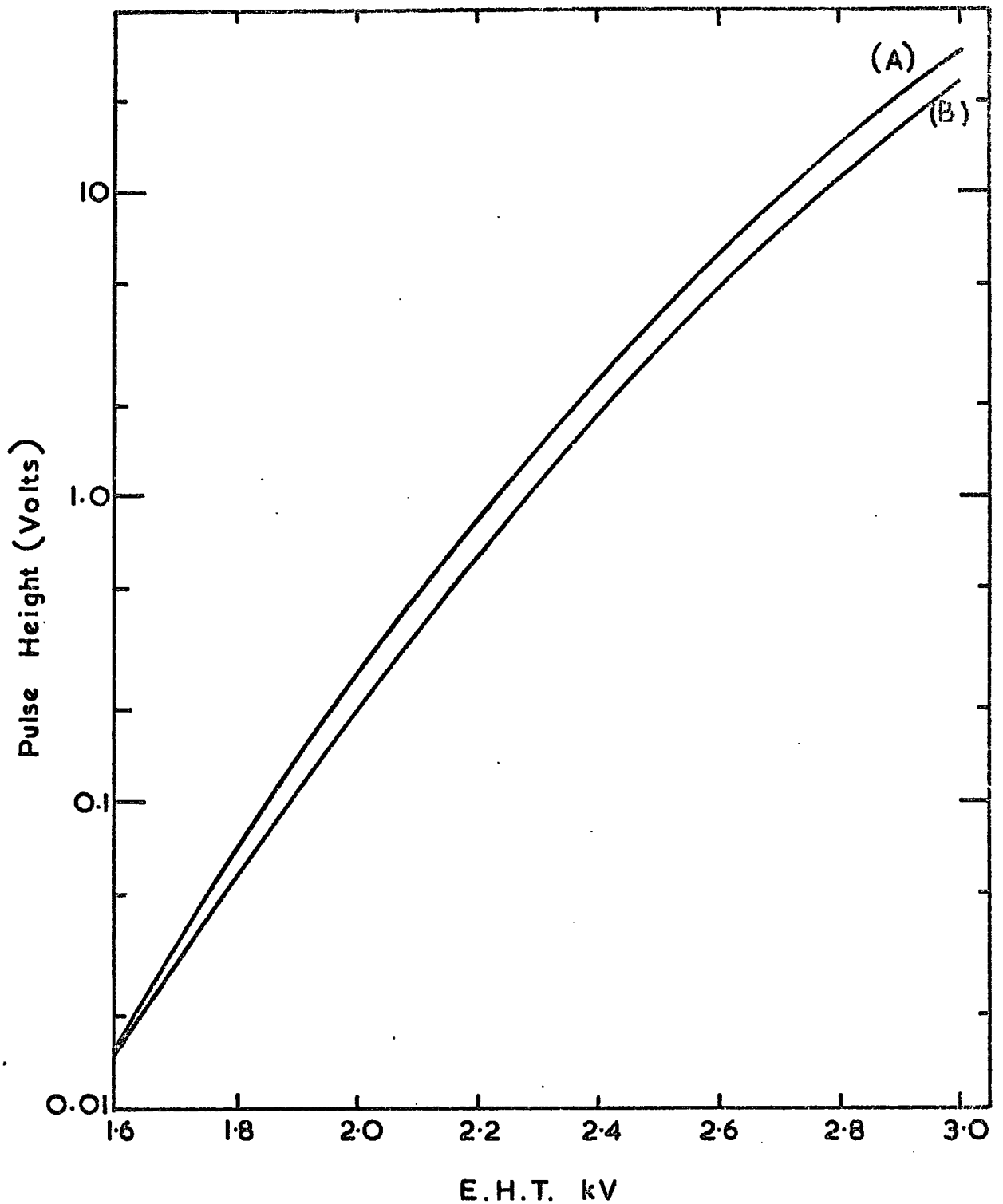

Figure 5.2 Variation of gain with E.H.T. for the two extra photomultipliers on S1

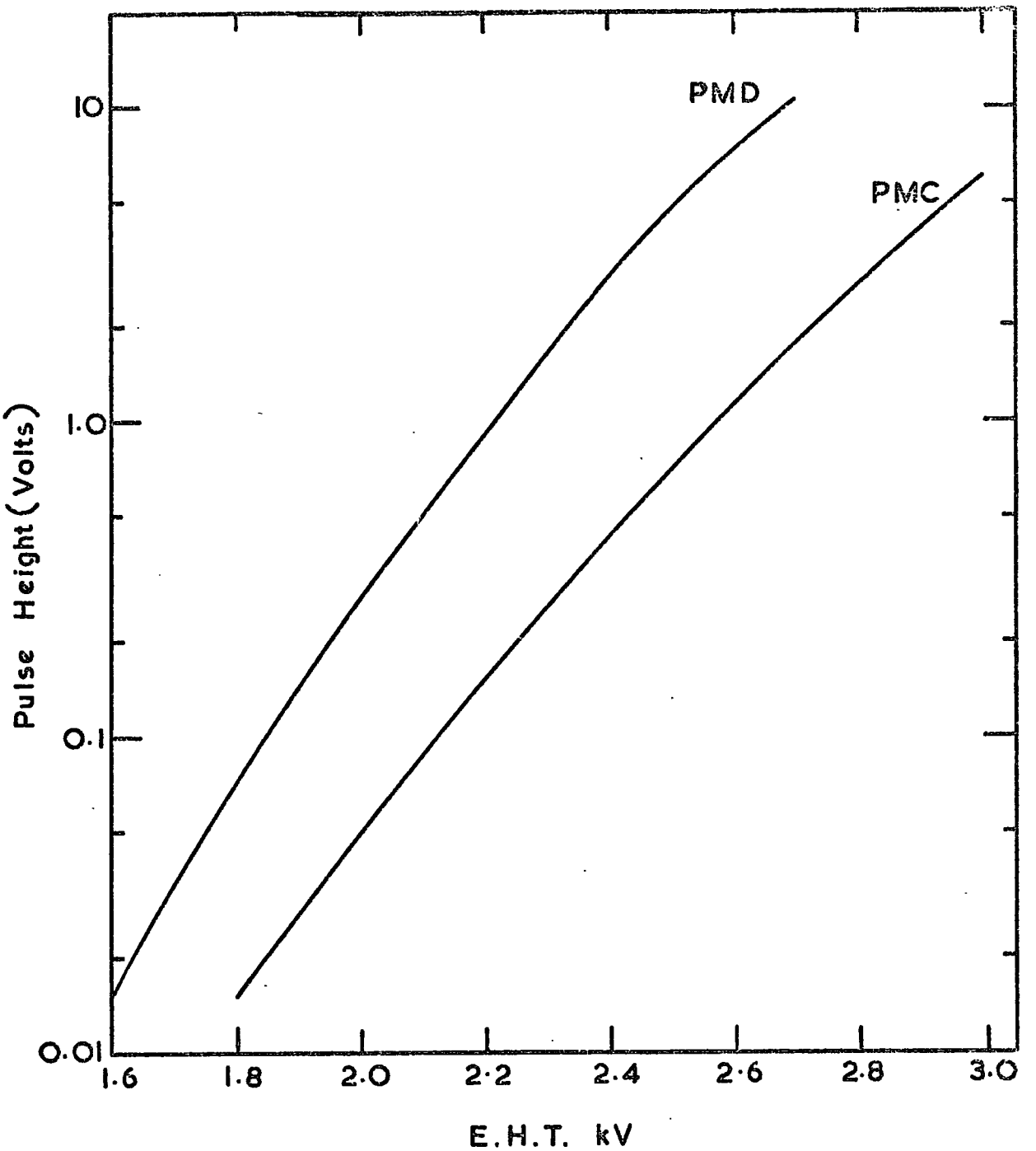

Figure 5.3 Variation of gain with E.H.T. for the two extra photomultipliers on S3

slides of film of variable transparency. The slides were calibrated first using a constant source of light and the Mullard ORP 60 photoresistor. By measuring the resistance of the cell for each slide, the intensity of light transmitted by each slide can be read off its characteristics curve. By normalizing these intensities to the smallest intensity between them, the relative transparency of each slide is obtained, which is independent of the light source. With the slides available the intensity could be varied over a range 100:1. The slides were then placed in turn between the photomultiplier and the light source and the output pulse height from the photomultiplier was measured. Measurements on each tube showed the pulse height to be proportional to the number of incident photons over the range of pulse height relevant to this experiment.

When the checks on the gain and linearity for all photomultipliers were finished, two photomultipliers were fixed on each scintillation counter (S1 and S3) in the positions shown in figure 5.4. Each photomultiplier was shielded from the magnetic field using the same arrangement as that described in Section 3.3.

5.2.2 Calibration of the counters

The scintillation counters were calibrated in their experimental positions in the spectrograph. The output pulse from each photomultiplier is fed to a head amplifier circuit with gain of unity. The output pulse from the head amplifier is then fed, for the two extra photomultipliers on each counter, to a linear adding circuit. Before adding the pulses the gains of the new photomultipliers on each counter were matched. This was achieved by selecting particles traversing the centre of the counter with the aid of two scintillator telescopes in the manner described in section 3.3.

After the gains of the photomultipliers were matched, the output from the adding circuit was used to study the uniformity of the counter along its

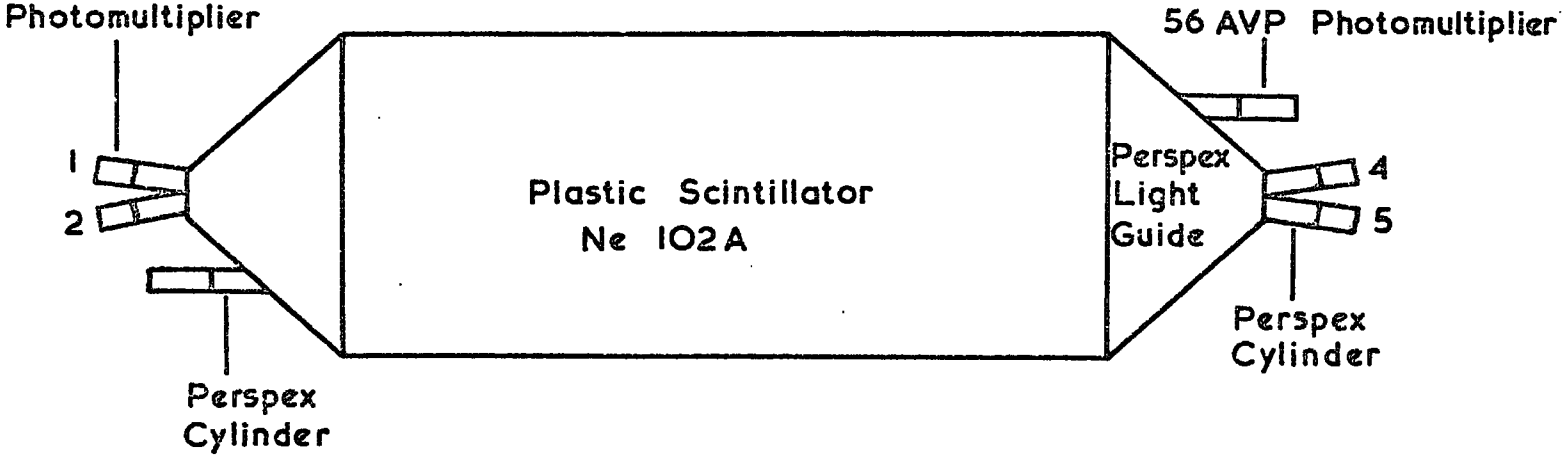

Figure 5.4 The modified scintillation counter in MARS

central axis using the method described in section 3.3. The result on the uniformity of the counter is given in figure 5.5. It can be seen that the curve is symmetric about the centre line of the counter and that the sensitivity increases outward towards the light guides. Therefore, for particles traversing the counter in the central region the pulse height will be less than the mean whilst for those particles traversing the phospher near to the photocathodes the pulse height will be higher than the mean. Thus the overall effect is for the pulse height distribution to be broadened about the most probable pulse height. The coefficient of variation in the uniformity of the counter is 24%.

The desired pulse height distribution for each counter is that due to a single vertical ionizing particle traversing the counter. The added pulse for each counter is fed to a linear inverter and then to a linear amplifier with variable gain. Considering S1 and S3 in turn the output pulse from the amplifier is fed to the P.H.A. and the P.H.A. is gated with the output pulse from the threefold coincidence. With this triggering mode vertical single ionizing particles traversing the counter were selected and a pulse height distribution, which is mostly due to vertical single vertical ionizing particle, was established for each counter. Since the scintillation counter is below the iron target, some of the counts obtained in the single particle distribution were due to pairs of particles, i.e. the muon plus a knock-on electron which has been produced in the target. However, their contribution to the single particle distribution is no more than 6% and therefore no corrections were applied. The pulse height distributions obtained for S1 and S3 are presented in figure 5.6. Each channel is equivalent to 3·5 mv.

5.3 Experimental conditions

5.3.1 Alignment of the spectrograph and the zero field run

Before running the red side of MARS to study the electromagnetic

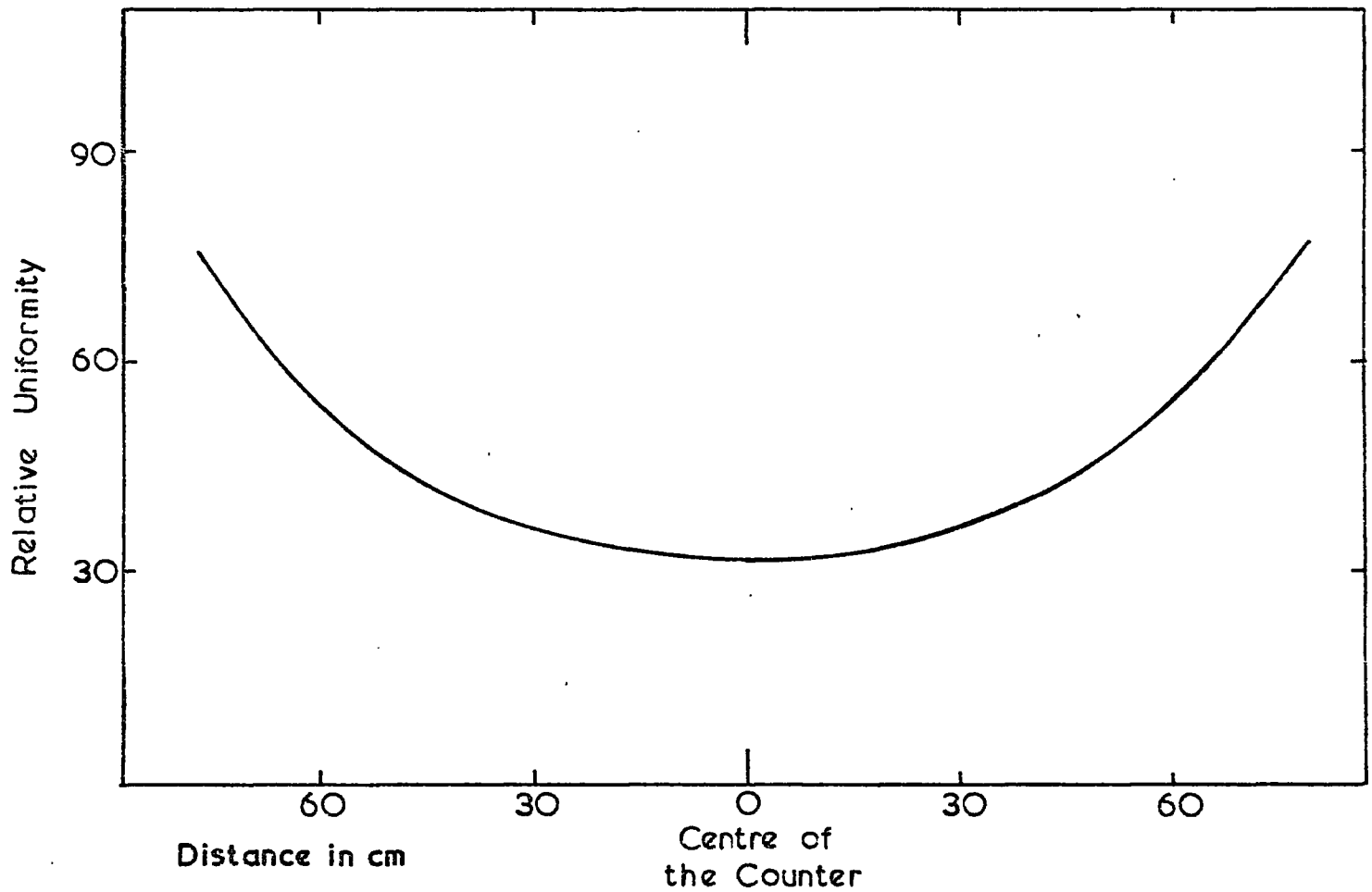

Figure 5.5 The response curve of the scintillation counter when using the added pulse from the new photomultipliers

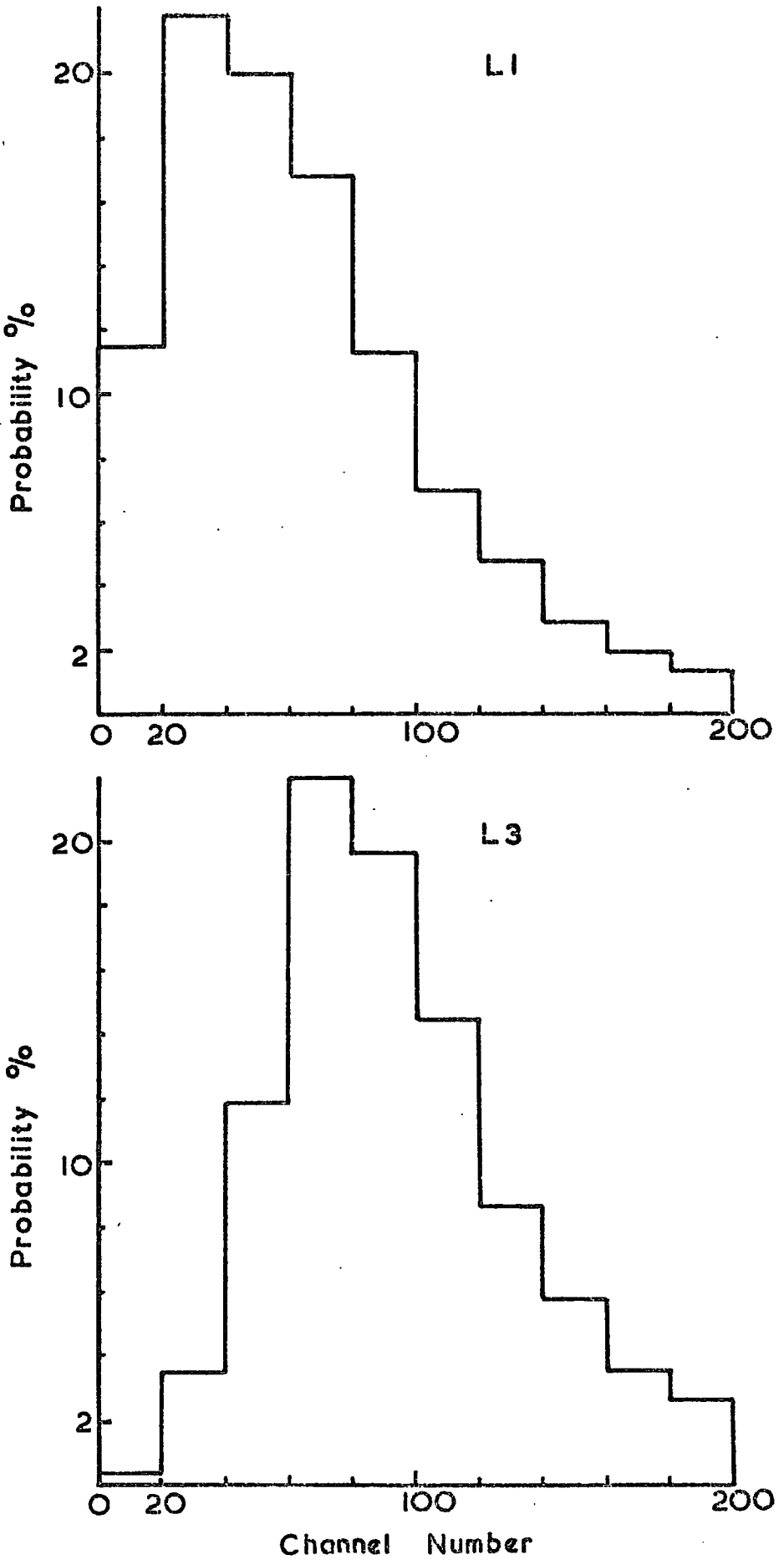

Figure 5.6 The pulse height distribution for vertical single ionizing particles traversing the red side of MARS.

interactions of cosmic ray muons, that side of the spectrograph, was aligned in the manner described in section 4.2.1. Also here, for more accurate location of the measuring tray positions, a zero field run was carried out in which single muons were used to trigger the instrument. The paralysis time used in this run was 13 sec which is longer than that used before (4 sec). The change was because it had been noticed that 4 sec was not long enough to get rid of all spurious flashes and therefore a longer paralysis time was to be preferred. The rate for single muon trigger is 4·0/min ± 1%. A total of 1000 events were photographed corresponding to a running time of about 4 hours.

5.3.2 Triggering mode

A block diagram of the electronics is shown in figure 5.7. The pulses from the new photomultipliers on S1 and S3 are fed to a linear adder circuit via a head amplifier. Considering the counters in turn, the output from the adder circuit is fed to a linear inverter whose output positive pulse is fed to a linear amplifier of adjustable gain. The amplifier output is fed to a discriminator. The output from each discriminator (one for each counter) is fed to a pulse shaper and the shaped outputs are fed into an 'OR' gate which gives an output when a negative pulse, at either inputs, arrives. The output from the 'OR' gate is fed to a coincidence gate with the output from the threefold coincidence. The output from the coincidence gate then represents the trigger pulse. One output is used to trigger the high voltage pulse for the flash tubes trays, another is fed to the cycling system and a third output is fed to a scaler to count the number of triggers. Another scaler is used to record the number of threefold coincidences (which is the same as the number of single muons traversing the spectrograph).

When a single particle traverses the spectrograph then triggering may or may not occur, depending on the settings of the discriminators for S1 and S3. If either discriminator level is low then triggering occurs when single

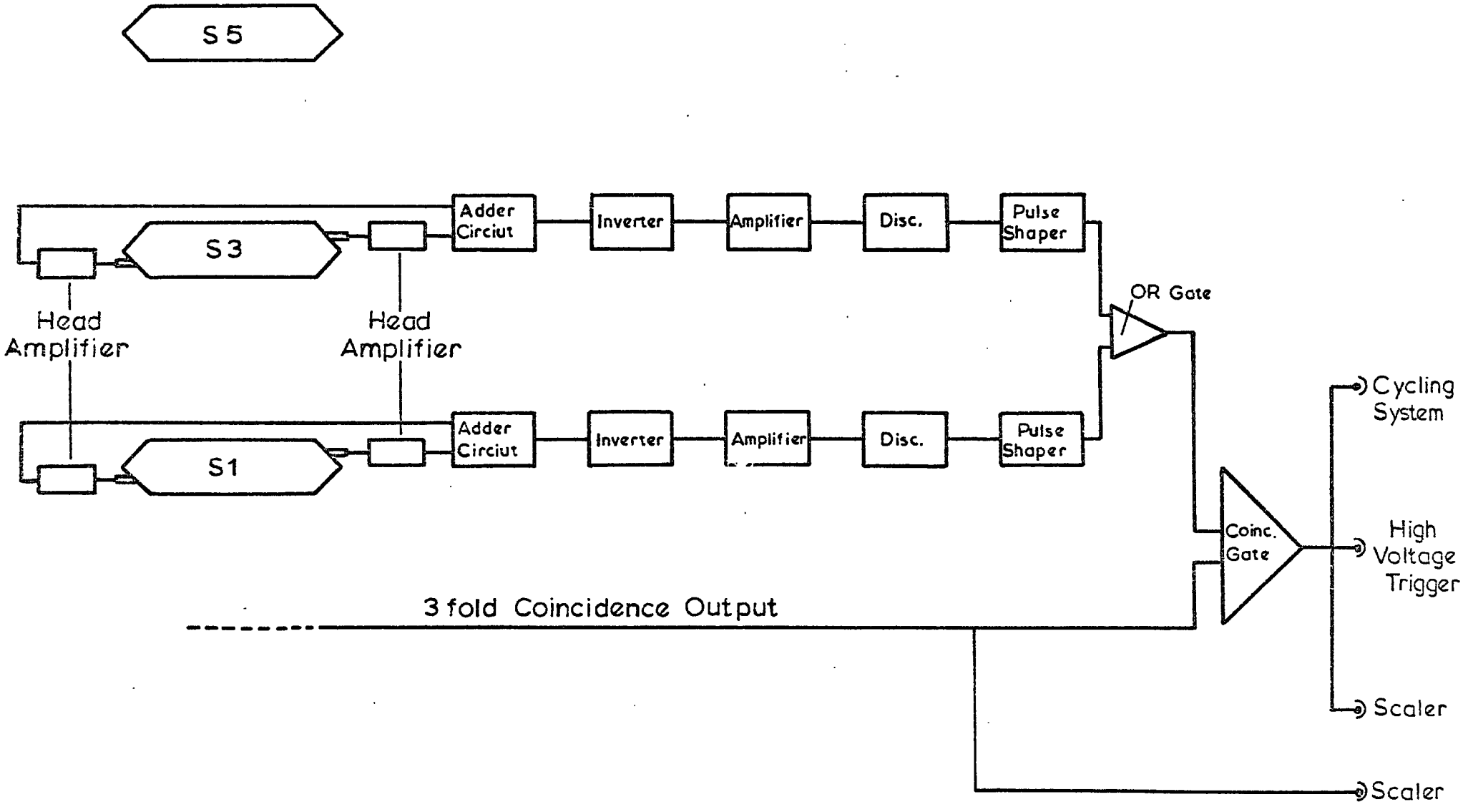

Figure 5.7 Block diagram of the electronics

particles traverse the spectrograph. However, if both discriminators are high (say equivalent to 3 or more particles) then, in most cases, triggering will occur only when the traversing particle undergoes an interaction in one or other of the magnet blocks above levels 1 and 3. With this sort of triggering requirement one can enhance the number of interaction events photographed and therefore the majority of the scanned events will be useful for interaction studies. Triggering can also occur when an extensive air shower or side shower falls on the spectrograph.

5.3.3 The field run

(A) The charge ratio run

The charge ratio of the muons is required for investigating the interaction asymmetry. Therefore a charge ratio run was carried out. The discriminator settings were turned down to accept single particles traversing the spectrograph. Every event was photographed and a paralysis time of 13 sec was used. The field direction was reversed and equal running time was obtained for each field direction. The total number of events photographed was about 4000.

(B) The interaction run

The discriminator setting selected for the interaction run must make a compromise between the single muon rate, the number of EAS and, most important, the rate of interaction events. The interaction events obtained with low discriminator settings are mostly single knock-on events with a few small bursts. Very high settings for the discriminators will have very few single muons but will also lose many of the smaller useful bursts. Also with high settings the rate of EAS events will be comparable with the rate of interaction events. Therefore, before the actual experimental run various discriminator settings were tried and the corresponding films were studied. The decision was to

select the discriminator setting which corresponds to the peak of the six-particle distribution, defined as 6 x the peak position of the single particle distribution (the distributions for single particles are given in figure 5.6). Accordingly each discriminator was set to the peak of 6-particles distribution in the following manner. Considering S1 and S3 in turn, a pulse generator was used to give an RC pulse similar to that obtained from the counter. Two identical outputs are taken from the pulse generator. One output was fed to the P.H.A., the other to the discriminator. The height of the pulse from the pulse generator was varied until the P.H.A. start counting exactly in the channel corresponding to the peak of the 6-particles distribution. The pulse generator output was then left unchanged and the output from the discriminator was used to gate the P.H.A. The discriminator level was then varied until the P.H.A. was about to stop counting. That discriminator setting was taken to represent the peak of the 6-particles distribution.

With both discriminator levels set to the required position, the experiment is ready to run for interaction studies. Because of the low rate of trigger ($\sim$ 12/hour) and the low probability of one interaction event occurring immediately after another ($< 1\%$), the experiment was run without paralysis. The triggering requirement was thus to have a burst in level 1 or level 3. The numbers of triggers and single muons traversing the spectrograph were recorded for each run. This enables a constant check on the operation of the instrument and is also useful in evaluating the absolute value of the interaction probability.

The main experimental run was from December 1971 to February 1972. The field direction was reversed every 24 hours and equal running time was obtained for each field direction. The total number of events photographed was 7733 in a useful running time of 637 hours.

5.4 Data analysis

The photographed events for the zero field run were scanned and analysed using the technique described in section 4.3. Only single muon events were scanned in this case (single muon events are defined in the manner given in section 4.3.2) and the results of the analysis gave an m.d.m. of at least 500 GeV/c, which was regarded as adequate for the present investigations.

The charge ratio films were scanned using the same projection system. The decision on the sign of the muon was taken by visualising its bending in the magnetic field. It is easy to decide, in most of the events, on the sign of the muon because the majority of the events are low energy muons and therefore bent considerably in the magnetic field. For example, a 100 GeV muon traversing the spectrograph suffers a deflection of $\sim$ 4 cm. Only when the event is due to very high energy muon (say $>$ 400 GeV) is it difficult to decide on the sign of the event. However, the rate of these events is very small (about 1/hour) and so any mistake on their sign will not affect the integral value of the charge ratio. Only an integral value of the charge ratio was obtained, because producing a charge ratio as a function of momentum needs very many events. In fact such data are not required because they have been produced in another experiment (Ayre et al., 1972) and all that is necessary is to check that the instrument gives the correct integral value. The integral value for the charge ratio obtained in our experiment was $1{\cdot}30 \pm 0{\cdot}04$. This is in a good agreement with the value obtained in experiment I ($1{\cdot}30 \pm 0{\cdot}03$) and is not inconsistent with the value of $1{\cdot}284 \pm 0{\cdot}004$ found by Ayre et al. (1972).

For the interaction run events the classification of events adopted is the same as that mentioned in section 4.3.2. However, two additional types of events were observed. One type is a multiple interaction event in which two or more trays exhibit interactions. This sort of event is either a multiple burst event or a mixture of burst and knock-on (knock-on and burst are defined

in the same way as given in 4.3.2). Because of the high discriminator level, the mean energy of the muons triggering the spectrograph is about twice that in interaction experiment I, which in turn enhances the probability of multiple interactions. The total number of multiple events observed in 2950 events scanned is 437. The other type of event observed in experiment II, which had not been observed in experiment I, showed multiple penetrating particles. By that is meant more than one muon traversing the spectrograph simultaneously. In some cases the penetrating particles are associated with an extensive air shower in tray 5. However, in most of the cases where only clean tracks are observed, at least one of the penetrating particles undergoes an interaction in the spectrograph. The number of such events observed is 12 in 7×10^5 single muon traversals. These penetrating muons are likely to be the remainder of small air showers whose electrons members have been absorbed in the atmosphere before reaching the spectrograph. They could in principle have also come from pair production of muons by muons, but the contribution from this process is thought to be very small due to its extremely small cross section in air. Typical events are presented in the plates 5.1 to 5.3.

Two types of film scanning were adopted. The first type is identical to that used in interaction experiment I (described in section 4.3). The second type is similar to the first one insofar as the projection system and the diagrams of the trays are concerned, but different in the method used to measure the position of the muon track in each tray. In the second method the scanner himself decides on the position of the muon track in the tray. He fits the best straight line to the track in the tray by means of a cursor whose intersection with the scale on the tray is read off and is taken to represent the position of the track in the tray. An independent computer programme was developed to find the momentum and the sign of the muon using the method of parabola fit.

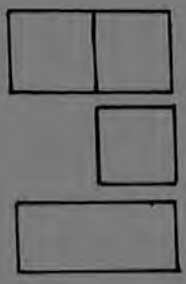

Plate 5.1

A Multiple Interaction Event

(i.e. Three bursts event)

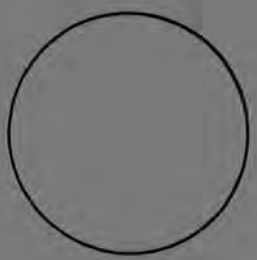

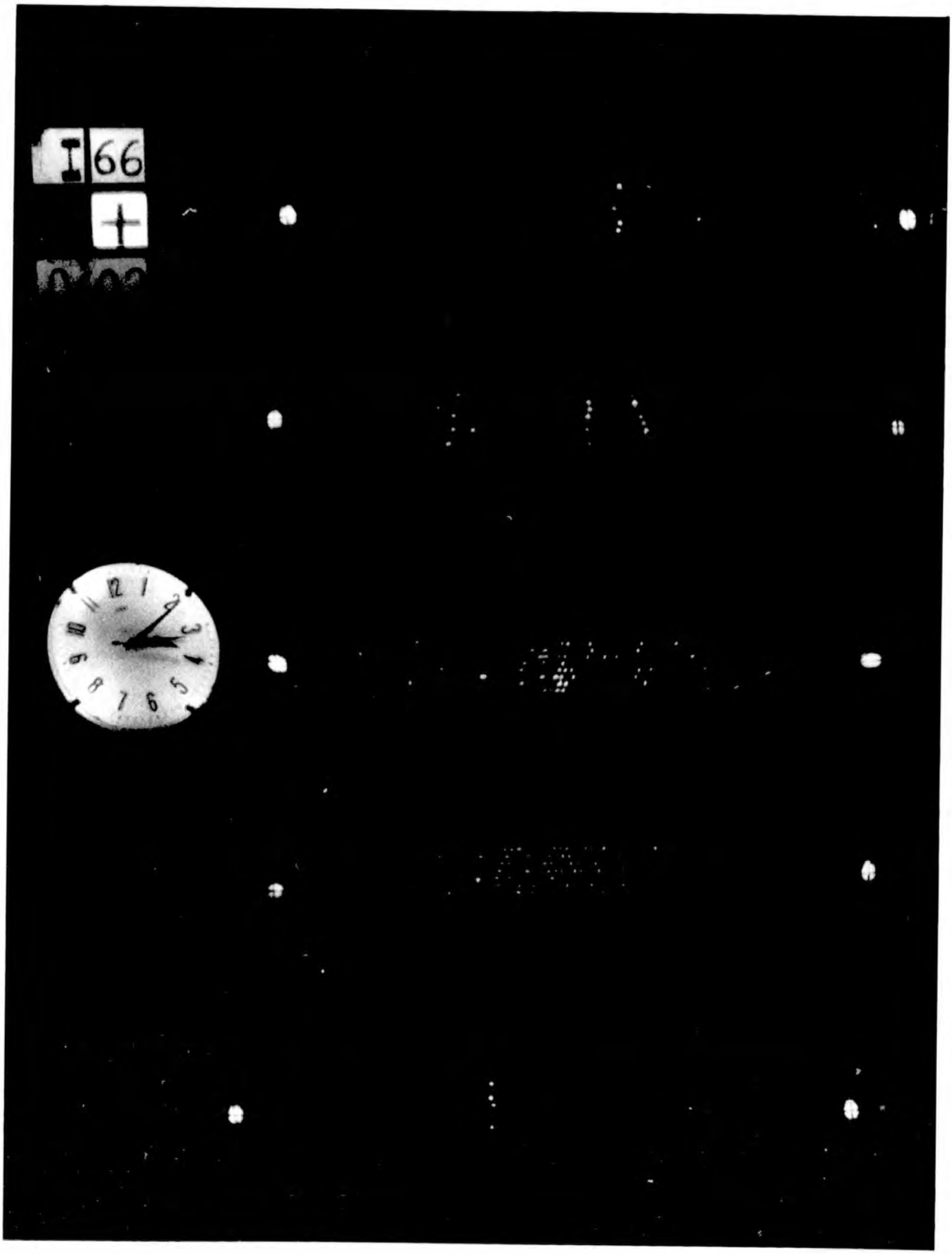
I66

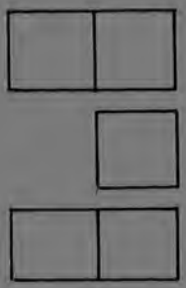

Plate 5.2

A Multiple Interaction Event

(i.e. One burst and two single

Knock-on Electron Event)

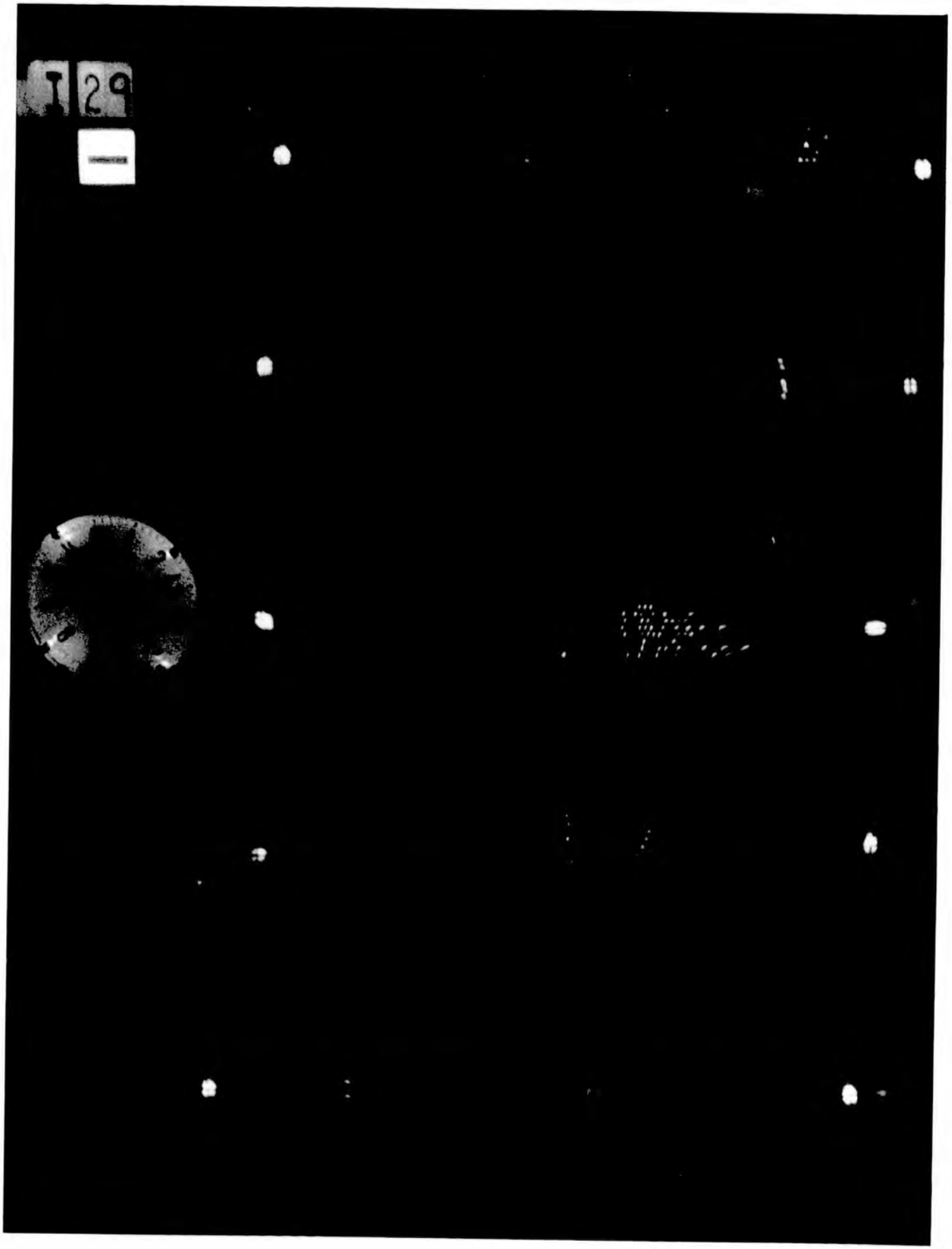

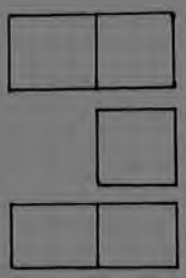

Plate 5.3

Two Muons Penetrating MARS

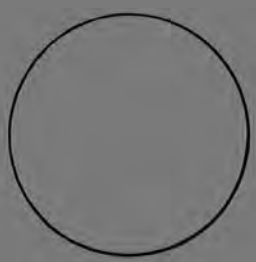

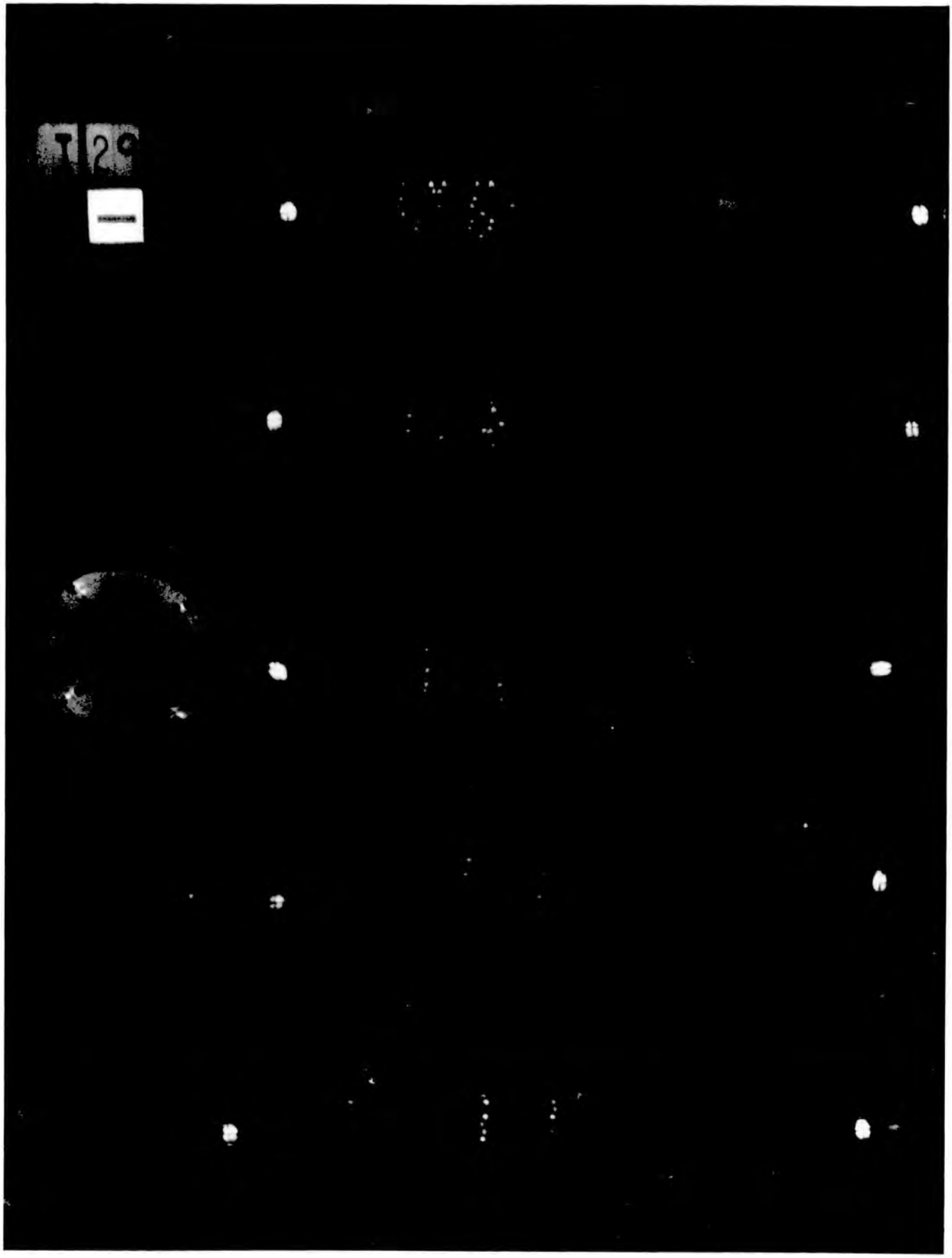

Both methods have been used independently to scan the same events. This was carried out for about 1000 events and then the sign and momentum for each event was compared. Good agreement was found between the two methods, in particular, no difference was observed in the sign of the muon. The reason for adopting two independent methods in determining the sign and momentum of the muon is to make quite sure of the validity of the results.

In scanning the films the selection criteria used were similar to those used in experiment I (section 4.3.4), the only difference being that single muon events were also scanned. These events were included because they may correspond to knock-on or small burst events where the secondaries are absorbed in the absorber on top of the measuring trays (the momentum selector and the scintillation counter in level 1 and 3). For each interaction event the pattern of the flashes was drawn. The method used in estimating the burst size of each event was identical to that used for interaction experiment I (section 4.3.4).

5.5 Charge asymmetry in muon interactions

5.5.1 Introduction

In this experiment (biased run) the total number of events scanned and analysed is 2950, this number being obtained from an effective running time of 350 hours. Events due to extensive air showers and side showers have been rejected from the analysis. Out of the 2950 scanned events 217 are single muons, 636 are single knock-on electrons and 2097 are burst events. It can be seen that about 70% of the analysed events are bursts.

The number of single knock-on electron events in this run is considerably less than that obtained in the unbiased run, therefore the value of the asymmetry obtained for these events in this experiment can only be considered as a rough check on that obtained in the previous run. The single muon events are very few and even if they do in fact correspond to interactions, including

them in the analysis will have a negligible affect on the value of the asymmetry

The energy transfers involved in this experiment extend to higher values than encountered in the previous one simply because of the longer duration of the experiment. It is estimated that the mean energy transfer is about 4 GeV. Therefore, in this experiment, too, the dominant interaction is the knock-on process.

The method used in analysing the data is identical to that used previously (section 4.4), that is using the number of flashes associated with each event. As mentioned before an event was accepted as a 'burst' if it had 15 or more flashes in one of the measuring trays, events with less than 15 but more than 6 flashes were considered to be single knock-on electron events . The information on momentum, sign and number of flashes in the interaction form the basic data for analysis.

5.5.2 Results

The interaction asymmetry, η , is defined in the manner given in section 4.4.2. In the asymmetry analysis the events were divided according to the sign of the associated muon. The overall value of the asymmetry obtained by comparing the overall interaction events for μ^+ with the overall interaction events for μ^- corrected by the charge ratio ($R = 1{\cdot}30 \pm 0{\cdot}04$) is $1{\cdot}04 \pm 0{\cdot}048$, this is to be compared with the value $1{\cdot}05 \pm 0{\cdot}04$ obtained in experiment I. The agreement is quite good. There appears to be no significant deviation from the theoretical prediction (unity) when if the single knock-on events are separated from burst events, the integral value obtained for the asymmetry in the two processes is $0{\cdot}99 \pm 0{\cdot}10$ and $1{\cdot}08 \pm 0{\cdot}06$ respectively. The value of the asymmetry for single knock-on electrons is consistent with that obtained in experiment I and it is in good agreement with the predicted value of unity.

The asymmetry obtained for burst production is statistically a factor of

two better in accuracy than that reported for experiment I. Although it is not inconsistent with unity, it is not inconsistent with there being a small asymmetry, although not as high as that given by Kotzer et al. (1965).

The asymmetry as a function of number of flashes, N_f, has been investigated. The interaction events for μ^+ and μ^- have been divided into cells of number of flashes associated with each event. The differential spectrum of the asymmetry as a function of number of flashes is presented in figure 5.8. As has been noted already, there seems to be no asymmetry for events with low number of flashes (single knock-ons), $\bar{N}_f = 11$. On the other hand quite a big asymmetry can not be ruled out for events with $\bar{N}_f = 20$. These events correspond to small bursts with energy transfer around 1 GeV. At higher values of N_f ($\bar{N}_f = 60$) there is no suggestion at all of an asymmetry. However, within the statistical accuracy of the data, there is no evidence against (or for) an asymmetry which increases with increasing energy transfer. The effect on the asymmetry caused by different celling of the data in terms of N_f is given in figure 5.9. It is clear that the data for different celling are consistent with each other and that what obtained in figure 5.8 is not due to a bias caused by one method of celling and not by another.

The dependence of the asymmetry for burst events on muon energy has also been investigated. The results are given in figure 5.10. Within the statistical errors, there is no dramatic change of the asymmetry with muon energy, a feature that had already been observed in the previous experiment. Although the mean values for the asymmetry, for muon energy < 100 GeV where knock-on process is dominant, are above unity, the difference from unity is again not statistically significant.

Kotzer et al. (1965) and Allkofer et al. (1971) reported that their results on the asymmetry suggests a decreasing asymmetry with increasing fractional energy transfer, with an asymmetry below unity close to the maximum transferable energy. The maximum value for the asymmetry was observed for

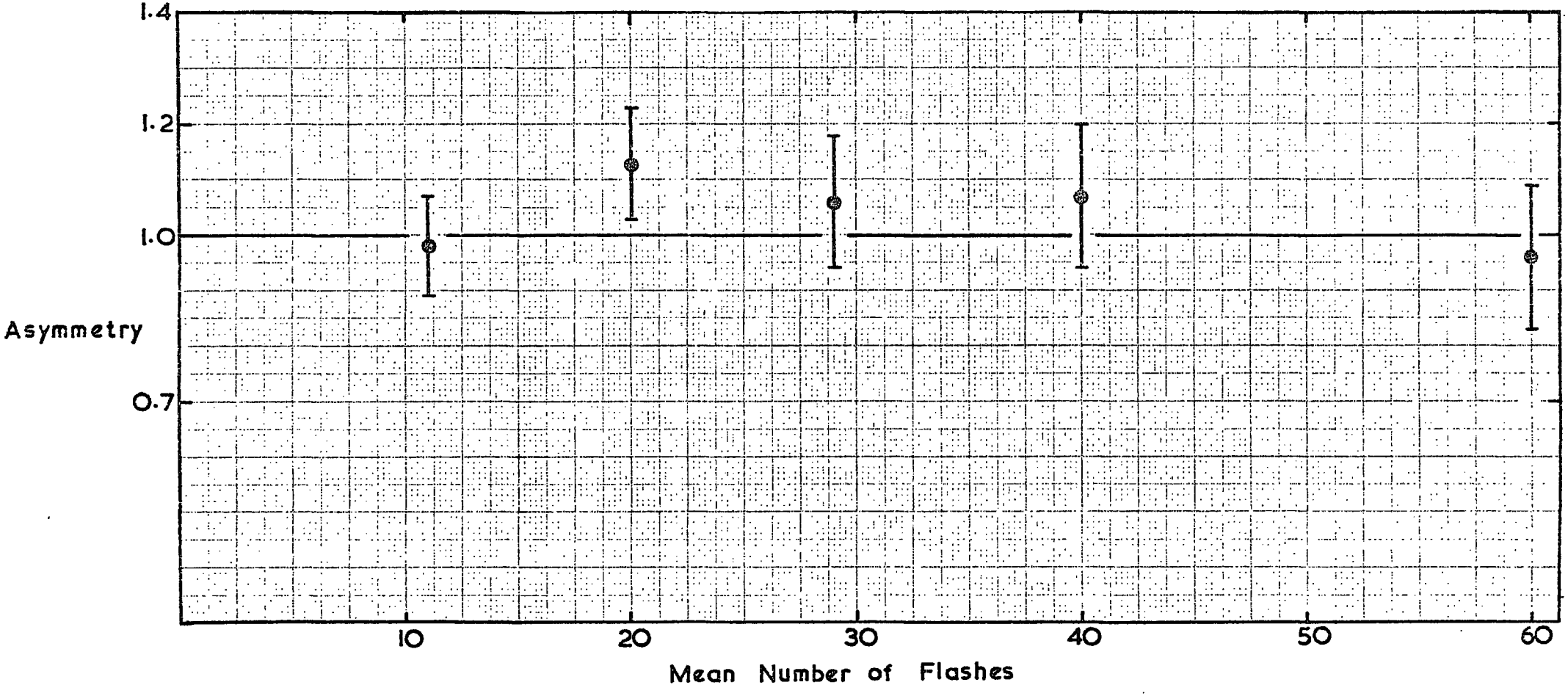

Figure 5.8 The differential spectrum of the asymmetry as a function of number of flashes

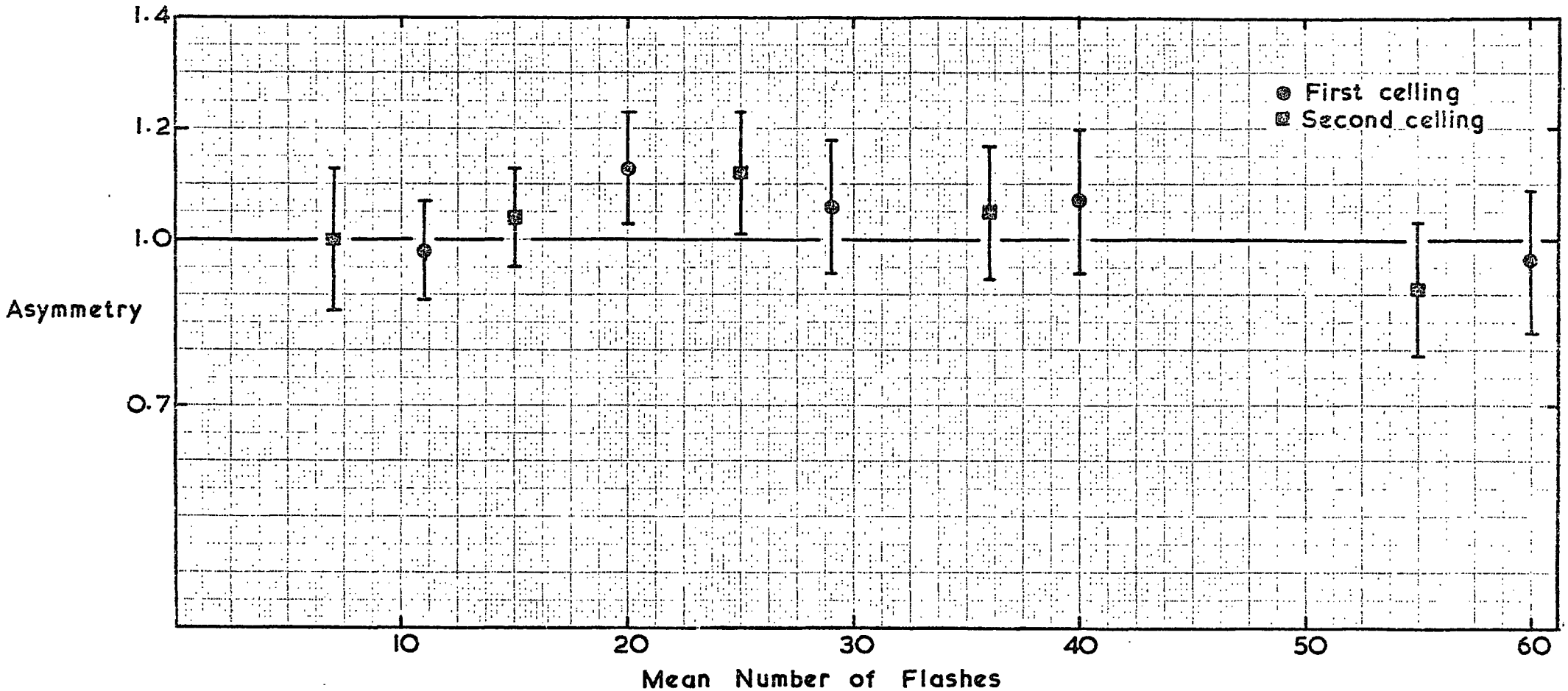

Figure 5.9 The dependence of the asymmetry on different celling for the data

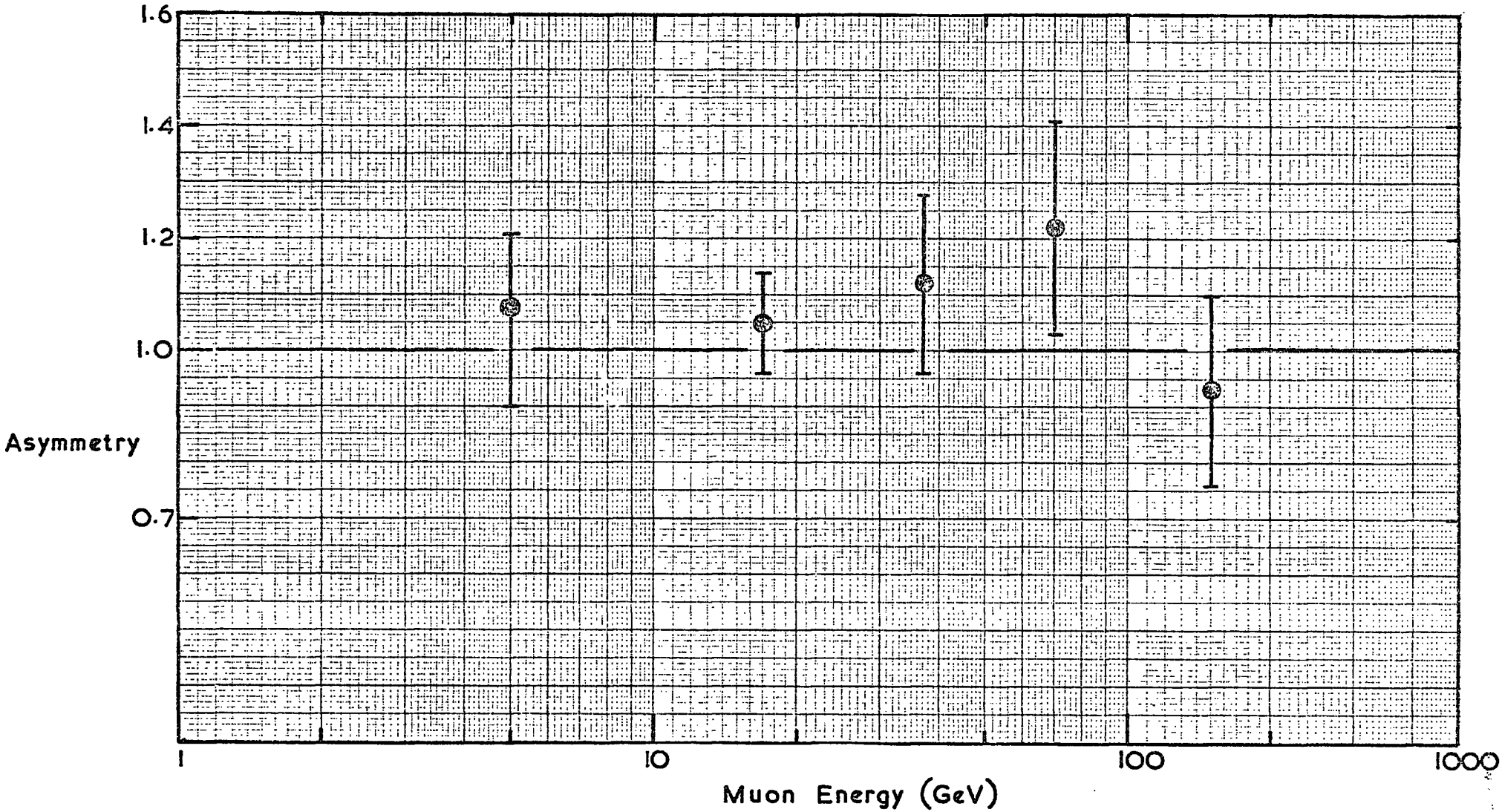

Figure 5.10 The asymmetry as a function of muon energy at interaction

small and medium energy transfers. Therefore, the data of this experiment have been analysed to investigate this effect. Since N_f is approximately proportional with energy transfer, N_f/E_μ is a quantity which is approximately proportional to the fractional energy transfer. In figure 5.11 the asymmetry is plotted against N_f/E_μ. Although the number of events in this work is at least a factor of two greater than that of Kotzer et al. (1965) and Allkofer et al. (1971), it is difficult to make any conclusion for or against their suggestion. It is true that the asymmetry at $N_f/E_\mu = 3$ is higher than at values of N_f/E_μ in both sides, but statistically it is consistent with the rest and indeed with unity. All that one can say is that within the statistical accuracy there is no evidence for significant asymmetry. In figure 5.11 a very approximate scale for fractional energy transfer is given.

It was mentioned earlier that a number of multiple interaction events had been observed. If the asymmetry is real, one would expect an increased effect amongst multiple events. Unfortunately the statistical accuracy is not good, the total number of double and triple interaction events observed being only 413 and 21 respectively. The double interaction events were divided into 'small' (N_{f1}, $N_{f2} < 15$), 'medium' ($15 \leq N_{f1}$, $N_{f2} \leq 35$) and 'large' (N_{f1}, $N_{f2} > 35$). If it is true that the asymmetry is confined to small burst events then one would expect a bigger asymmetry for 'medium' double events. The values of the asymmetry obtained for small, medium and large double burst events are 0.96 ± 0.25, 1.18 ± 0.35 and 0.77 ± 0.72 respectively. It can be seen that the asymmetry for medium double burst events is indeed higher than the rest, but once more the statistical accuracy is not adequate and all three values agree with each other within one standard deviation, therefore the difference could be due to statistical fluctuations. The asymmetry obtained for the triple interaction events, considering events

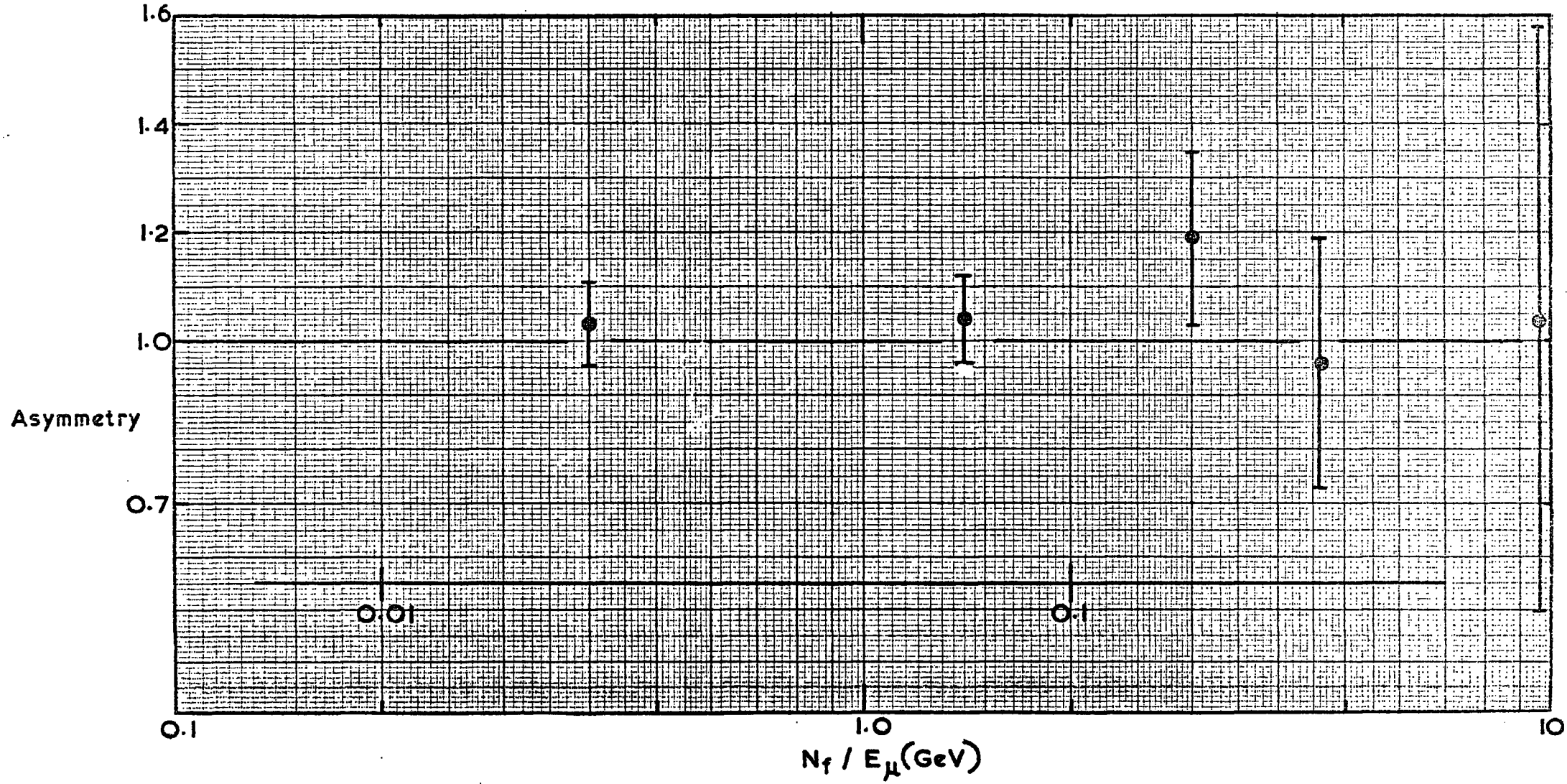

Figure 5.11 The dependence of the asymmetry on the ratio N_f/E_μ. An approximate fractional energy transfer is given

with N_{f1}, $N_{f2} \geq 8$ is $1{\cdot}25 \pm 0{\cdot}54$. If only events with N_{f1}, $N_{f2} \geq 10$ flashes are considered then the value of the asymmetry drops below unity.

Only three events with four interactions were observed in a total of 2950 event scanned. The average number of flashes for these events is 18. All three events were induced by positive muons.

5.6 Conclusion

The results obtained for the asymmetry in interaction experiment II is in a good agreement with that obtained in interaction experiment I (a detailed comparison between the results of the two experiments is given in the next chapter), which confirms the reproducibility of our results. All the results firmly suggest no asymmetry for single knock-on electron production (correspond to some tens of MeV in energy transfer) which is in agreement with the theoretical prediction. The integral value of the asymmetry obtained for bursts production ($1{\cdot}08 \pm 0{\cdot}06$) is statistically the most accurate reported so far. This value, is in agreement with unity, (the probability of being consistent with unity is 77%), although it can not rule out the possibility of a small asymmetry ($\sim 10\%$), especially in the region of energy transfer around 1 GeV (where N_f is ~ 20). If there is really a small asymmetry then the statistical accuracy needed to establish it is of the order of 1%. Only then will a firm conclusion about the asymmetry and its dependence on muon energy and energy transfer be possible.

CHAPTER 6

COMBINED RESULTS ON THE INTERACTION ASYMMETRY

6.1 Introduction

The object of this chapter is to give a direct comparison of the results of the interaction experiments of the present work and to examine their consistency. Also given are more details of the experiments mentioned in Chapter 2. Finally, a direct comparison between the results from all the experiments on the interaction asymmetry is presented.

6.2 Comparison of results for interaction experiments I and II

The main results from the two interaction experiments are the dependence of the asymmetry on muon energy and on energy transfer. The method of analysis used in both experiments are identical and therefore the results are directly comparable. The comparison is presented in figures 6.1 and 6.2. Figure 6.1 compares the dependence of the asymmetry on muon energy and Figure 6.2 compares that on energy transfer.

Consider figure 6.1. The comparison is carried out for burst events (i.e. events with $N_f \geqslant 15$). As can be seen, the agreement between the two experiments is quite good and, within the statistical errors, they both suggest no appreciable dependence of the asymmetry on the muon energy for the range of muon energies covered (6 - 200 GeV). It is interesting to note that the mean values are above unity, although the difference from unity is not statistically significant. The integral values of the asymmetry for burst events, presented in figure 6.1 , for experiments I and II are respectively $1{\cdot}12 \pm 0{\cdot}12$ and $1{\cdot}08 \pm 0{\cdot}06$. The two values are in good agreement with each other and the statistical accuracy for the value obtained from experiment II is much better in view of the greater number of detected events.

Consider figure 6.2, where the dependence of the asymmetry on energy transfer is presented. It can be seen that the agreement between the two

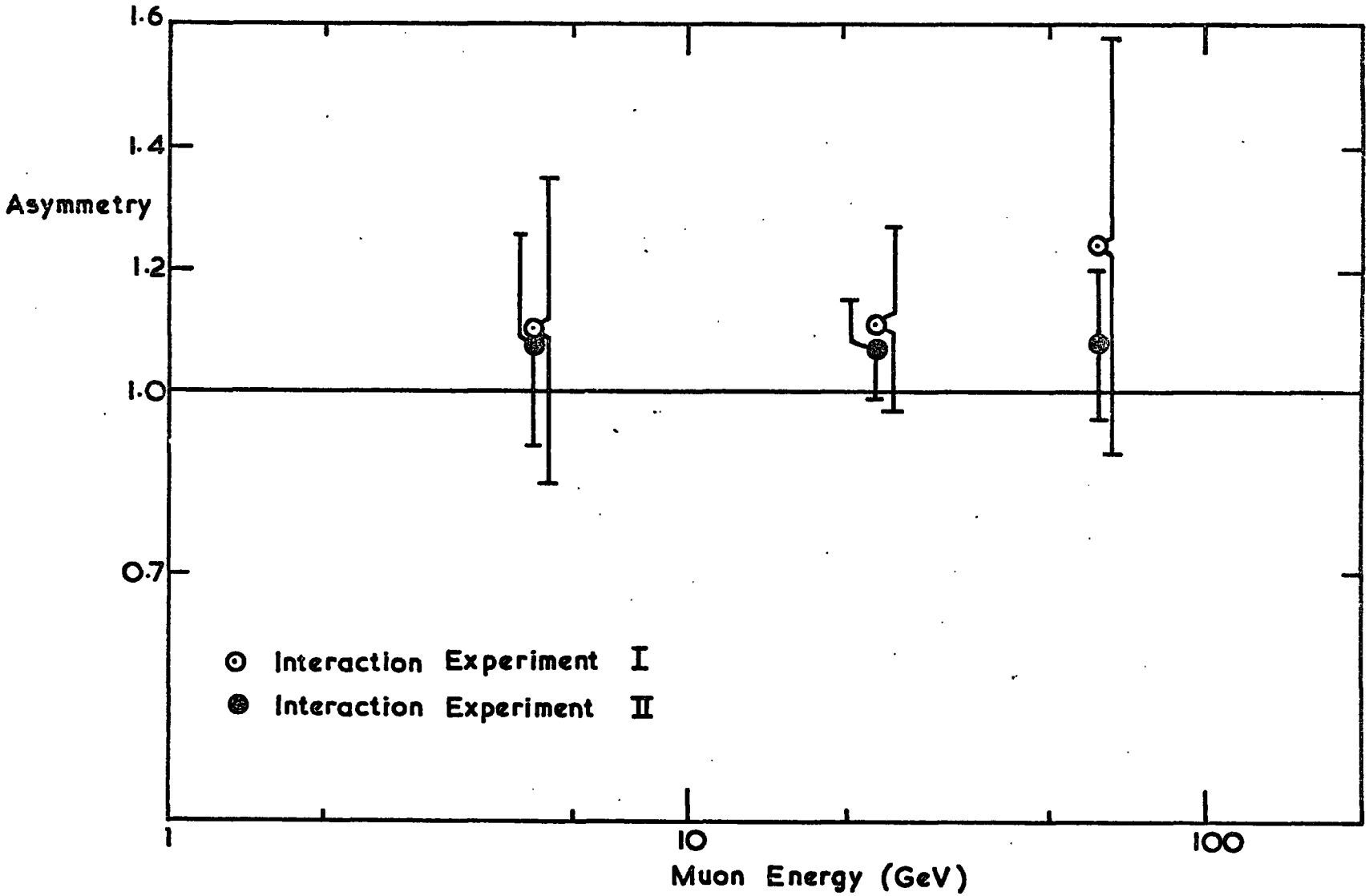

Figure 6.1 Comparison of the asymmetry as a function of muon energy for interaction experiments I and II

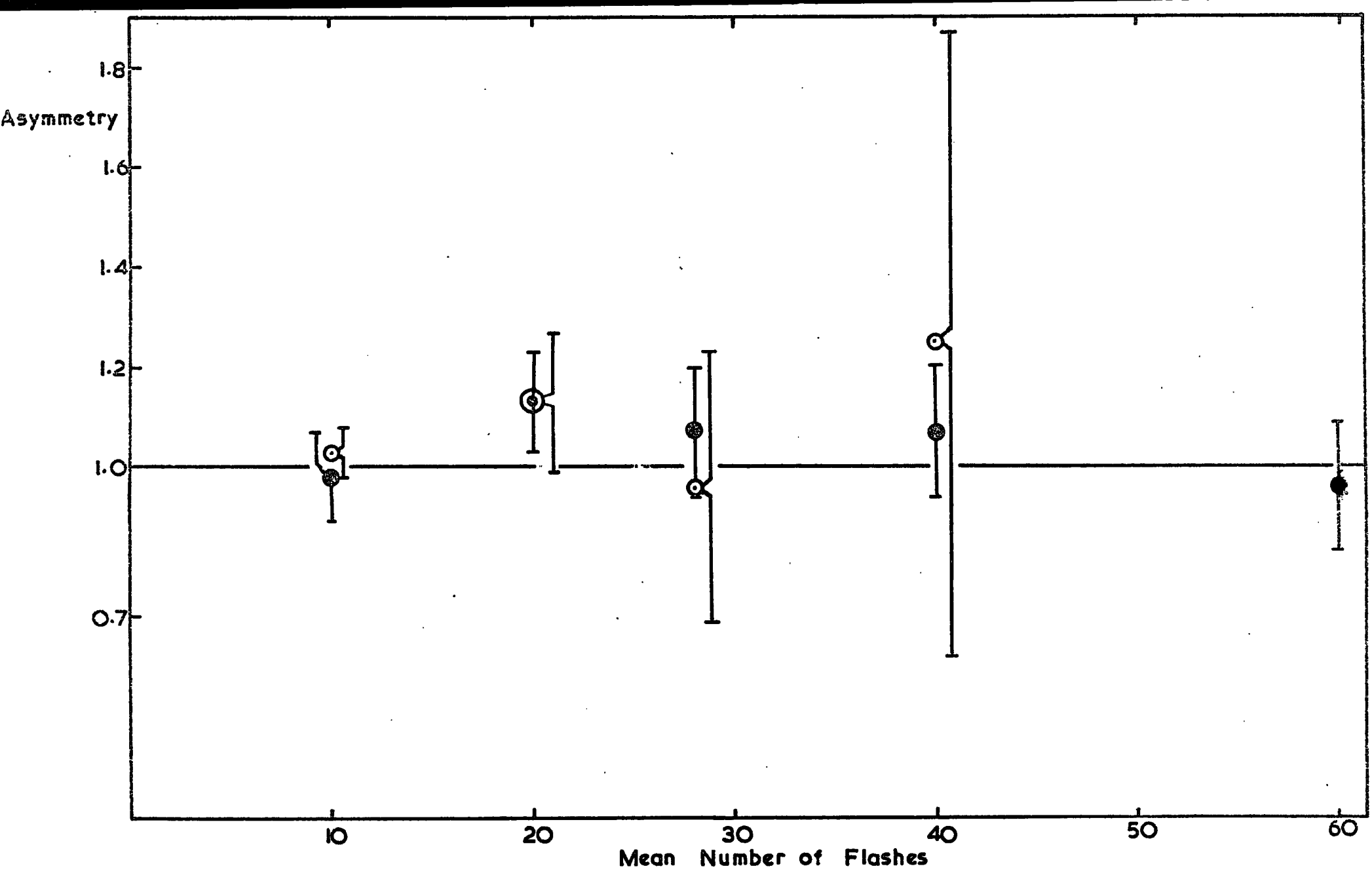

Figure 6.2 Comparison of the asymmetry as a function of number of flashes for interaction experiments I and II

experiments is quite good. Both experiments are consistent with there being no asymmetry for single electron production ($\bar{N}_f$ = 10, equivalent to some tens of MeV in energy transfer), the asymmetry values given by experiments I and II are respectively 1·03 ± 0·053 and 0·99 ± 0·10. For large bursts there seem to be no asymmetry too and again the statistical accuracy of experiment II is much better. Neither experiment is inconsistent with there being a small asymmetry ($\sim$ 10%) for events with energy transfer around 1 GeV or so ($N_f \sim 20$), but whether this asymmetry is real or is due simply to a statistical fluctuation is very difficult to say. It is regarded that the agreement with theory for energy transfer around 1 GeV is satisfactory and is excellent for low and high energy transfers. These results hold under different celling of the data.

The overall values for the asymmetry obtained in experiments I and II are, respectively, 1·05 ± 0·04 and 1·04 ± 0·048 in excellent agreement with each other.

6.3 Results from previous cosmic ray experiments

6.3.1 Kotzer and Neddermeyer (1965, 1967)

This experiment, which was originally set up to investigate the production probabilities of knock-on electrons by cosmic ray muons, was used afterwards to study the interaction asymmetry of the muons. The apparatus was described briefly in section 2.2.1 and will be described here in more detail to emphasise some of its features.

The instrument consisted of three cloud chambers placed vertically on top of each other and were immersed in a magnetic field of 11 k gauss. The production target was, in one experiment (experiment A), carbon (0·52 r.ℓ.), and in a second experiment, (experiment B) paraffin (0·359 r.ℓ.). The target was placed above the upper cloud chamber. Events were selected by a fourfold coincidence between two trays of geiger counters, one above the target and the other 30" below the bottom of the chamber assembly under

14" of lead absorber, and two proportional counters, the first being placed between the target and top of the upper chamber while the second was placed on top of the second cloud chamber. The tray of geiger counters placed on top of the target is a double tray, one or more discharged counters being required in each tray to complete the coincidence. The proportional counters were biased to permit efficient selection of interaction events. Two lead plates one ½" in thickness placed at the bottom of the upper chamber and the other of 1" thickness placed at the top of the lower chamber, were used to give identifications of the secondaries and primaries and were also used for electron energy determinations.

A 14" lead shield was placed above the entire arrangement to remove the incident electromagnetic component of cosmic rays. A 30" space was left between the lead shield and the target to permit the fringing field of the magnet to deflect the shower particles coming from the lead shield (in the case of a shower or interaction in the shield) so that they did not get confused with those originating in the target.

Unfortunately the details of the results on the interaction asymmetry observed in this experiment were not given by the authors. Only a few remarks were published which summarised the state of the experiment and the results and the integral value obtained for the asymmetry.

Kotzer et al. (1965) reported that although the experimental distributions of energy transfer to the electron for negative and positive muons are of the same shape, that due to the negative muon is in agreement with the predictions of the Bhabha theory whereas that due to the positive muon persisted in showing an upward deviation. Out of 54 interaction events observed, 33 were due to positive muons and 21 to negative ones. The integral value quoted for the asymmetry for these events was $1{\cdot}30 \pm 0{\cdot}30$, and when they included some more data obtained from the same experiment by Deery et al.(1961),

the integral value for the asymmetry rose to $1{\cdot}60 \pm 0{\cdot}30$. This is to be compared with an expected value of unity.

The experiment was then modified by replacing the middle cloud chamber with a second carbon target. For events occurring in the middle target, the primary particle could be observed both before and after the interaction. The results for the top target are similar to those obtained in the first experiment, that is, there is no significant difference in the form of the distribution resulting from positive and negative primaries, but as before, there is an abnormal positive excess suggesting a higher cross section for positive than for negative muons. The middle target results differ in that the distribution agrees with the one calculated from the normal Bhabha cross section. Due to the difference in results obtained for the top and bottom target, they suggested that the difference could be due to a process in the lead shield which results in the appearance of μ-e like events from the top target.

On further work on those cosmic ray muon events interpretable as μ-e scattering in carbon, Kotzer et al. (1967) concluded the following:

1. Normal behaviour for negative muons.
2. For energy transfer around 1 GeV a generally larger cross section for positive than for negative muons.
3. A significantly lower cross section for positive than for negative muons for large fractional energy transfer.

In view of the results from accelerator experiments (kirk and Neddermeyer 1968) which found a good agreement with prediction, they suggested that the anomaly may be caused by an abnormal behaviour of those muons arising from the decay of kaons.

6.3.2 Allkofer et al. (1971)

The experimental arrangement used by Allkofer et al. (1971) was described in section 2.2.2 and some more information will be given here. It is represented

by a spark chamber calorimeter and Kiel spectrograph which are operated in coincidence. With the spectrograph the momentum and sign of each muon is determined before entering the calorimeter where the interactions are observed.

The calorimeter is a stacked assembly of multiplate spark chambers, targets and large area solid iron magnets. The multiplate spark chambers act as track detectors. The authors state that the iron magnets are used to broaden the lateral distribution of the secondary particles and hence improve the multi-track efficiency. The targets consisted of iron and aluminium plates corresponding to 325 gm/cm^2 and 18 gm/cm^2 respectively.

The energy transfer for each interaction occurring in the calorimeter was determined from the range-energy relation or from the associated shower development in the calorimeter. Energy transfers in the range 0·2 - 100 GeV were observed. Thus, for every interaction event it was possible to determine the muon energy, muon sign and the transferred energy and these formed the main parameters in investigating the asymmetry. The obtained asymmetry as a function of muon energy and energy transfer are shown in figures 6.3 and 6.4 respectively. These results were based on about 1000 interaction events with energy transfer in excess of 0·2 GeV. It can be seen from figure 6.3 that within the statistical accuracy it is not possible to make any conclusion about the dependence of the asymmetry on muon energy. The statistical accuracy for events with muon energy above 100 GeV is very poor, and considering the experimental points below 100 GeV there seem to be no significant change with muon energy. Although all the experimental points are above unity the agreement with unity in most cases is within one standard deviation. The largest deviation from unity is in the points belonging to mean muon energies of 13 and 45 GeV, which suggest an asymmetry of $1{\cdot}20 \pm 0{\cdot}13$ where the difference from unity is less than two standard deviations.

As for the dependence of the asymmetry on energy transfer (figure 6.4),

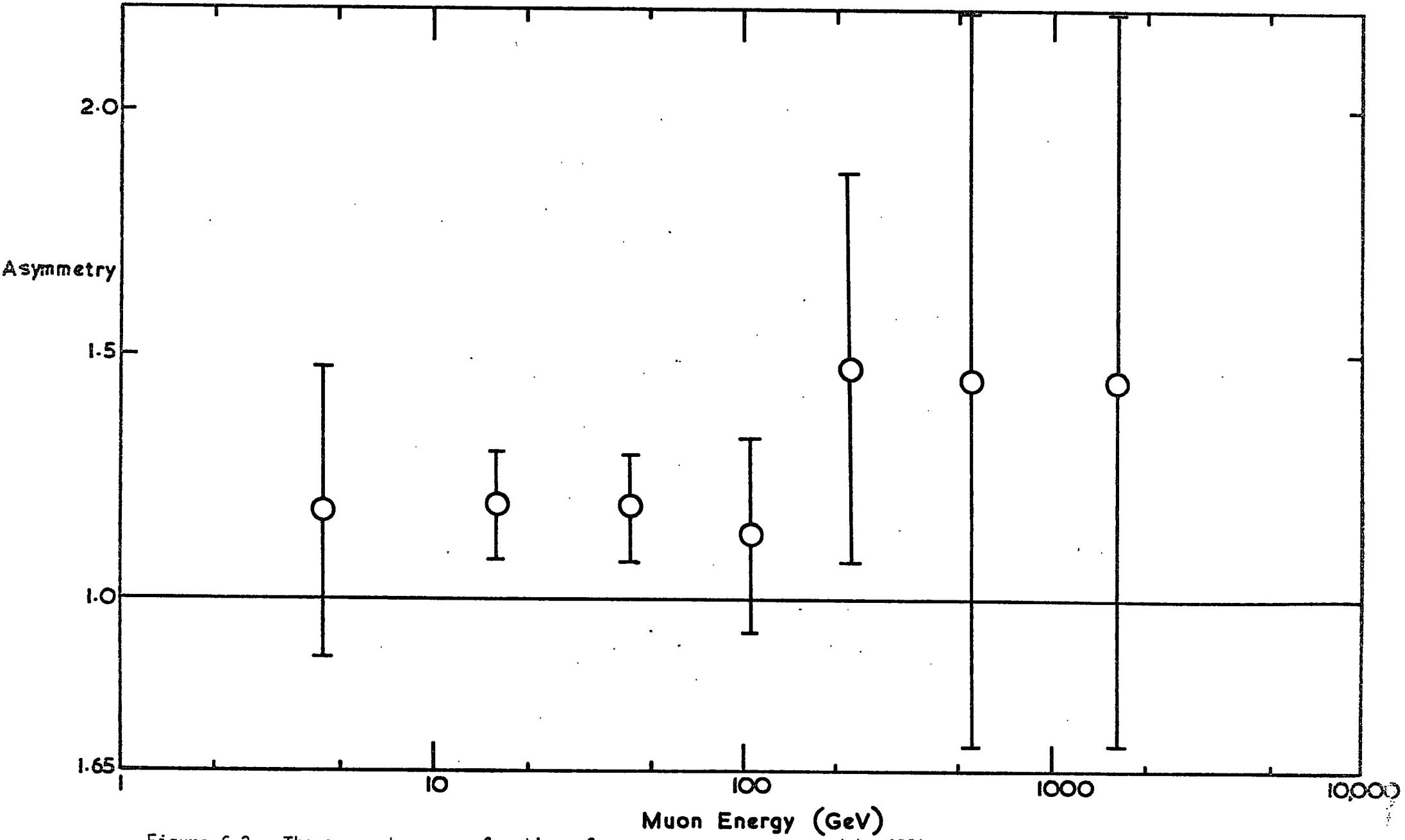

Figure 6.3 The asymmetry as a function of muon energy as reported by Allkofer et al. (1971)

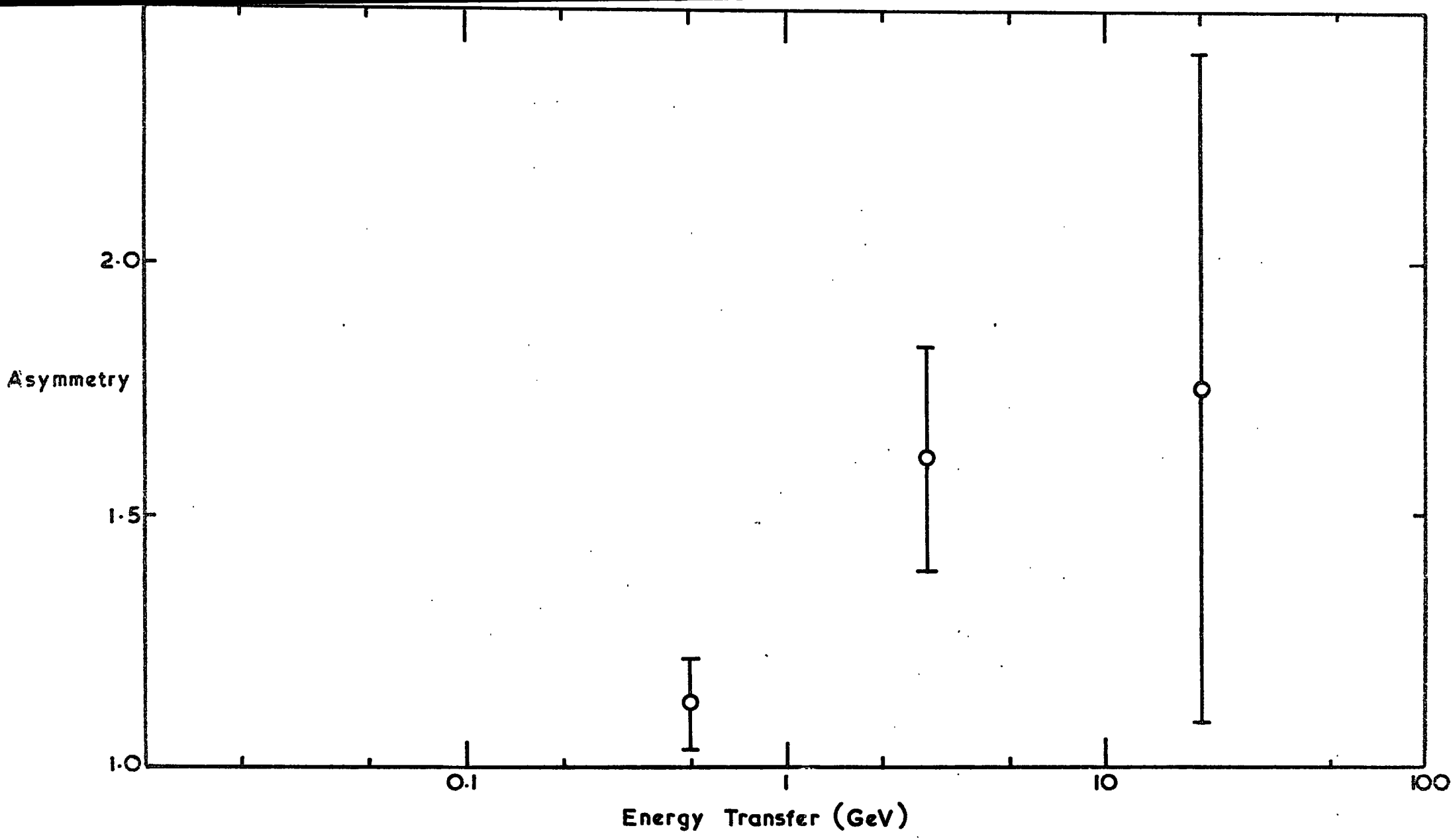

Figure 6.4 The differential spectrum of the asymmetry as a function of energy transfer as reported by Allkofer et al. (1971)

the largest excess was observed in the region of energy transfer around 3 GeV, where the observed asymmetry is $1{\cdot}63 \pm 0{\cdot}24$ over two standard deviations from unity. At higher energy transfers the statistical accuracy is poor and the quoted asymmetry is $1{\cdot}75 \pm 0{\cdot}66$.

Recently, another result has been reported, which gives the dependence of the asymmetry on the fractional transferable energy, this result is presented in figure 6.5. It can be seen there is an indication of a decreasing asymmetry with increasing fractional energy transfer, a result which agrees with that of Kotzer et al. (1967).

In general, the results of Allkofer et al. (1971), which are statistically more accurate than those of Kotzer et al. (1965, 1967), suggest an asymmetry for events with energy transfer > 0·2 GeV, the quoted integral value being $1{\cdot}20 \pm 0{\cdot}11$.

6.3.3 The Durham Mk II Horizontal Spectrograph

A brief description of the spectrograph is given in section 2.2.3; a detailed description was given by Said (1966). The spectrograph was set at a mean zenith angle of 87° and it consisted essentially of two solid iron magnets to bend the incident particle and therefore enable momentum determination, they also served as targets for interactions to take place. The spectrograph was triggered by trays of geiger counters. Visual information concerning the incident particle trajectory was obtained from five trays of flash tubes. One tray of flash tubes was placed behind each magnet to enable an estimate to be made of the energy transfer involved in the interaction.

The data on muon interactions in the spectrograph were re-analysed in 1971 by the present author in order to investigate the interaction asymmetry. The films were rescanned and only those events associated with $\geqslant 15$ flashes in either flash tube tray (the ones behind each magnet) were selected. Those events were considered as interaction events with two or more electrons. The total

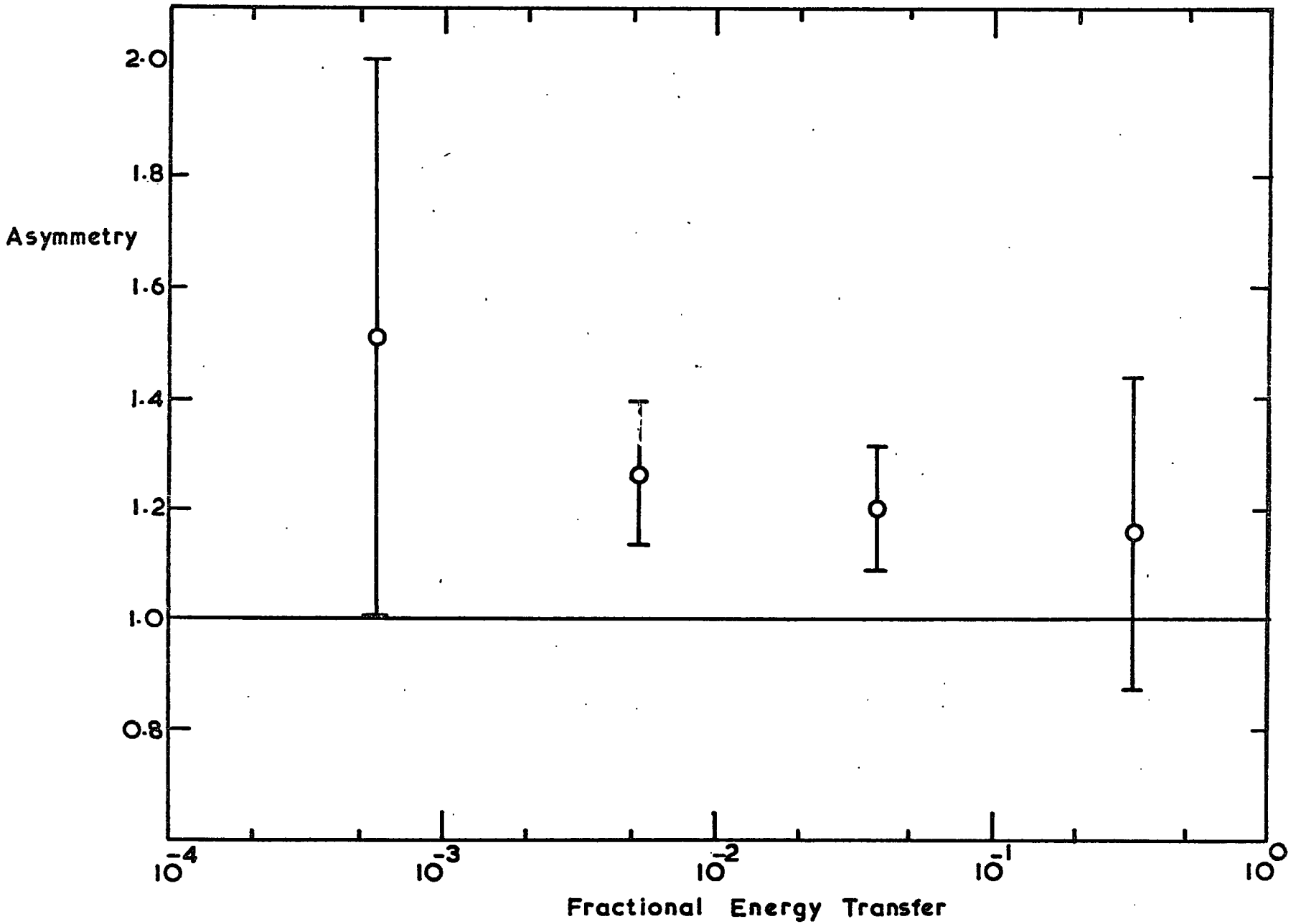

Figure 6.5 The asymmetry as a function of the fractional transferable energy as reported by Allkofer et al.(1971)

number of such events obtained was $\sim$ 300. Events with a single electron, i.e. corresponding to $7 \leqslant N_f < 15$ were not considered because there was no suggestion of an anomaly for these events in the earlier work of Lloyd and Wolfendale (1959) and also in the interaction experiment I.

Information concerning the momentum and the sign of the muon producing the interaction and the charge ratio of single muons traversing the spectrograph was obtained from the previous analysis of the data by Said (1966). The data were divided in terms of the muon sign and the dependence of the interaction asymmetry on muon energy and on number of flashes (being proportional to energy transfer) was investigated. The value of the charge ratio used is $1{\cdot}19 \pm 0{\cdot}04$ and the obtained asymmetry as a function of muon energy and energy transfer are given in figures 6.6 and 6.7 respectively. The integral value for the asymmetry is $0{\cdot}97 \pm 0{\cdot}11$. As can be seen, although the statistical accuracy is not great, all the experimental points are statistically consistent with unity and with there being no asymmetry greater than about 11%.

6.4 Results from accelerator experiments

6.4.1 Kirk et al. (1968)

The interaction asymmetry of the muons was studied using beams of positive and negative muons at Brookhaven AGS with momenta peaked at 5·5 GeV/c and 10·5 GeV/c respectively. The pion contamination was less than 10^{-6}. The beams were prepared and observed in an identical way, they differed only in the sign of charge of the beam particles.

The instrument essentially consisted of three water filled Cerenkov counters and one shower detector. The Cerenkov counters recorded the passage of fully relativistic particles and were used to provide pulse height information for event selection. The shower detector consisted of sixteen plates of plastic scintillators interleaved with fifteen lead plates each of which was $\frac{1}{4}$" thick. Its purpose was to promote the rapid build up of electromagnetic

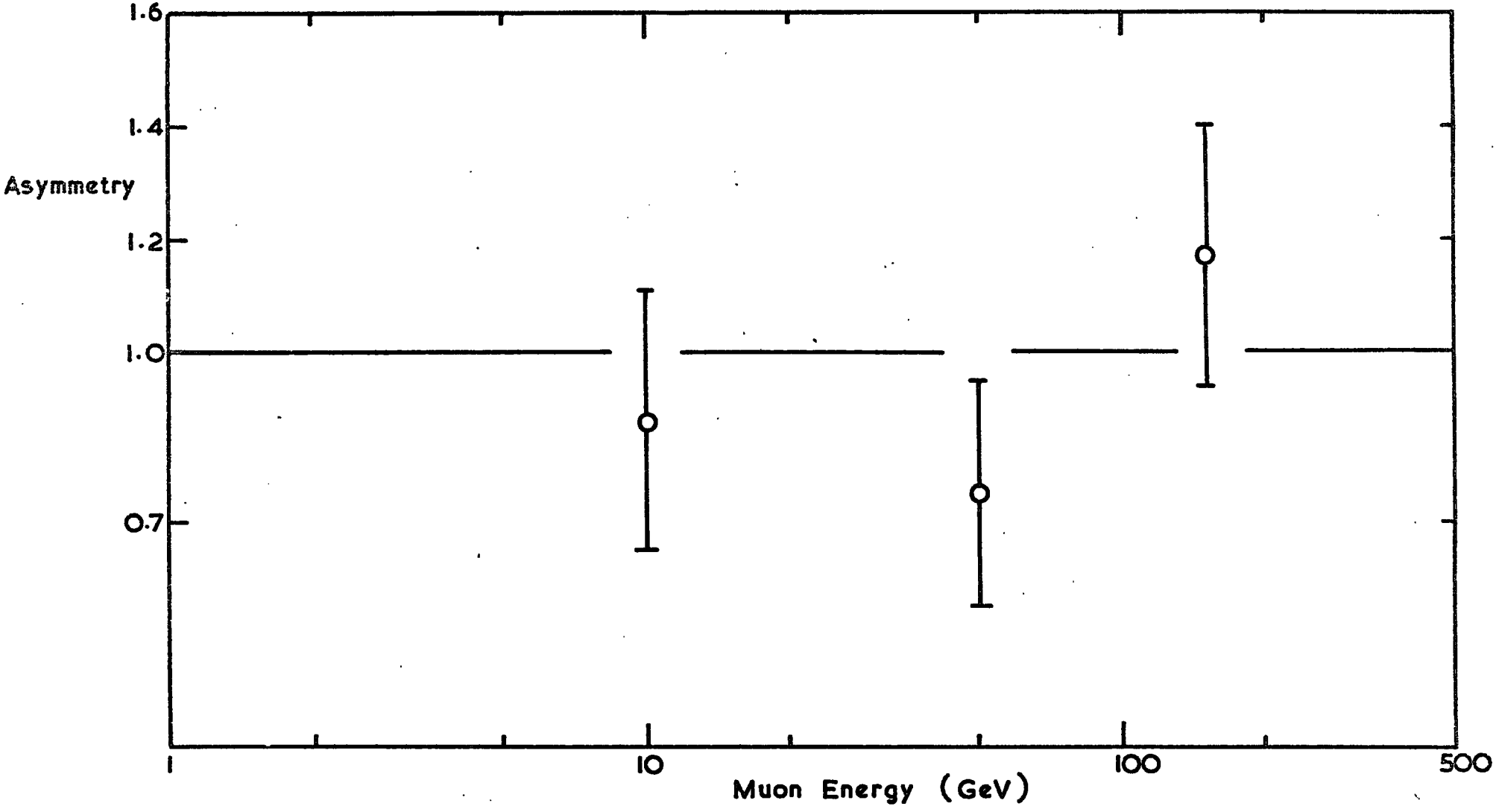

Figure 6.6 The asymmetry as a function of muon energy (the Durham Mk II horizontal spectrograph)

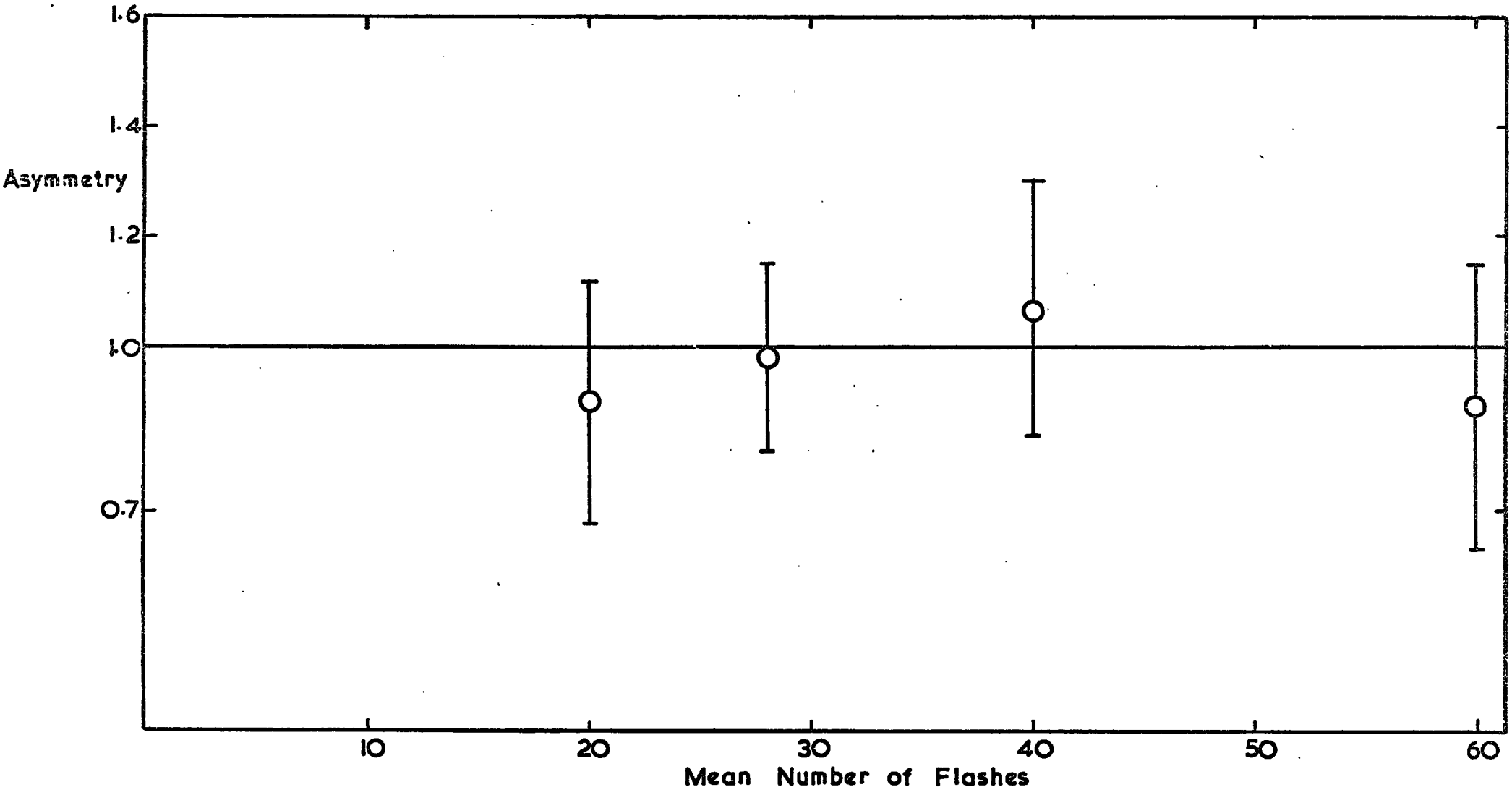

Figure 6.7 The differential spectrum of the asymmetry as a function of number of flashes (the Durham Mk II horizontal spectrograph)

showers initiated by high energy electrons to enable energy estimation. Beam telescope counters were also used, consisting of variously shaped pieces of plastic scintillators coupled to photomultipliers. These were placed in front and at the back of the apparatus, they were used to record the passage of the charged particles.

The data were of two types. In the first type, a minimum trigger was used which required only a muon traversal of the beam telescope. In this case the target was unlocalized and consisted of all the material in the beam path. In the second type of data, a selection system was introduced to enhance the selection of the knock-on electron events in the middle Cerenkov counter. In all cases the pulses from the counters were digitized and stored.

The asymmetry was measured by observing the number of knock-on electrons produced by beams of positive and negative muons. Figure 6.8 presents some of the results for the asymmetry as determined from both the Cerenkov-selected and unselected runs. The results for both runs are consistent with each other and with there being no asymmetry $\geq \pm 10\%$ for knock-on interaction process by muons with energies up to 13 GeV. The integral value obtained for the asymmetry is $0{\cdot}98 \pm 0{\cdot}10$. Such a result is obviously in good agreement with theory.

6.4.2 Jain et al. (1970)

Three small stacks of Ilford G-5 nuclear emulsions were exposed to a positive muon beam of momentum peaked at 10·1 GeV/c and negative muon beams of momenta peaked at 5·0 GeV/c and 14·5 GeV/c, at the Brookhaven AGS, in order to investigate the process of knock-on interaction for differently charged muons. The general features for the production of the three beams were similar and the contamination of pions was less than 10^{-7}.

The scanning was done by following the incident muon path through the emulsion. Since the greatest interest is in the high energy knock-on electron events, the scanning was confined to scattered events whose projected angles

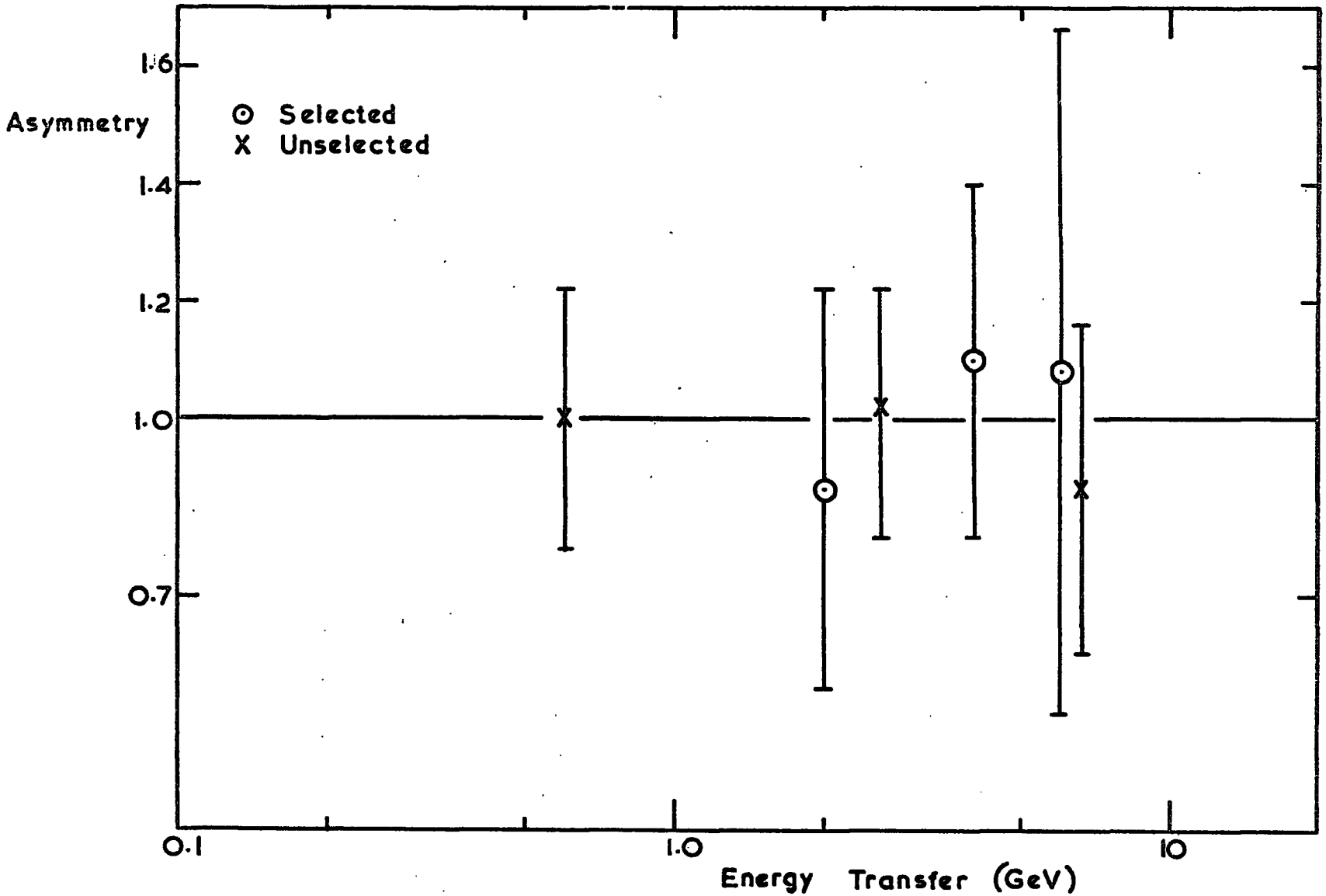

Figure 6.8 The differential spectrum of the asymmetry as a function of energy transfer as reported by Kirk et al. (1968)

were below 10°. For an interaction to be accepted for measurements as a possible knock-on electron event, it had to satisfy the following:

(i) There should be an apparent vertex coincident with the primary track.

(ii) The secondary had to be straight for at least one field of view and sharp scatters were not included.

(iii) The vertex had to be a three particles vertex (without any recoil of nucleus).

(iv) The projected angle was less than 10°.

(v) The secondary track was indeed like an electron.

The events satisfying the above criteria for analysis were also checked for coplanarity and energy-momentum balance. The energies of the secondary electrons were carefully measured using the technique of multiple coulomb scattering.

The total number of events accepted was 189. Comparison between the measured and predicted cross section (based on Bhabha theory) as a function of energy transfer was carried out for each beam. In all cases, for energy transfers > 200 MeV the experimental points agreed with expectation within one standard deviation. Below 200 MeV agreement with theory was obtained only after corrections to the loss in scanning efficiency. The authors did not present a graph to give a direct comparison between the positive and the negative muon cross sections as a function of energy transfer. The statistical accuracy however is not good (the results were based on 55, 48 and 86 events for 5, 10·1 and 14·5 GeV/c muon beam respectively) and on calculating the asymmetry from their data for energy transfers $\geqslant$ 1 GeV using the results given for 10·1 GeV/c and 14·5 GeV/c muons, the value obtained is: $1{\cdot}28 \pm 0{\cdot}46$. Although the agreement with unity is within one standard deviation, the statistical accuracy is so poor that their result can not be taken for or against an asymmetry.

6.5 Comparison of results on the interaction asymmetry

Up-to-date six experiments have investigated the interaction asymmetry of the muons. Four of these are cosmic ray experiments and the other two are accelerator experiments. All these experiments were undertaken in different ways, different experimental biases, different mean muon energy and, in addition, different zenith angles in the case of cosmic ray experiments, therefore they are not directly comparable and any comparison between them will be only approximate. In figure 6.9 an attempt is made to summarise the dependence of the asymmetry on energy transfer. It should be mentioned that some estimations were necessary before being able to present the results in such a form. This is mainly due to the fact that the experiments measure the energy transfer in different ways. In table 6.1 the integral values of the asymmetry obtained in the different experiments are listed.

TABLE 6.1

Integral values of the asymmetry

Authors' Names	Year	η
Neddermeyer et al.	1965, 1967	$1{\cdot}60 \pm 0{\cdot}30$
Allkofer et al.	1971	$1{\cdot}20 \pm 0{\cdot}11$
Durham MkII horizontal spectrograph	1971	$0{\cdot}97 \pm 0{\cdot}11$
Interaction Experiment I	1971	$1{\cdot}12 \pm 0{\cdot}12$
Interaction Experiment II	1972	$1{\cdot}08 \pm 0{\cdot}06$
Kirk et al.	1968	$0{\cdot}98 \pm 0{\cdot}10$
Jain et al. (for energy transfer $\geqslant 1$ GeV)	1970	$1{\cdot}28 \pm 0{\cdot}46$

In figure 6.9 the results from the MARS interaction experiments I and II have been combined, because these results are consistent with each other and by adding them a slight improvement in the statistical accuracy is achieved.

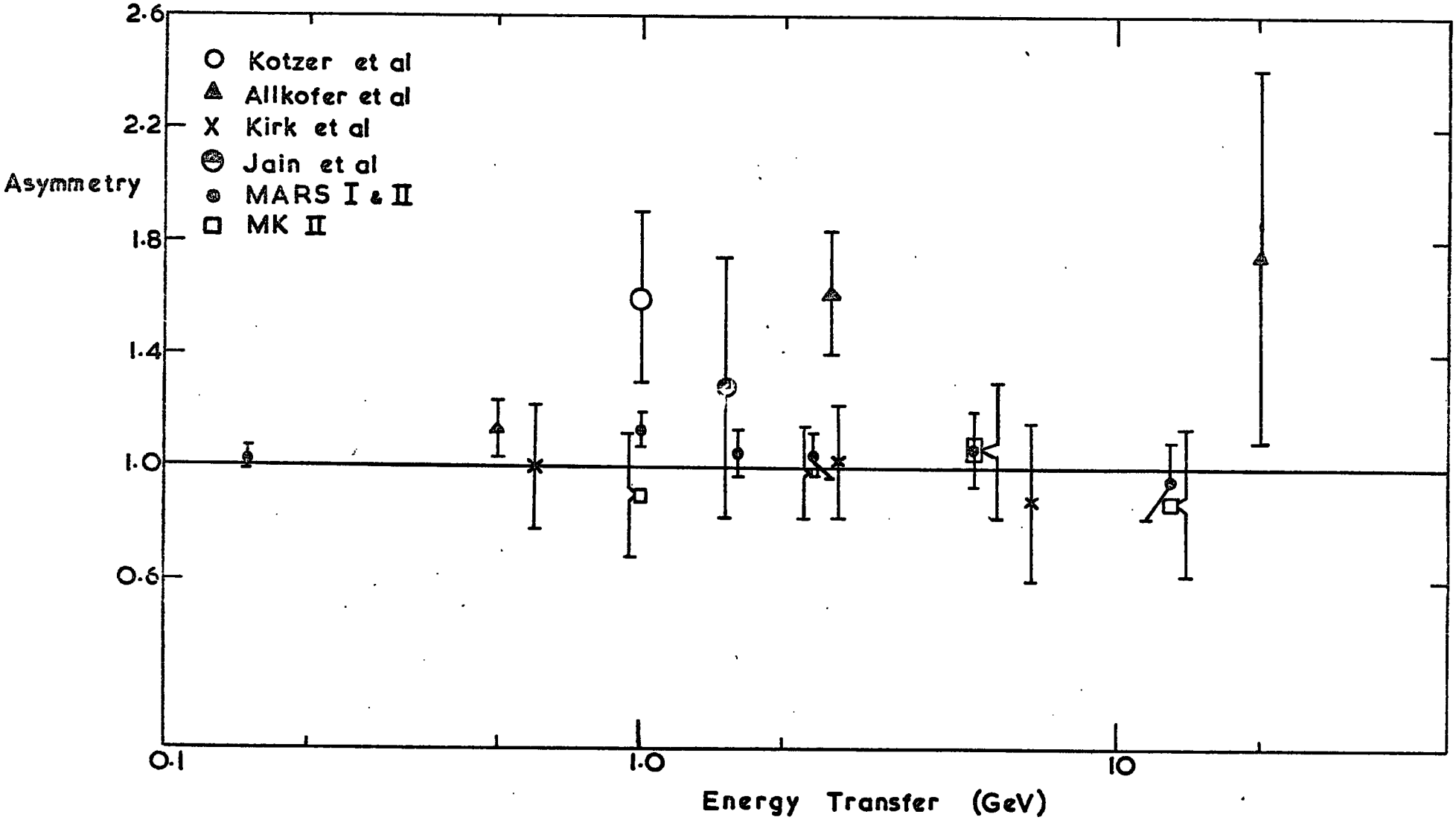

Figure 6.9 Comparison of results on the asymmetry as a function of energy transfer

The results of MARS are the most recent and the most accurate reported so far. All the measured points are consistent with a predicted value of unity within one standard deviation, apart from the point at 1 GeV whose difference from expectation is within two standard deviations. Such a deviation, however, is to be expected on the basis of statistical fluctuation (statistically only $^2/_3$ of the number of measurements are expected to lie within one standard deviation from the expected value). At any rate, if the deviation for the point around 1 GeV energy transfer is real, then it would suggest an asymmetry which is probably as high as 20% for that energy transfer. Such a value seems lower than that quoted by Allkofer et al. ($1{\cdot}63 \pm 0{\cdot}24$) and that estimated for Kotzer et al. ($1{\cdot}60 \pm 0{\cdot}30$). It is interesting to note that the statistical accuracy of the results of Kotzer et al. and Allkofer et al. is not great and their points around 1 GeV in fact agree with ours within two of their standard deviations, whereas for our point to agree with their point five to six of our standard deviations would be required which is statistically most unlikely.

Another experiment with cosmic ray muons which give results supporting the theory is the Durham Mk II horizontal spectrograph. This experiment suggested no asymmetry $> \pm$ 11%. This result is in agreement with the MARS result and is in conflict with that of Kotzer et al. and Allkofer et al. However, such a conclusion is not definite because if the asymmetry is real, it is possible to have a variation with zenith angle on the basis of postulating a new lepton (Grupen and Hamdan, 1971).

Results from the accelerator experiment of Kirk et al. (1968) are consistent with the MARS results too. They suggested no asymmetry $> \pm$ 10%. The accelerator experiment of Jain et al. (1970) did not give a useful result in view of their poor statistics. Although agreement with theory was claimed by Jain et al., a careful examination of their data shows that an asymmetry as high as 20 - 30% for energy transfers $\geq$ 1 GeV can not be ruled

out. For energy transfers $\geqslant 0{\cdot}5$ GeV the integral value of their asymmetry is $1{\cdot}10 \pm 0{\cdot}20$.

CHAPTER 7

Electromagnetic Burst Production in Iron

7.1 Introduction

In the previous chapters the data of the present work were analysed to investigate the interaction asymmetry of cosmic ray muons with no reference to the absolute values of the interaction probability. In this chapter, however, the data analysed to investigate the absolute magnitude of the interaction probabilities for producing single electrons and electron bursts of various sizes from the knock-on, direct pair production and bremsstrahlung processes as a function of muon energy. The main method of analysis adopted is to predict a burst spectrum for level 1 and level 3 assuming the validity of Q.E.D. Comparison of the measured and predicted spectra will then indicate the accuracy of the interactions cross sections.

This chapter gives the details of the data analysis and the results. Results from some previous experiments on muon interactions are also discussed.

7.2 Theoretical considerations

7.2.1 Introduction

Before going into the details of the theoretical treatment of the problem of electromagnetic bursts produced by muons, it is desirable to give a reasonable amount of theoretical background first. The known interaction processes by which the muon can lose energy in traversing matter are: knock-on electron production, bremsstrahlung, direct pair production and nuclear interactions. The first three processes produce comparatively frequent energy transfers and therefore are of importance in the present work. The contribution of the nuclear interaction to the probability of burst production in the present experiment is insignificant and therefore has not been included.

7.2.2 Knock-on electron production

The collision probability for particles of mass m and spin $\frac{1}{2}$ has been

derived by Bhabha (1938) and is given by Rossi (1952). In the derivation it was assumed that the electromagnetic field of the particle can be described as being due to a point charge down to distances smaller than 10^{-13} cm from the centre of the particle and that the magnetic moment of the particle has the value predicted by Dirac theory. It is also assumed that the energy transfer is sufficiently large so that the atomic electrons may be regarded as free.

The differential probability is given by

$$\phi_{coll}(E,E')dE' = \frac{2C\, m_e c^2}{\beta^2} \cdot \frac{dE'}{E'^2} \cdot \left[1 - \beta^2 \frac{E'}{E'_m} + \tfrac{1}{2} \left(\frac{E'}{E+mc^2} \right)^2 \right] \qquad \ldots\ldots\ldots(7.1)$$

where $\phi_{coll}(E,E')dE'$ is the probability/gm cm^{-2} of a charged particle of kinetic energy E transferring an energy between E' and E' + dE' to an atomic electron.

$C = \pi N \frac{Z}{A} r_e^2 = 0{\cdot}15 \frac{Z}{A}$ gm^{-1} cm^2 represent the total area covered by the electrons in one gram, each considered as a sphere of radius r_e ($r_e = \frac{e^2}{m_e c^2}$ is the classical radius of the electron).

Z and A are respectively the atomic number and the atomic weight of the absorber.

N is Avogadro's number

βc is the velocity of the incident particle

E'_m is the maximum transferable energy and is given by

$$E'_m = 2\, m_e c^2 \frac{p^2 c^2}{m_e^2 c^4 + m^2 c^4 + 2 m_e c^2 (p^2 c^2 + m^2 c^4)^{\frac{1}{2}}} \qquad \ldots\ldots\ldots\ldots(7.2)$$

where p is the momentum of the incident particle.

It can be seen from equation 7.1 that the differential probability for the knock-on process varies inversely with the square of the transferred energy and is almost independent on the energy of the incident particle. The

dependence of this probability on muon energy and energy transfer is shown in figure 7.1.

7.2.3 Bremsstrahlung

The differential probability for the emission of radiation by charged particles of mass m, spin $\frac{1}{2}$ and normal magnetic moment has been calculated by Christy and Kusaka (1941). In their calculations they assumed that the energy of the particle is large compared with its rest mass, that the screening of the outer electrons is negligible and the potential of the nucleus is that of a point charge for distance larger than the nuclear radius, r_n, and is constant for distances smaller than r_n. The general expression for the radiation probability is:

$$\phi_{rad}(E,E')dE' = \alpha N \frac{Z^2}{A} r_e^2 \left(\frac{m_e}{m}\right)^2 \cdot \frac{dE'}{E'} F(U, v) \quad \ldots\ldots\ldots\ldots\ldots\ldots (7.3)$$

where $\phi_{rad}(E,E')\,dE'$ is the probability /gm cm^{-2} that a particle of rest mass mc^2 and kinetic energy E will emit a photon of energy between E' and E' + dE'.

U is the total energy of the incident particle

α is the fine structure constant

$v = E'/U$ is the fractional energy transfer

F(U,v) is a slowly varying function of U and v and depends on the nuclear radius r_n. It has the following form:

$$F(U,v) = 4\left[1 + (1-v)^2 - \frac{2}{3}(1-v)\right] \times \left[\ell n\left(\frac{2U}{mc^2} \times \frac{\hbar}{mcr_n} \frac{1-v}{v}\right) - \tfrac{1}{2}\right] \ldots\ldots (7.4)$$

where $r_n = 0{\cdot}49\, r_e\, A^{1/3}$

$\hbar$ = Planck's constant / 2π

The dependence of ϕ_{rad} on the energy transfer, E', is mainly through $\frac{1}{E'}$. The differential probability given in equation 7.3 is thought to be correct up to a primary energy of the order of $\left(\frac{1}{\alpha} \frac{(mc^2)^2}{m_e c^2} \times Z^{-1/3}\right)$ where the

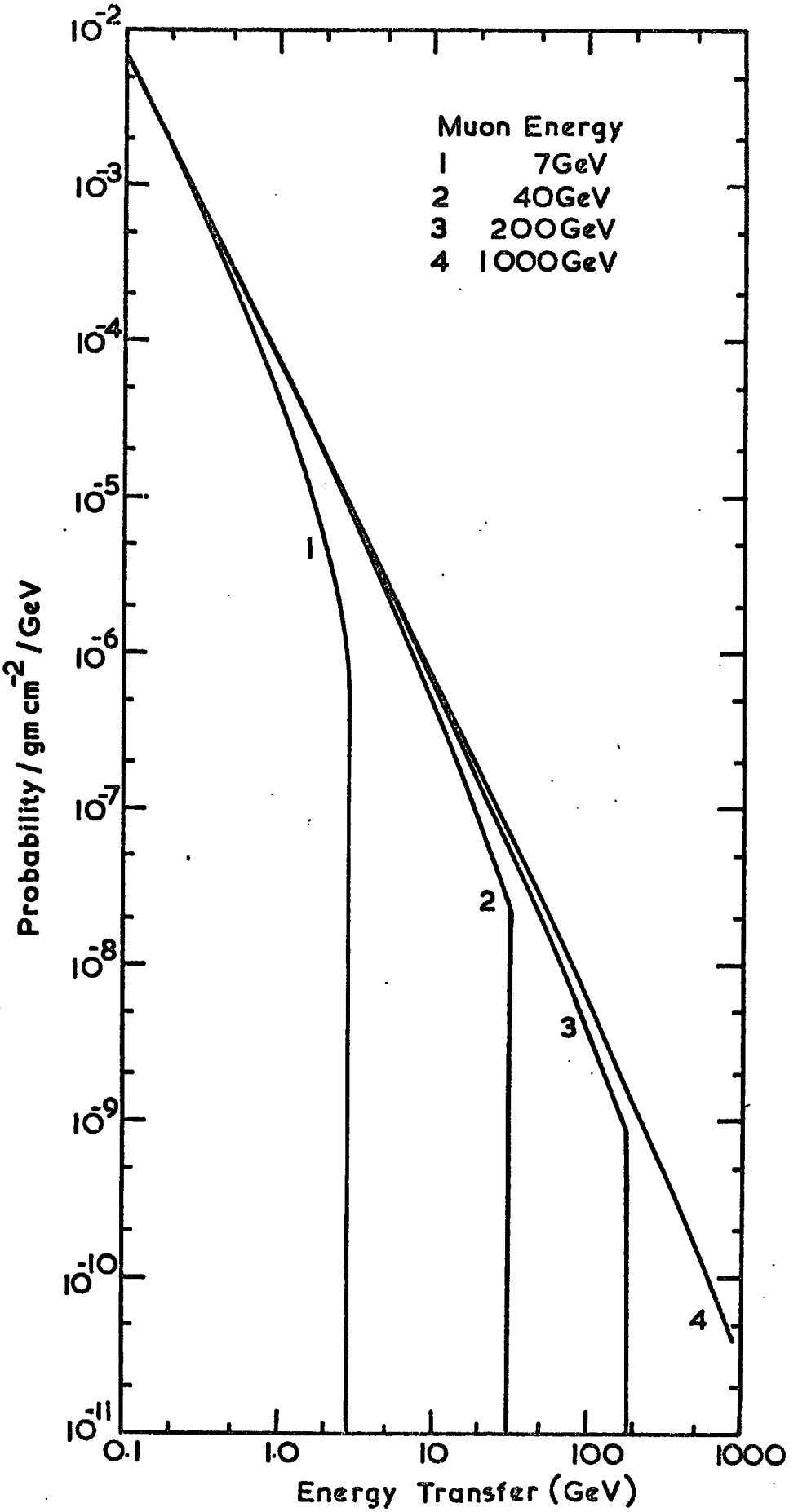

Figure 7.1 Differential probability of energy transfer for knock-on process in iron

screening effect becomes important. In the case of muons in iron screening becomes important for U $\gtrsim$ 1000 GeV.

Recently two other workers have worked out the cross section for bremsstrahlung process. Erlykin (1965) examined the influence of the atomic electrons and the finite size of the nucleus on muon bremsstrahlung. He concluded that the effect of the atomic electrons is higher, up to muon energy of 1000 GeV, than that usually taken into account by the replacement of Z^2 by Z(Z+1) and that the correction due to the finite dimensions of the nucleus is less than that used by Christy and Kusaka.

Petrukhin and Shestakov (1967) investigate the effect of the nuclear form factor on muon bremsstrahlung cross section for momentum transferred to the nucleus greater than the muon mass. They concluded that the effect implies a smaller cross section for bremsstrahlung than that given by Christy and Kusaka.

The three above-mentioned results on the bremsstrahlung cross section have been compared with each other for different muon energies and over the whole range of energy transfer. The result that emerges is that the difference in the predictions is mainly at low energy transfers, < 0·1 GeV where the screening effect is important. The difference decreases with increasing energy transfer and increases with increasing muon energy. Over the range of muon energy and energy transfer relevant to this experiment, the maximum difference is $\sim$ 20%. The reflection of this difference in the burst spectra is much smaller and hence it is not possible with the present experimental accuracy to resolve the difference between the theories. Therefore, the interaction probability given by Christy and Kusaka is accurate enough and this is what has been used in the present analysis. The dependence of the interaction probability on muon energy and on energy transfer is illustrated in figure 7.2.

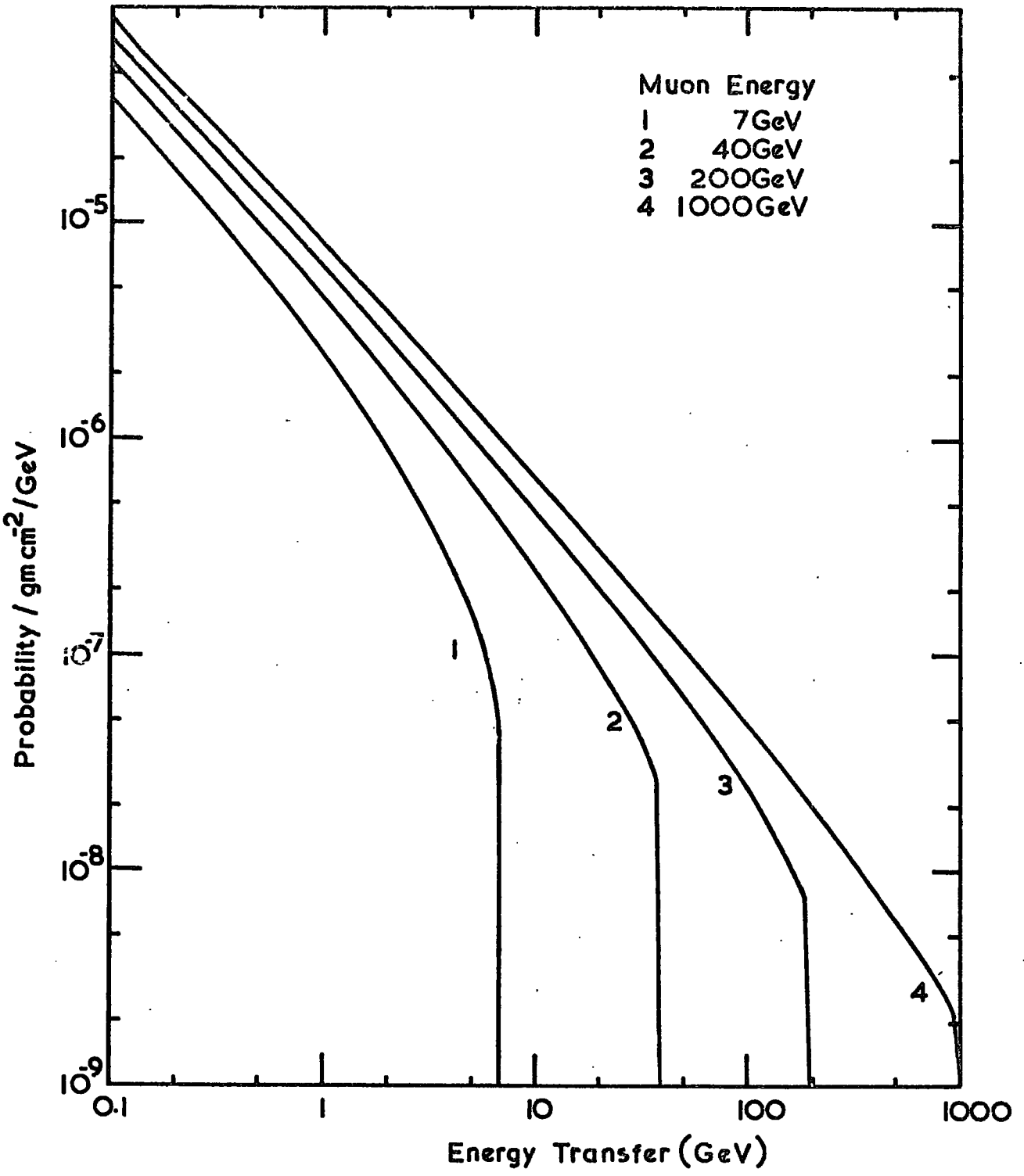

Figure 7.2 Differential probability of energy transfer for bremsstrahlung process in iron

7.2.4 Direct pair production

The theory of electron pair production by a charged particle of spin $\frac{1}{2}$ have been worked out by several authors, firstly by Bhabha (1935) and independently by Nishina et al. (1935) and by Racah (1937) using classical quantum electrodynamics. Their calculations give a correct description only when the energy transferred to the pair is small compared with the energy of the incident particle. The results of Nishina et al. and Racah, while in good agreement with each other, led to numerical values which was considerably lower than those of Bhabha. Block et al. (1954) improved the approximations used by Bhabha and by so doing obtained results in good agreement with those of Racah.

A more recent treatment of the theory of direct pair production is that due to Murota et al. (1956, abbreviated MUT), who calculated the cross section in a manner more precise than that of Bhabha and others, using the Feynmann-Dyson method. Their results are valid as long as the participant particles have energies large compared with the respective rest masses. The MUT theory has at least one arbitrary parameter, α, which is of the order of unity. It is introduced in the theory as a cut-off factor in the momentum transferred from the primary particles to the pair.

Kelner and Kotov (1967) have recalculated the cross section for pair production by an incident charged particle. They obtain an exact expression for the cross section in the non-screening and screening regions.

Kokoulin and Petrukhin (1969) gave a good survey for the cross section given by the previous workers, and obtained a united analytical expression for the cross section. Their results are in good agreement with that of Kelner and Kotov, the maximum difference being only 2%. The difference in values obtained by using the theory of Kokoulin et al. and the MUT theory depends on the value assigned to the parameter α in the latter. Using a value of two for α (results from several experiments favour this value for α), the

difference between values obtained from the two theories over a wide range of energy transfer and muon energy is <30%. Again, the reflection of this difference in the burst spectrum analysis is much smaller and therefore it is not possible to test the validity of one theory on the other with the present analysis. In fact any experiment set to investigate the difference needs an enormous amount of statistical and systematic accuracy.

In the present analysis of the burst spectrum the interaction probability given by the MUT theory has been adopted. Due to the complicated form of the formula, it will not be presented here, only reference to it is given. The formula used to calculate the differential probability is formula 23 given by Murota et al. (1956). This formula was evaluated for both the screening and non-screening cases. The dependence of the interaction probability on muon energy and energy transfer is shown in figure 7.3.

7.2.5 Comparison of the interaction probabilities

In the present experiment it is impossible to discriminate between the three interactions processes in individual interactions because it is not possible to see the initial signature of the interaction. It is possible, however, to make a measure of discrimination for a group of particles in view of their different dependence on muon energy and energy transfer. The knock-on process probability is nearly independent of muon energy and so is dominant at low muon energies (< 40 GeV). It varies inversely as the square of the energy transfer. The direct pair production probability increases more rapidly with muon energy than the other two, but it falls off very rapidly with energy transfer. Direct pair production is dominant at muon energies > 100 GeV. The bremsstrahlung interaction probability is relatively small and decreases rather slowly with increasing energy transfer. It is dominant at high fractional energy transfers. Comparison between the three interactions probabilities for 10 and 100 GeV muons in iron is given in figures 7.4 (a)

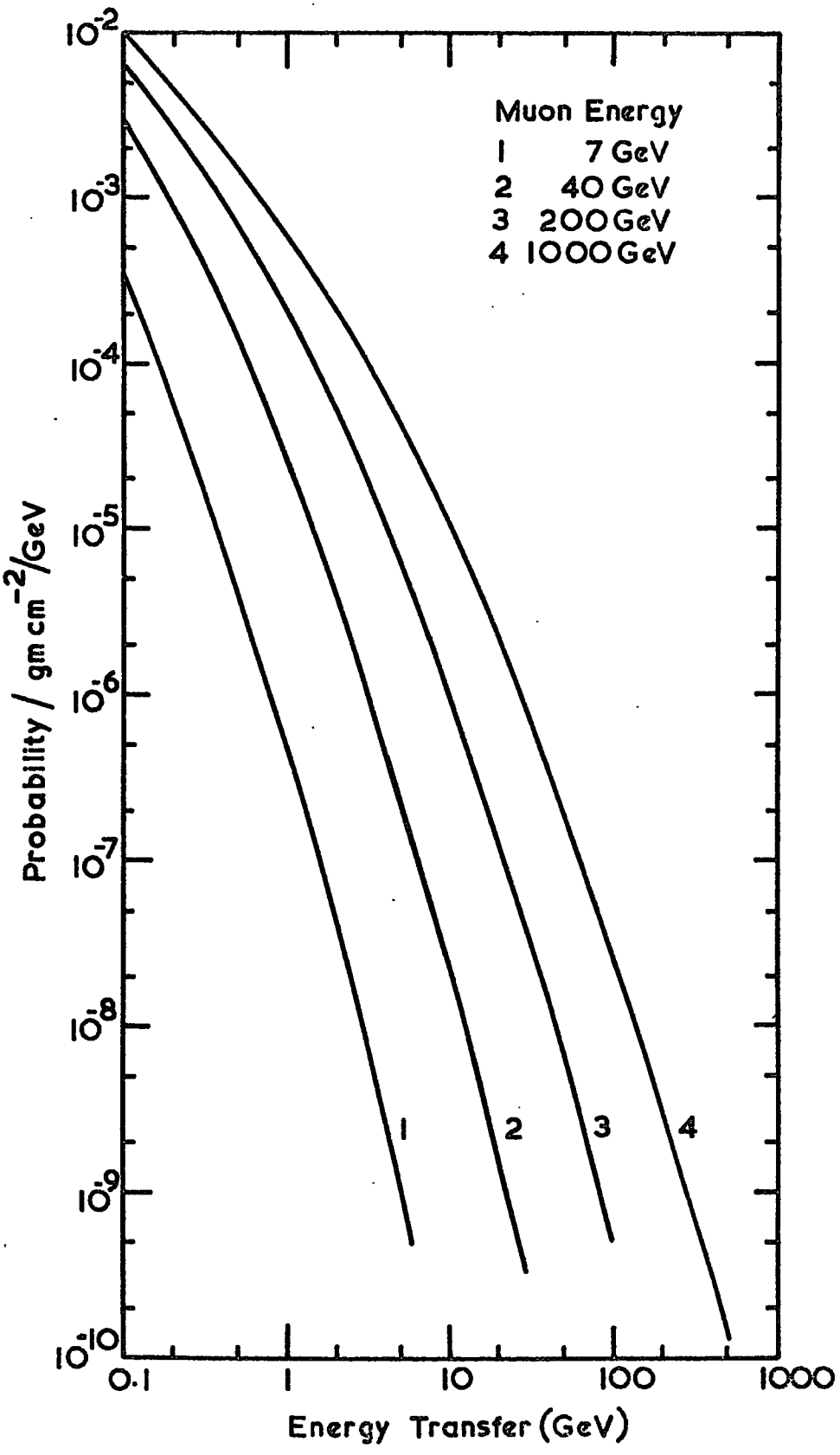

Figure 7.3 Differential probability of energy transfer for direct pair production process (MUT theory) in iron

and (b).

In figure 7.5 the differential probabilities are given as a function of muon energy for four representative energy transfers: 1, 2, 5 and 10 GeV. Curves for other energy transfers can be obtained similarly and it is possible to see which interaction process predominates for a given muon energy and given energy transfer. For instance, at an energy transfer of 1 GeV, bremsstrahlung predominates for all muon energies $< 3{\cdot}7$ GeV, whereas for an energy transfer of 10 GeV it is predominant for all muon energies $< 17{\cdot}5$ GeV. Direct pair production predominates at an energy transfer 1 GeV for muon energy $>$ 83 GeV, whereas for an energy transfer of 10 GeV it predominates for muon energy $>$ 170 GeV. Therefore for an energy transfer of 1 GeV the knock-on process dominates for muon energies in the range 4 - 70 GeV, whereas for an energy transfer of 10 GeV it dominates for muon energies in the range 18 - 160 GeV. These arguments have been used to give the approximate regions of predominance for the three interactions and the results are given in figure 7.12.

7.2.6 Cascade shower in iron

In traversing matter an electron loses energy mainly by collision and by the radiation process i.e. bremsstrahlung, and for energies greater than the critical energy of the medium (ε_o), radiation losses predominate. On passing through the coulomb field of the nucleus, there is a significant probability of a photon being emitted with energy close to that of the primary electron E_o. The secondary photon has a probability of producing an electron-positron pair or it can undergo Compton scattering. In either case the resulting charged particles can emit further photons, which in turn produce more electrons. Thus, at a certain depth in the medium instead of there being one electron of energy E_o, there are several electrons and photons whose total energy is close to E_o. This phenomena is known as the 'electromagnetic cascade'. As the cascade process goes on the number of particles increases and their average

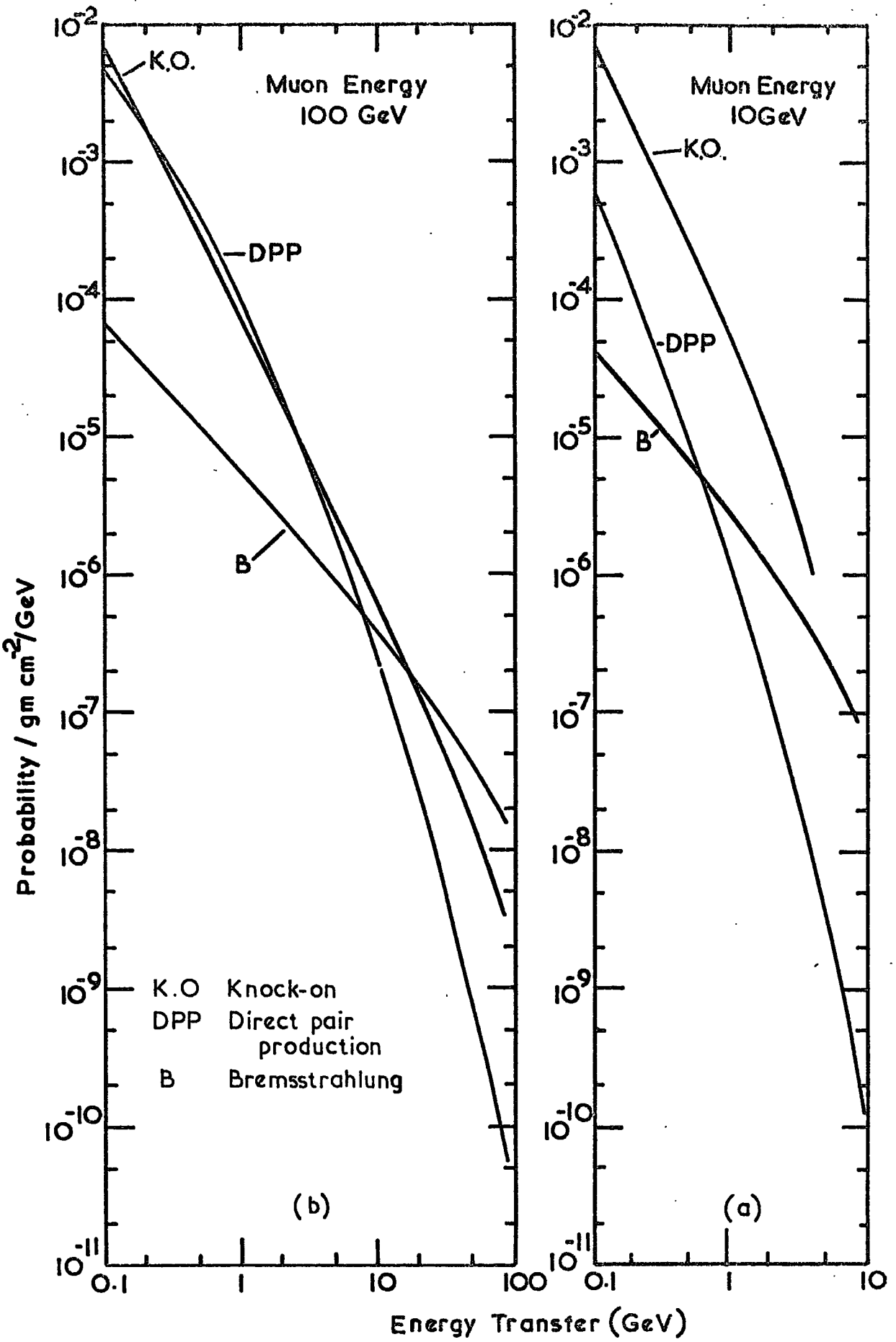

Figure 7.4 Comparison between the three interaction probabilities of muon in iron

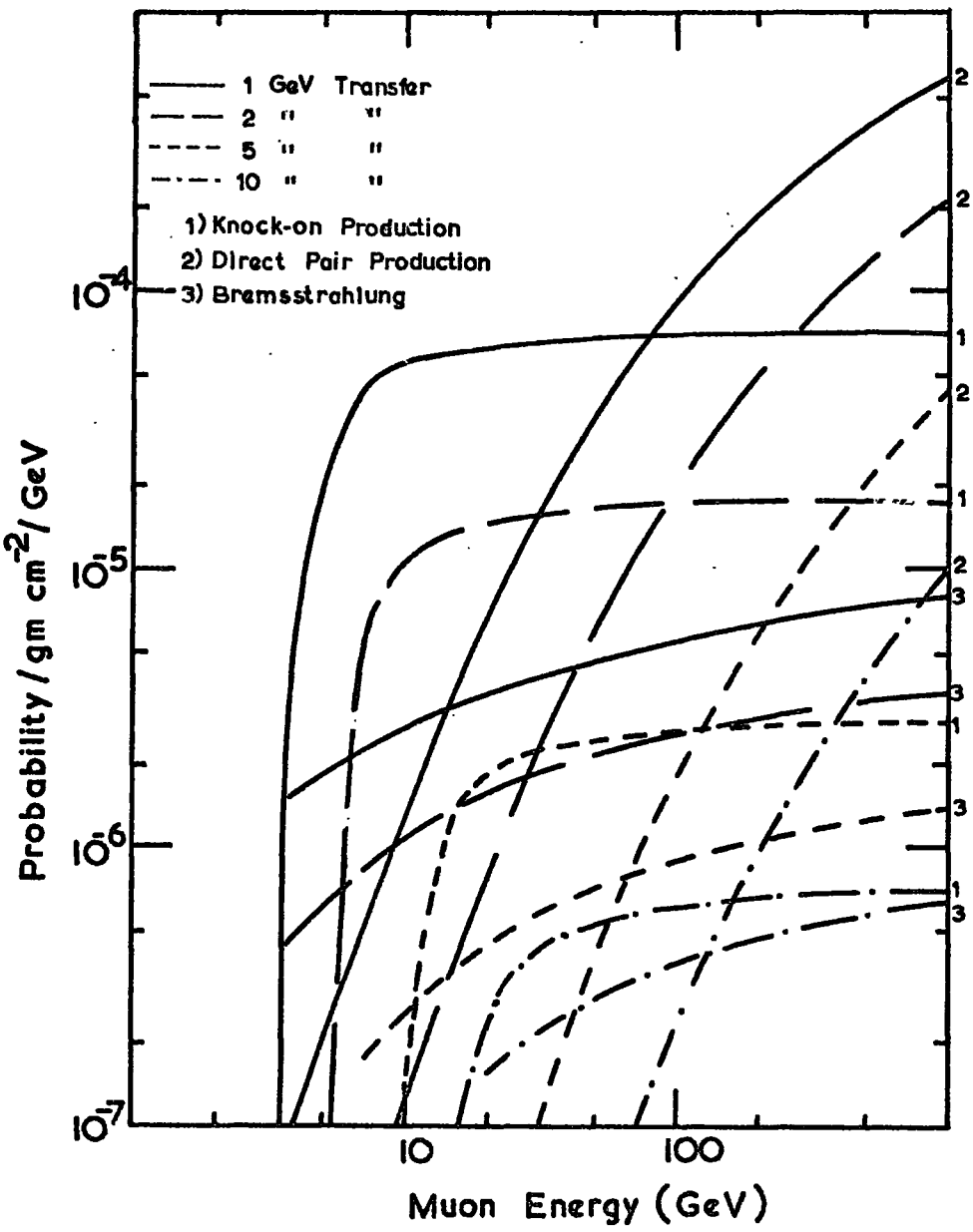

Figure 7.5 Interaction probabilities for the three processes as a function of muon energy for four different energy transfers

energy decreases and so more and more electrons fall into an energy range where collision losses predominate and the cascade begins gradually to die out.

The theory of cascade showers determines the probability that in the element of solid angle $(\Omega,\Omega+d\Omega)$ and in the energy interval (E, E+dE) there exist at a certain depth, N_1 electrons and N_2 photons at a distance (r, r+dr) from the shower axis. Mathematically this problem is very complicated and to obtain the more important characteristics of the shower it is sufficient to know the average number of electrons and photons at a given depth. Consequently only the average behaviour of the shower is calculated and any specific probability is calculated as a deviation from the average behaviour. This problem is known as the fluctuation problem.

In all elementary processes at high energies, the angle at which secondary electrons and photons emitted are extremely small, of order of $m_e c^2/E_o$, where E_o is the energy of the primary particle. In any target of low Z Rutherford scattering of charged particles is also small and hence the shower develops essentially in the direction of motion of the primary particle. In heavy elements, however, this is not true because the shower multiplication continues to lower secondary electron energies, where Rutherford scattering becomes important. In fact the assumption of a one-dimensional shower in a heavy element is justified only if attention is restricted to the behaviour of the more energetic shower particles. In general the approach adopted is to treat the cascade as being one-dimensional and then to make corrections for the increased track length due to scattering. A comprehensive article on the theory of the electron-photon cascade shower and the various methods adopted by several workers is given by Belenkii et al. (1959).

In the present experiment bursts corresponding to energy transfers in the range 1 - 30 GeV have been observed, hence any cascade theory employed in a theoretical prediction must cover this range of energy transfer and also

pertain to iron. Ivanenko et al. (1959, 1967) have calculated the cascade curves for iron for primary electrons or photons, taking into account the energy dependence of the total photon absorption coefficient and multiple scattering. These curves have been employed to calculate the theoretical burst spectra in this experiment, because the Ivanenko theory is, in general, in good agreement with the available experimental measurements for iron (Backenstoss et al., 1963, Murzin et al., 1963 and Takbaev et al., 1965).

The shower development curves of Ivanenko et al. (1967) for showers initiated in iron by primary electrons and primary photons are shown in figures 7.6 and 7.7 respectively for an electron threshold energy of 2 MeV. All energies are in units of $0{\cdot}437 \times \varepsilon_o$, where ε_o is the critical energy for iron.

7.2.7 Fluctuations

The theory of cascade showers describes only the average behaviour of the showers. The study of the fluctuations from the average behaviour represents a much more complicated problem and has not yet received a satisfactory solution. There is no general agreement on this problem in the theory of electromagnetic cascade.

Bhabha and Heitler (1937) postulated the Poisson distribution on the basis of genetical independence of the shower particles. This is not quite true due to the nature of radiation and pair production processes. In general any deviation from the average behaviour occurring in the early development of the shower reflects itself upon successive generation amplified by the multiplication process.

Another attempt was made by Furry (1937) who obtained a distribution as the solution of a differential equation based on the actual mechanism of the shower. However, ionisation losses were ignored in the derivation of the distribution and electrons and photons were treated as identical particles. The effect of ionisation losses becomes increasingly important with increasing

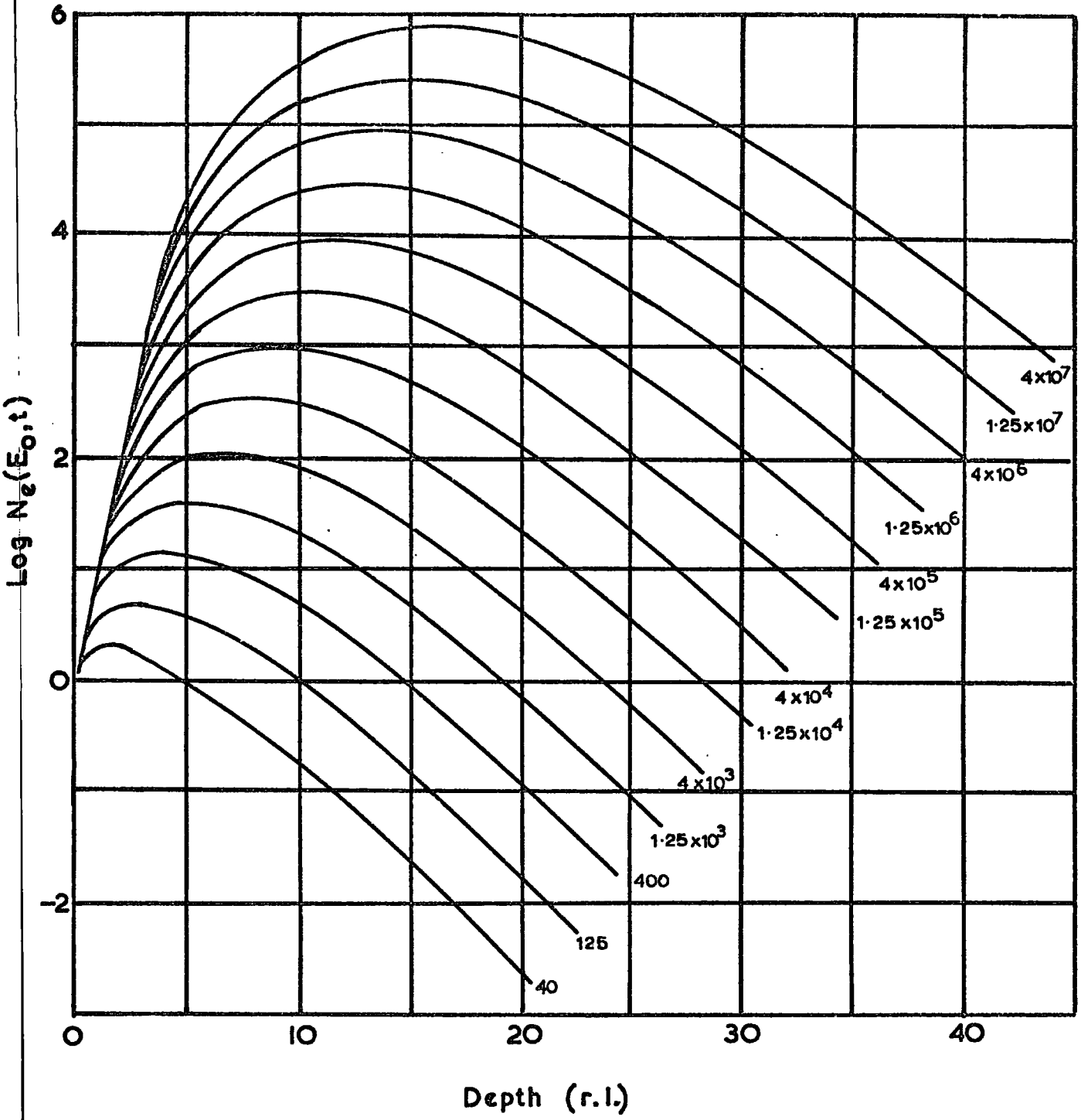

Figure 7.6 Showers initiated by primary electrons in iron, after Ivanenko et al. (1967). Electron threshold energy is 2 MeV.

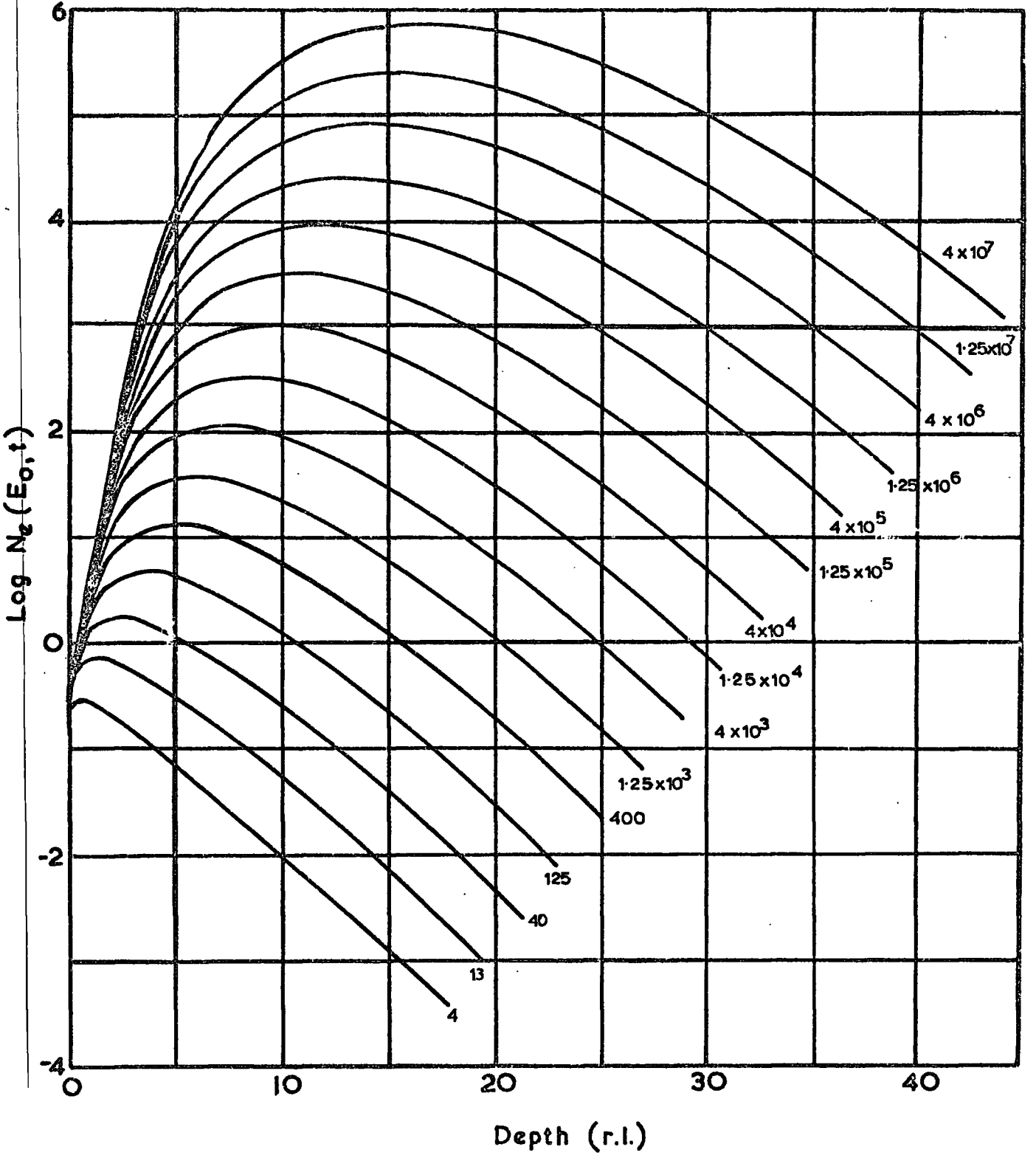

Figure 7.7 Showers initiated by primary photons in iron, after Ivanenko et al. (1967). Electron theshold energy is 2 MeV.

depth, so the Furry distribution might be expected to apply only over the first few radiation lengths (r.ℓ.).

The experimental mean square deviation from the average is too large to fit a Poisson distribution and too small to fit the Furry distribution. The experimental data seem to suggest the following:-

1. At small depth ($t < 2$ r.ℓ.) the distribution is approximately Furry.
2. At large depth ($t > 17$ r.ℓ.) the distribution is approximately Poisson.
3. At the shower maximum and its neighbourhood the distribution is normal.

At small depths, the shower is young and the fluctuations are large because there are some highly energetic particles. Near shower maximum, the fluctuations are smaller due to the larger number of particles present.

As most observed bursts are predominantly produced by showers close to the maximum of their development, it is reasonable to expect that the Poisson distribution (which becomes Gaussian for large numbers of particles) would give a reliable estimate of the effect of fluctuations on the burst spectrum. Therefore Poissonian fluctuations have been adopted. The effect of the fluctuations is to increase the burst frequencies by an amount which is greater for lower muon energies where the slope of the differential cross-section as a function of energy transfer is steeper. The effect on the slope is not very great.

7.3 Results from previous experiments

7.3.1 Introduction

The results of work done up to 1957 are contained in a review article by Fowler and Wolfendale (1958). Up to that time the results on the knock-on process were in agreement with the theoretical prediction of Bhabha for energy transfers below 1 GeV and up to 100 GeV transfer with the theoretical prediction of Christy and Kusaka in the case of the bremsstrahlung process.

In the following paragraphs brief descriptions are given for some of the

more recent experiments on the electromagnetic interactions of the muons. These experiments are divided into two groups. One group contains experiments where the authors claim inconsistency with theory. The other group contains experiments where the authors claim consistency with theory.

7.3.2 Experiments inconsistent with theory

1. Roe and Ozaki (1959)

This experiment was mainly carried out to study direct pair production of electrons by muons with energy in the range 8 - 120 GeV. The interactions were observed at S.L. (sea level) in a multiplate cloud chamber which was placed under the Cornell magnetic spectrograph. The chamber contained nine type metal plates (essentially lead) each of 1·06 r.ℓ. The experiment was carried out in two stages, in one stage the spectrograph was in the vertical and in the other stage at a zenith angle of 68°. In order to determine the energy transfer for each interaction event extrapolations were made of Wilson's Monte Carlo results (Wilson, 1950) to obtain the theoretical shower curves for the energy region from 200 MeV to over 1 GeV. Their results indicate that for energy transfers $>$ 200 MeV the direct pair production cross section is about half the predicted by the MUT theory.

2. Gaebler et al. (1961)

Gaebler et al. (1961) operated a multiplate cloud chamber 1032 ft underground to study the electromagnetic interactions of cosmic ray muons. The cloud chamber contained twelve $\frac{1}{8}$" lead plates and was triggered by vertical muons by coincidence of Geiger-Muller counter trays above and below it.

Showers primarily due to direct pair production and knock-on processes were observed. The energies of the cascade showers were determined by comparing the showers with those obtained using a Monte Carlo method (Wilson, 1952). The results indicate that there is agreement with knock-on theory but that the direct pair production cross section is about $\frac{1}{2}$ that predicted by MUT theory

for energy transfer below 1 GeV. At 1 GeV and above the agreement with theory is better.

3. Kearney and Hazen (1965)

Kearney and Hazen (1965) studied the production of knock-on electrons and electron pairs by cosmic ray muons of mean energy > 50 GeV, using a multiplate cloud chamber operated at a depth of 1132 ft underground. The chamber contained 21 lead plates, $\frac{1}{8}$" thick as production target. It was triggered by coincidence pulses from plastic scintillators mounted above and below the chamber. During the first part of the experiment the chamber was operated in a vertical position, in the second part, the chamber and the plastic scintillator assembly were set to a zenith angle of 66° in order to favour the observation of high energy muons. The energies of the electrons that initiated the showers were obtained from an experimental calibration. The energy transfer observed was in the range 85 MeV to 10 GeV. The observed frequency was compared with the expected frequency calculated from the theory of Bhabha for knock-on electrons and MUT for electron pair. A satisfactory agreement was found with pair production theory, whereas the prediction of knock-on theory was significantly lower than the observed frequency for energy transfers around 1 GeV.

4. Matano et al. (1968)

The Tokyo air shower array was used to observe horizontal air showers in order to study the high energy interactions of muons. Horizontal air showers are produced most probably by bremsstrahlung and by nuclear interaction of the muons. A shower produced by bremsstrahlung is almost entirely electromagnetic and the number of nuclear active particles and muons in the shower is very much less than in a shower produced by the nuclear interactions of muons. Therefore a shower can be classified as nucleonic if it contains nuclear active particles and (or) muons.

A total of nine large angle air showers of size greater than 10^4 and

zenith angle above 70° were observed. Two of these showers showed evidence that they were not pure electromagnetic showers but nucleonic showers. There was no information for the other seven showers to determine whether the shower was nucleonic or not. When the size spectrum of the horizontal showers was compared with the calculated one, assuming that the nuclear interaction of high energy muons was negligible, the observations were much higher than the prediction, which tends to suggest an unusually high muon nuclear interaction cross section.

5. Alexander et al. (1969)

Alexander et al. (1969) studied electron showers incident on the large angle EAS detector at Durham at a mean zenith angle of 73°. On analysing the data in terms of muon interactions in the atmosphere, the results were in agreement with those of Matano et al. (1968), in that there was an excess of events for burst sizes above a few hundred particles. A very high nuclear interaction cross section (approaching 20 mb) would be required to explain the results. A possible reason for the excess (as given by the authors) is that the lateral distribution of electrons and conversion from measured densities to shower size are not well represented by simple shower theory. Later work by Kiraly et al. (1971) in this field is referred to later in Section 7.6.

6. Allkofer et al. (1971)

Allkofer et al. (1971) investigated the electromagnetic interactions of cosmic ray muons in the energy range 7 to 1000 GeV. Details of their instrument were given before (section 2.2.2). They found reasonable agreement between the experimental results and the theoretical predictions except in the region of energy transfer around 1 GeV where deviation is claimed from Bhabha's theory for knock-on process and the MUT theory for direct pair production process.

7.3.3 Experiments consistent with theory

1. McDiarmid and Wilson (1962)

McDiarmid and Wilson, (1962), studied the electromagnetic interactions of cosmic ray muons in iron and lead targets using a multiplate cloud chamber at S.L. The chamber was triggered by two trays of geiger counters and two scintillation counters. The two scintillation counters were biased to give an output only when ≥ 9 particles present at the level of either sintillator. Therefore interaction events were selected by requiring a coincidence between the top tray of geiger counters, one counter in the bottom tray and one of the scintillators. Estimates of the total shower energy were made from the observed total track length in the chamber, using a value of 30 MeV per radiation length for the average energy dissipated by an electron.

When bremsstrahlung is the dominant process, the measured production probabilities are in good agreement for energy transfers in the range 8 - 40 GeV. When the production of knock-on electrons is the dominant process, good agreement with theory is obtained for energy transfers around 4.5 GeV, but only fair agreement is obtained for higher energy transfers.

2. Chaudhuri and Sinha (1964)

Direct pair production of electrons by cosmic ray muons in an iron target was studied using a multiplate cloud chamber set vertically underground at a depth of 148 m.w.e. The method used was to select a beam of cosmic ray muons with the aid of geiger counters and then observe their interactions in the iron plates placed inside the chamber. In one experimental run the cloud chamber contained twelve 1·6 cm thick iron plates and one 1·25 cm thick lead plate. In this run the chamber was triggered by a fourfold coincidence between the geiger counters placed above the chamber. In the other run the chamber contained nine 0·54 cm iron plates and 1·25 cm lead plates and the chamber was triggered by a coincidence between three geiger counters, two of

which were placed above the chamber, the third under 5 cm of lead below the chamber.

The events selected were those in which a single penetrating particle traversed the chamber and was accompanied by two or more electrons originating in any of the iron target plates. In order to determine the energy transfer (between 40 MeV - 1 GeV) use was made of the results of Hazen (1955) on cascade showers in copper, on the other hand for energy transfer > 1 GeV conventional showers theory as given by Bhabha and Chakrabarty (1948) was used. For pairs of energy < 40 MeV, the results of Wilson's Monte Carlo calculations (Wilson, 1951) were used.

In both runs the results obtained were in good agreement with the predictions of the MUT theory ($\alpha = 2$) for energy transfers in the range 35 - 1000 MeV.

3. Barton et al. (1965)

Barton et al. (1965) studied the electromagnetic interactions of high energy cosmic ray muons using six large area liquid scintillation counters interleaved with five sheets of lead each of thickness 2·5 r.ℓ. The apparatus, which was set in vertical direction, was placed at depth of 60 m.w.e. underground. The instrument was triggered by index trays above and below the apparatus, also a pulse was required from the fourth scintillation counter which was placed below the middle target. The experiment was run with different biasing level for the fourth scintillation counter.

The energy transfer in the interaction was estimated from the number of particles at the shower maximum using the cascade theory of Buja (1963). For the measured range of energy transfer (0·1 - 50 GeV) good agreement was found with theory.

4. Ashton et al. (1968)

The electromagnetic interactions of cosmic ray muons, in iron, incident

at sea level in the zenith angle range 50° - 90° was studied. The apparatus consisted of two iron targets, each of ~ 14 r.ℓ., and two scintillation counters, one behind each target. A high energy electron or photon produced in either targets by an electromagnetic interaction of a muon, generated a burst of electrons and photons. The scintillation pulse produced by the passage of this burst was used for the selection of such events and also to determine the size of the burst. Visual information about each event was obtained from five trays of flash tubes.

A differential burst spectrum was calculated using the cascade curves of Ivanenko et al. (1959). The contributions to the burst were mainly coming from the knock-on process and bremsstrahlung. The effect of the fluctuation on the burst spectrum was included assuming a Poisson distribution. The experimental results they obtained are in agreement with theory.

5. Chin et al. (1969)

Chin et al. (1969), studied nuclear interactions by muons at a depth of 40 m.w.e. underground using a large calorimeter. The calorimeter consisted of two kinds of detectors, scintillation counters and multiwire proportional counters to detect the shower particles at each layer, and spark chambers to identify penetrating particles among the shower secondaries. Iron and lead plates were inserted between the detectors to act as a target in producing interactions and also to give shower multiplication.

The total energy transferred to a shower from an incident muon was calculated from the pulse height in the shower detector. The majority of the showers observed were due to muon bremsstrahlung. The measured burst spectrum was in agreement with the predicted one and no unusual nuclear interaction cross section was observed.

6. Misaki et al. (1969)

Showers induced by high energy cosmic ray muons were observed at a depth

of 5 m underground with an emulsion chamber arranged horizontally. The chamber consisted of nuclear emulsion plates, X-rays film and lead plates, the thickness of each being 1 - 2 r.ℓ. Showers produced in the chamber by muon bremsstrahlung, with energy transfer 1 to 8 TeV, and muon nuclear interaction were detected. Bremsstrahlung showers were recognised from their single core structure, whereas those due to nuclear interaction gave multiple cores. Good agreement was found with theory and it was concluded that the showers observed were mainly due to muon bremsstrahlung. No deviation was claimed from the theoretical nuclear interaction cross section.

7.4 Analysis of results from the present experiment

7.4.1 Experimental analysis

As mentioned in the previous chapters, two interactions experiments were carried out. In the first experiment the triggering requirement was that a single muon traversed the red side of MARS. Interaction events were then selected by film scanning. In this experiment most of the interaction events observed involved a low energy transfer (small burst events).

In interaction experiment II, the triggering requirement was different from that in experiment I, that is although we still triggered on single muons traversing the red side, it was also required that the muon produced a burst (≥ 6 particles) in either level 1 or 3. This was achieved by using a high discriminator setting for these levels. In this case most of the triggering muons were associated with bursts larger than six particles. Ideally there should have been no events with burst size < 6 particles, but, because of the nonuniformity of the counter, the angle of incidence of the shower particles on the counter and effects associated with photons, this was not the case, and a few events with burst size < 6 particles were also observed.

Interaction experiment I provided a good statistics for small burst events, whereas experiment II provided good statistics for large bursts. Combining the

results for each level (1 and 3) from the two experiments gives good statistics for all burst sizes up to eighty particles or so and therefore it is possible to produce a burst spectrum for these levels.

The burst size for each event has been estimated using the method described by Rogers (see section 4.3.4). Corrections have been made, where necessary, for each burst size to take into account the nonuniformity of the shower density. The method adopted for the corrections was to divide the shower under consideration into small cells. The number of particles in each cell was then calculated using Rogers's method of uniform density. The burst size for the shower was then obtained by adding the numbers of particles obtained for each cell. This number is the one used in the burst spectrum analysis. The method was not used for burst events where the number of tracks could be counted directly.

The data were divided according to whether the burst was in level 1 or 3. There are more burst events in level 3 than 1 as expected on account of the different muon energy spectrum. Considering level 1 and 3 in turn, the data for each level were divided into cells of muon energy and burst size. The number of single muons for each cell of muon energy was obtained from the muon energy spectrum corresponding to the considered level. By comparing the number of bursts with size $\geq N$, for different values of N, with the total number of single muons of all energies a total integral burst spectrum was established for each level. The probability/muon of observing a burst $\geq N$ as a function of muon energy is obtained by comparing the number of bursts with size $\geq N$ produced by a muon of mean energy (E_μ) with the total number of single muons of that energy traversing the spectrograph.

7.4.2 Theoretical burst spectra

A) Incident muon spectrum

In order to calculate the expected burst spectra for level 1 and 3, the

energy spectra of the muons incident upon the interaction region must be knwon. This was calculated for levels 1 and 3 by folding the acceptance function of the apparatus (given in section 3.5) into the vertical muon energy spectrum (Ayre et al., 1971) and taking into account the energy loss in the iron block ($\sim$ 1·8 GeV/block). It was assumed that only the last 10 cm of each block contributes to the observed burst. The energy spectra of muons for the measuring levels 1 and 3 are shown in figure 7.8. As can be seen, the mean energy at level 3 is higher than that at level 1. This is because of the energy loss in the bottom half of the spectrograph. It is therefore expected that the measured spectra of burst at these levels, will be somewhat different.

B) Electromagnetic cascade

The object of this section is to illustrate the approach adopted to calculate the integral burst spectrum for muons of unique energy and also the total burst spectrum. Afterward a rough calculation for the probability of single knock-on electron production as a function of muon energy will be given.

In the present calculations a threshold energy of 2 MeV for the electrons in the shower is used as it is estimated that this is the minimum energy for the electrons to be detected by the measuring trays of flash tubes. Transition effects associated with the non-iron absorbers (scintillator and momentum selector trays) between the magnets and the measuring trays are not expected to be great and so have been neglected in this analysis.

In the calculations the cross sections for the various interaction processes given in section 7.2 have been used together with the electromagnetic cascade curves given by Ivanenko et al. (1967) and shown in figures 7.6 and 7.7. Since the cascade curves initiated to primary electrons are almost identical to those initiated by primary photons, only one of them is used

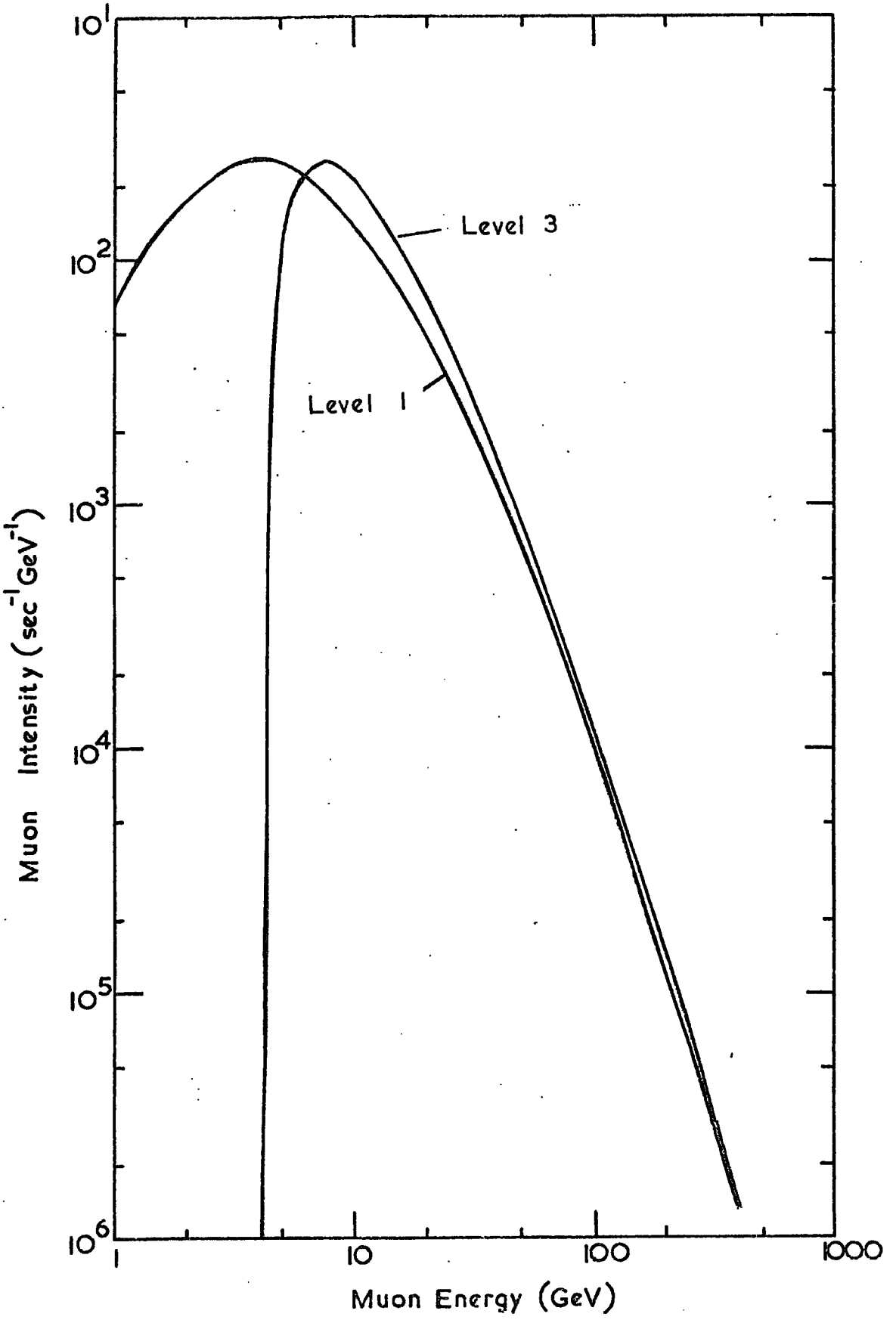

Figure 7.8 The differential spectrum of muons at the two levels in MARS where interactions are studied

in the present analysis. Consider the cascade curves given in figure 7.6, the effective target thickness, $T(E', \geqslant N)$, for energy transfer E' in producing a burst $\geqslant N$ can be read off. The dependence of the effective target thickness on energy transfer for different integral burst sizes is given in figure 7.9.

The probability for a muon of energy E_μ to produce a burst of size $\geqslant N$ in traversing the iron block is given by:

$$P(E_\mu, \geqslant N) = \int_{E'_{min}}^{E'_{max}} \phi_{total}(E_\mu, E')\, T(E', \geqslant N)\, dE' \qquad \ldots\ldots\ldots\ldots(7.5)$$

where $\phi_{total}(E_\mu, E')$ is the total probability (i.e. $\phi_{k.o.} + \phi_{Bremss.} + \phi_{Dpp}$) for a muon of energy E_μ to transfer energy E' in iron. $T(E' \geqslant N)$ is defined above and its values can be read off figure 7.9. E'_{min} is the minimum energy transfer required to produce a burst of size N and, E'_{max} is the maximum energy transfer for a muon of energy E_μ. E'_{max} is usually very close to E_μ.

In order to obtain the total integral burst spectrum, equation 7.5 is modified to the following form:

$$P(\geqslant N) = \frac{\int_{(E_\mu)_{min}}^{(E_\mu)_{max}} \left[\int_{E'_{min}}^{E'_{max}} \phi_{total}(E_\mu, E')\, T(E', \geqslant N) dE' \right] I(E_\mu) dE_\mu}{\int_{(E_\mu)_{min}}^{(E_\mu)_{max}} I(E_\mu)\, x\, dE_\mu} \qquad \ldots\ldots(7.6)$$

$P(\geqslant N)$ is the probability/muon of seeing a burst $\geqslant N$.

$I(E_\mu)$ is the intensity of a muon of energy E_μ given by the muon spectrum in figure 7.8.

$(E_\mu)_{min}$ is the lower limit of muon energy in figure 7.8.,

$(E_\mu)_{max}$ was taken as 1000 GeV, the contribution from higher muon energies being

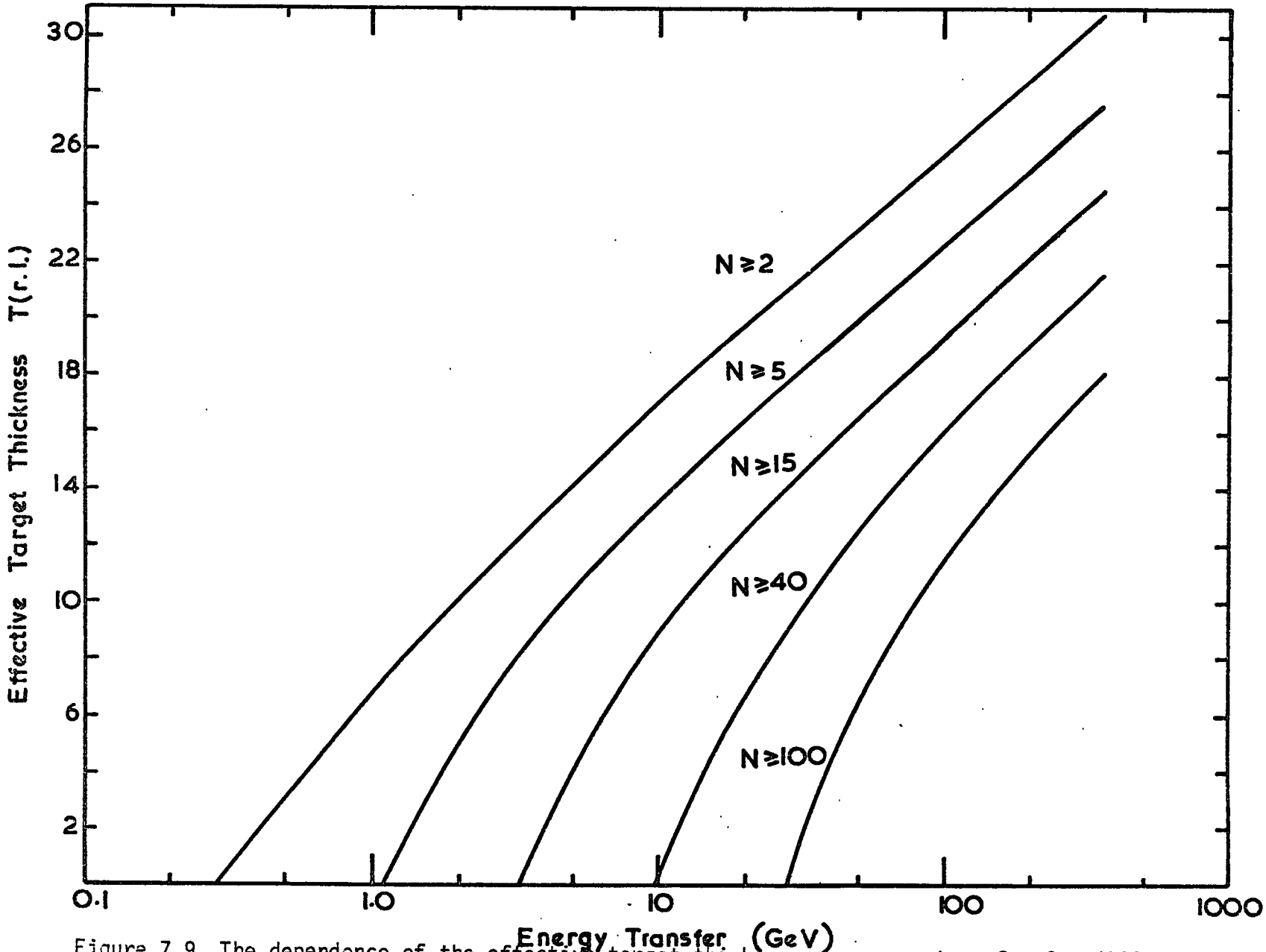

Figure 7.9 The dependence of the effective target thickness on energy transfer for different values of integral burst size.

negligible. Thus, considering levels 1 and 3 in turn the total integral spectrum for each can be calculated.

The probability of observing a single electron, emerging from the magnet block, as a function of muon energy, has been calculated considering the knock-on process and direct pair production for which only one electron emerges. The contribution from the bremsstrahlung process is negligible and has therefore been neglected. The lower limit for knock-on electron was taken as 15 MeV and the upper limit as 150 MeV. Many of the electrons produced with energy < 15 MeV will not emerge and an electron with energy > 150 MeV will have a good chance of generating a shower. The limits taken for direct pair production process are 30 MeV and 300 MeV respectively. The effective target thickness has been taken as 1 r.ℓ. This method of calculations is very approximate since the above limits on the electron energy are not exact and the effective target thickness is not accurately known. The lack of interest in this process arises because it is well known and there is not much doubt that conventional theory is applicable at least for small energy transfers.

The total integral burst spectrum for levels 1 and 3, the probability as a function of muon energy of observing a burst of size $\geq N$ and for single knock-on electron production are given in figures 7.10, 7.11, 7.12, and 7.13 respectively.

7.4.3 Comparison of experiment and theory

The total measured integral spectra for level 1 and 3 are compared with prediction in figures 7.10 and 7.11. The experimental data are absolute and no normalization factor has been used. In experiment I the discriminator levels were set to accept single particle (i.e. the muon) and therefore no loss in burst events was suffered. In experiment II, however, because of the high biasing level, there was considerable loss of small burst events.

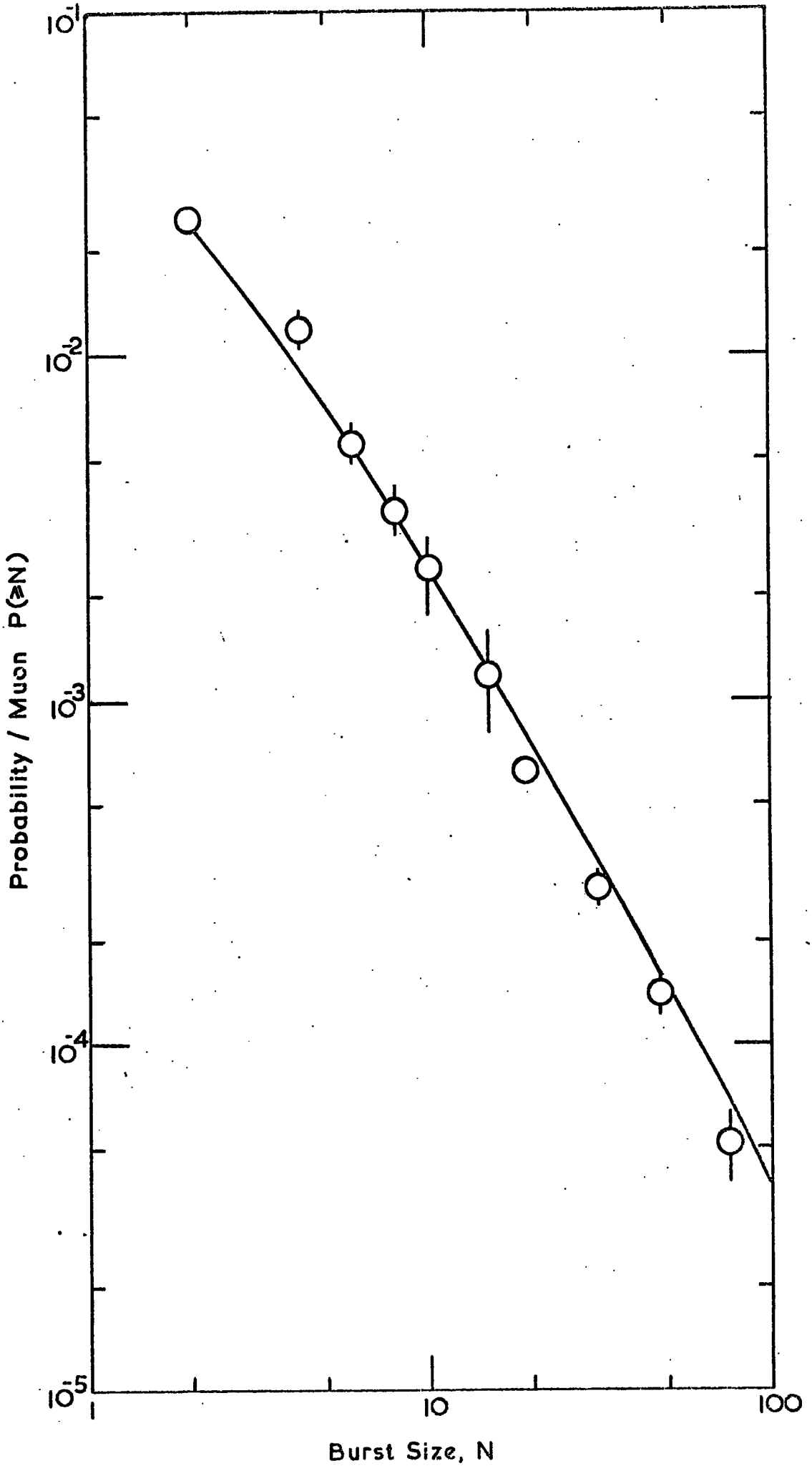

Figure 7.10 The total integral burst spectrum for level 1.

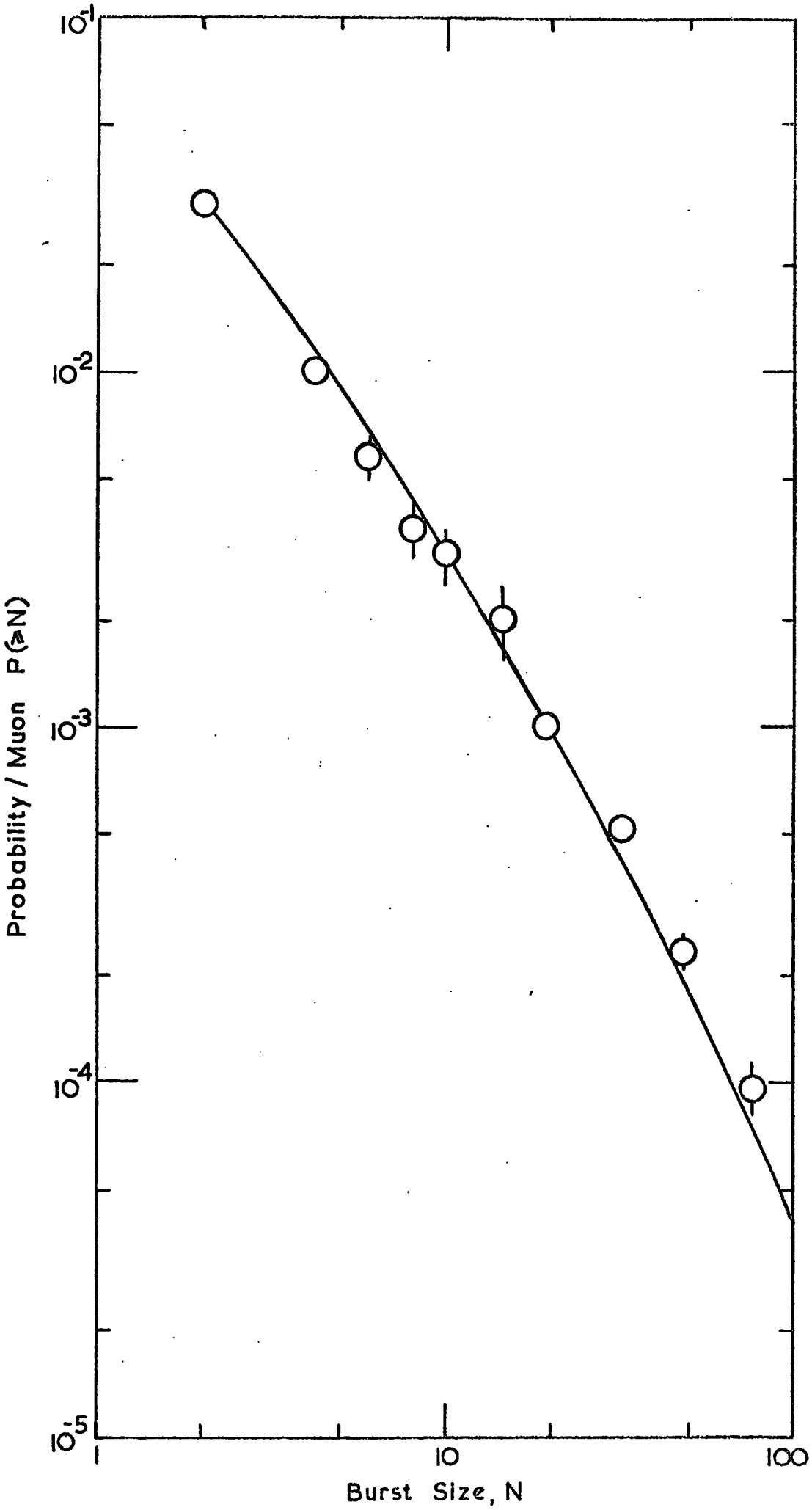

Figure 7.11 The total integral burst spectrum for level 3.

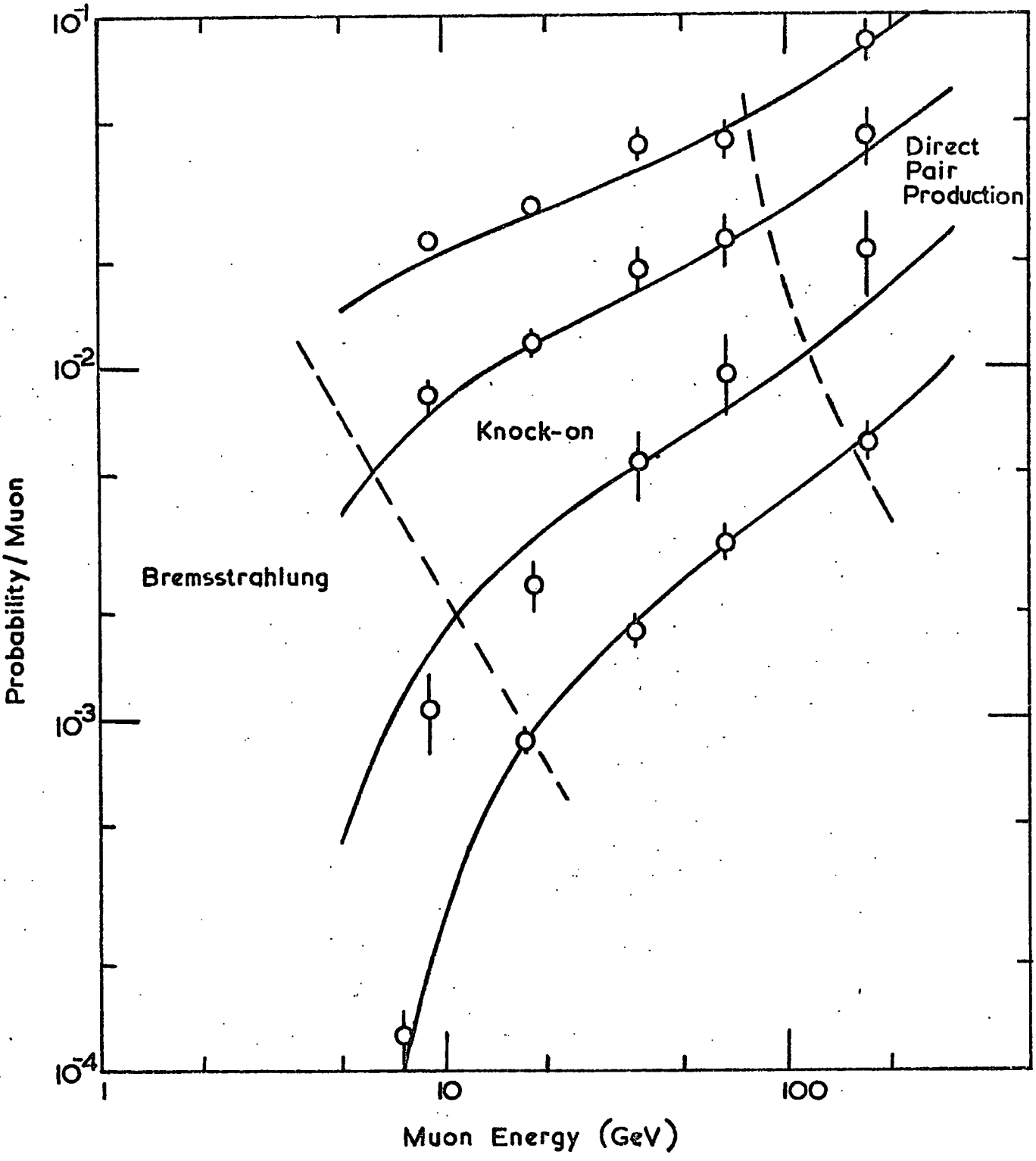

Figure 7.12 Integral burst size probabilities as a function of muon energy. The regions of predominance are shown.

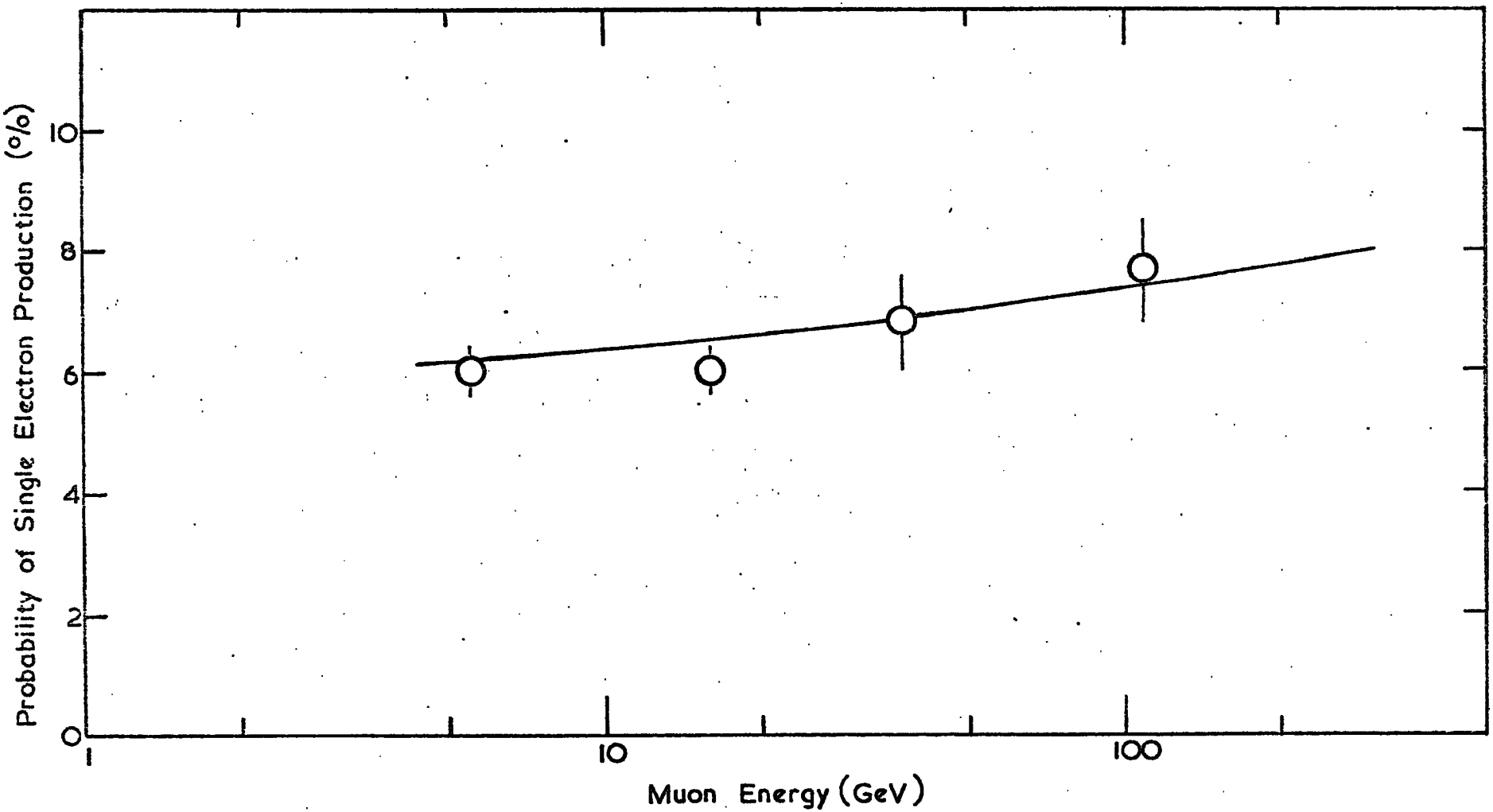

Figure 7.13 The probability of observing a single electron as a function of muon energy

Therefore in constructing the experimental burst spectra all the data from experiment I were used while only those with burst size > 15 particles in experiment II were considered. Because only a few events with bursts size > 15 particles were observed in experiment I, most of the events indicated come from experiment II. The experimental points for burst size < 15 and > 15 particles preserve a consistent slope. As expected, the burst spectrum for level 3 is higher than that for level 1 and they both agree reasonably well with predictions. In the burst spectrum for level 1, the experimental point at N = 3 is higher than expected, but in view of good agreement found for the corresponding point in the burst spectrum for level 3, no significance is attached to it. For large burst sizes the experimental points for level 1 are lower than expected, whereas those for level 3 are higher than expected. In both cases the difference from the expected values is statistically not significant. If the data for both levels are grouped together, the agreement with expectation is very good.

The comparison for the absolute interaction probabilities as a function of muon energy for burst and for single electrons are shown in figures 7.12 and 7.13 respectively. For burst probabilities, the overall data were used for burst size $N \geq 20$ and data from experiment I only were used for $N \geq 2$, 4 and 10. For single electrons only data recorded on levels 2 and 4 in experiment I were used. This is due to the fact that these measuring levels are just underneath the magnet, whereas single electrons detected in levels 1 and 3 may come from the magnet block, the momentum selector tray or the scintillation counter.

It can be seen from figures 7.12 and 7.13 that there is a satisfactory agreement between experiment and theory for the whole range of energy transfer and over the range of muon energy investigated.

7.5 Comparison with previous results on muon interactions

The results from this experiment together with results from previous

experiments mentioned in this chapter, on the electromagnetic interaction of cosmic ray muons are compared with the theoretical prediction in figures 7.14 and 7.15. Although the absolute probabilities in the present experiment are probably not accurate to better than $\sim$ 30%, the relative probability is thought to be accurate and there is seen to be no evidence for significant deviation from the theory. Therefore the present experiment results do not lend any support to those experiments in which a deviation from the accepted theory was claimed.

7.6 Critical analysis of previous experiments

At this stage it is desirable to examine rather critically some of the previous experiments which have been mentioned and in which inconsistency with theory was found.

Consider the experiments of Roe and Ozaki (1959) and Gaebler et al.(1961). As mentioned earlier these two experiments were carried out using cloud chambers and they found a cross section for electron direct pair production which was about $\frac{1}{2}$ the value predicted by the MUT theory. One common feature in analysing the data from the two experiments is that they both use Wilson Monte Carlo results (Wilson, 1950, 1952) to estimate the energy transfer of the showers observed. According to Hazen et al.(1965) Wilson's shower curves underestimate the energy transfer of the shower event by a factor of about 2 compared with their own calculations and with the calculations of Crawford and Messel (1962). Therefore if we now use the latter shower curves then a reasonable agreement with theory will occur.

Another point relevant to the observed discrepancy is the muon momentum spectrum used. Accurate knowledge of the muon spectrum falling on the chamber is necessary because the direct pair production process does depend on muon energy. In the experiment of Roe and Ozaki this may not be a serious source of error, because the experiment was carried out at S.L. where the muon momentum spectrum in the range relevant to their experiment is believed

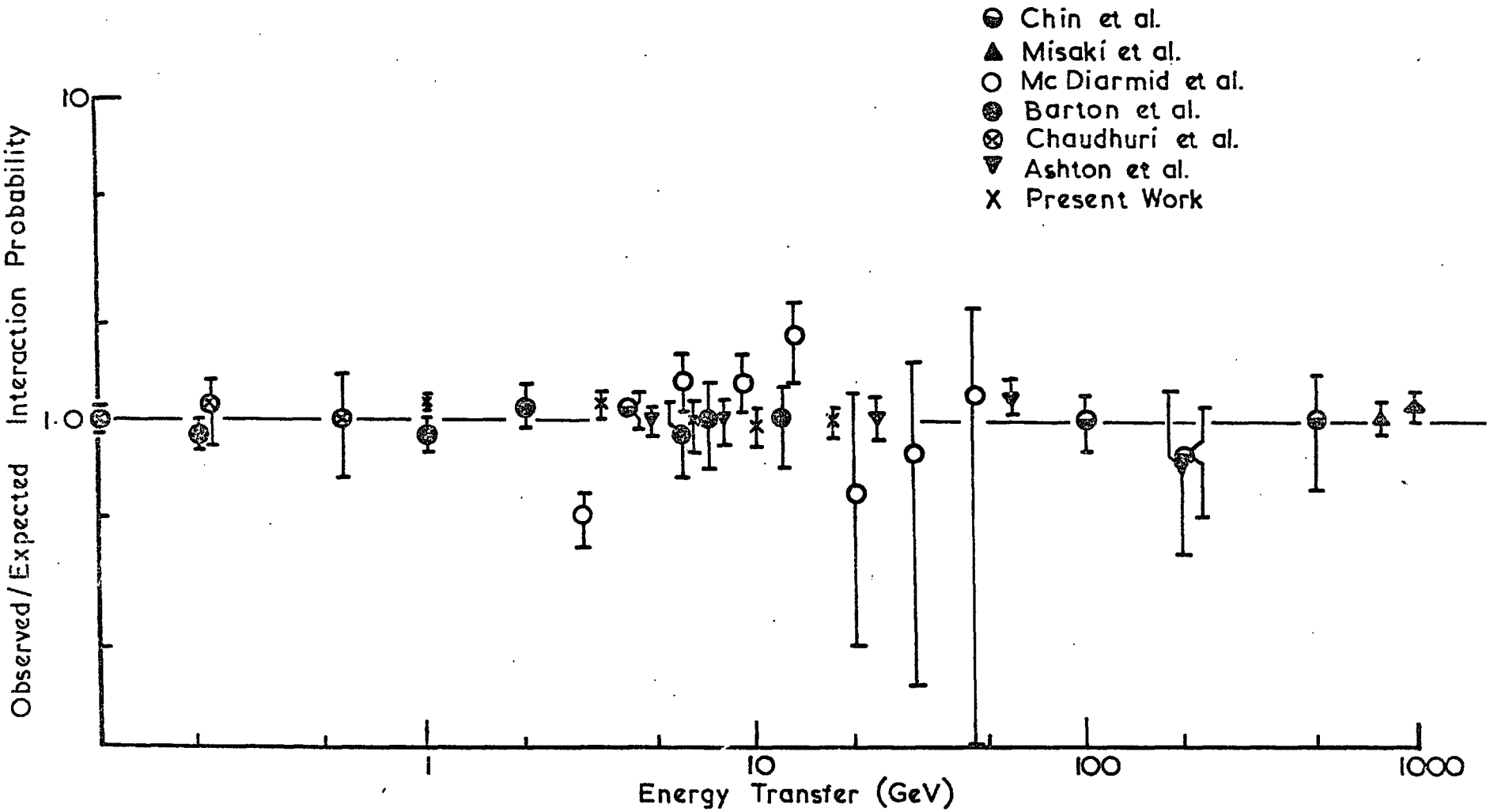

Figure 7.14 Results from experiments consistent with theory.

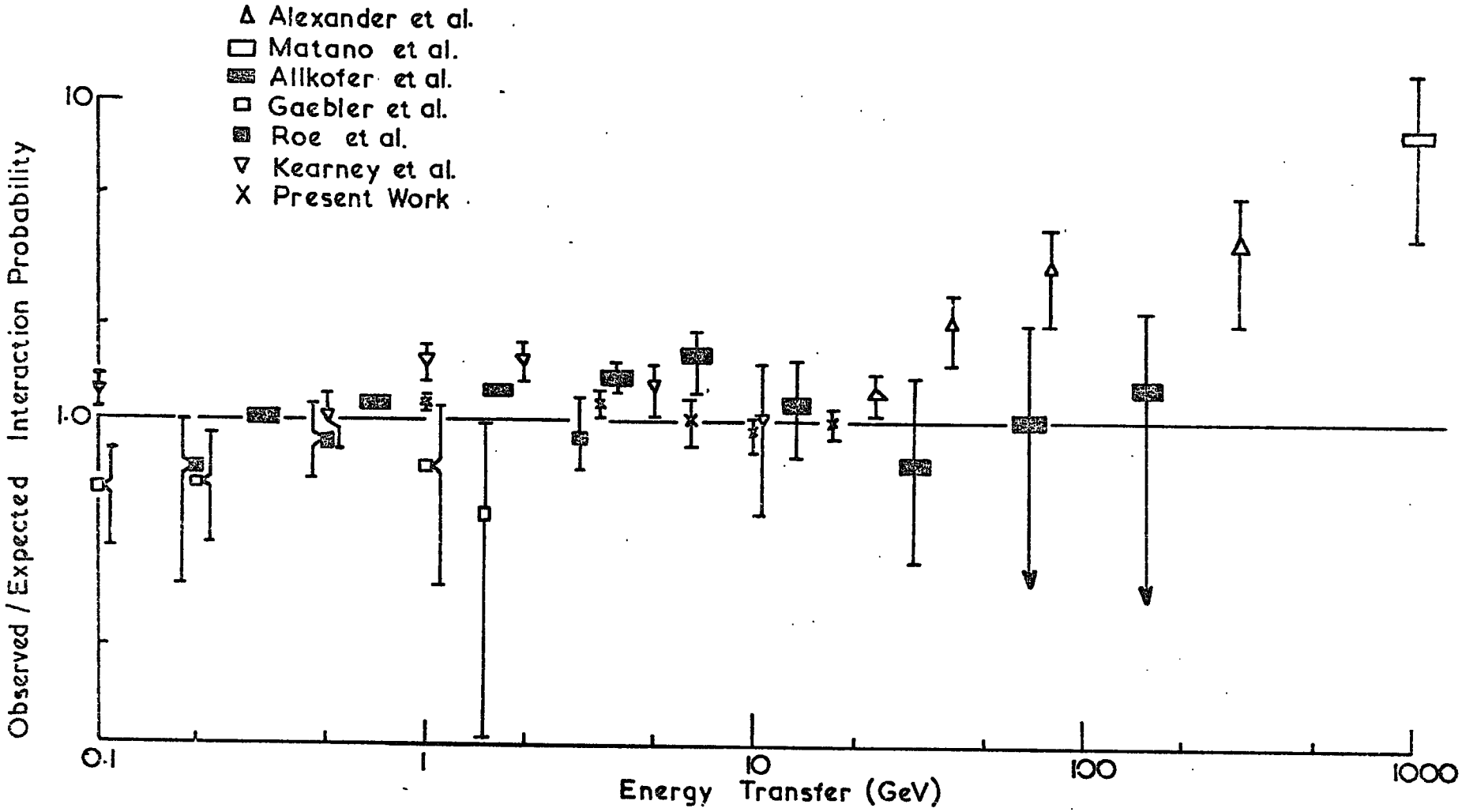

Figure 7.15 Results from experiments inconsistent with theory together with results from the present experiment

to be known reasonably well. This may not be the case in the experiment of Gaebler et al. however, because this experiment was carried out underground and the muon spectrum used has to be derived from the depth intensity measurements and the range energy relation (for example, as given by Barrett et al., 1952).

In view of possible underestimation of the energy transfer and some uncertainty in the muon momentum spectrum used, one may conclude that the discrepancy in these two experiments is not significant and does not necessarily imply a breakdown in the direct pair production theory.

The experiment of Kearney et al. (1965) suggested a possible discrepancy with Bhabha theory for knock-on production. This experiment was carried out by operating a cloud chamber underground. In a cloud chamber, the energy transfer involved in the interaction is determined by counting the number of track segments associated with each event. Some tracks might fall outside the illuminated region of the chamber in which case the energy transfer would be underestimated. Conversely, background tracks might be mistaken for shower tracks. On account of the steepness of the energy transfer spectrum a small error in the energy transfer estimation could make a considerable difference in comparison with theory. One way of overcoming this problem is by normalization. In fact the slope presented by their experimental points is in reasonable agreement with prediction. The uncertainty in the muon momentum spectrum can not contribute significantly to the discrepancy because of the knock-on process being almost independent of muon energy.

In the experiment of Allkofer et al. (1971) the same sort of discrepancy but smaller, was found. On examining their experimental points, the slope agrees with the theoretical one reasonably well. Allkofer et al. did not rule out the possibility that the discrepancy is due to an error in estimating the energy transfer. In fact, with the errors they quoted in estimating the energy transfer, the agreement between theory and experiment is within one

standard deviation for all their measured points.

One important fact which has not been mentioned is the effect of the fluctuations on the predicted values. None of the above experiments, which claim a discrepancy, corrected their theoretical predictions for fluctuations. The effect would be to cause the experimental points to be too high and in some cases the necessary correction is quite significant.

The discrepancy in the experiments of Matano et al. (1968) and Alexander et al. (1969) can probably be understood (Kiraly et al., 1971) if allowance is made for uncertainties in recorded shower size.

While results from the Deery and Neddermeyer experiment (1961) suggest an excess of events over the number predicted by the Bhabha theory in the region around 1 GeV, results from Backenstoss et al. (1963) are in good agreement with theory. Of the two experiments that due to Backenstoss et al. is more accurate, and so is possible that the result of Deery et al. is due to a statistical fluctuation.

In general the results from accelerator experiments are in good agreement with theory. In these experiments the statistical accuracy is generally better than in cosmic ray experiments, and the experimental conditions are much better controlled, however, the muon energy is limited ($\lesssim$ 20 GeV) and there are still problems concerning absolute frequencies.

7.7 Conclusions

In view of the approximations used, and the fact that there is no general agreement on the fluctuation problem, the absolute probabilities in the present experiment are probably not accurate to better than 30%. However, the relative probability is accurate and there is no evidence for significant deviations from expectation which are either muon energy - or burst size - dependent.

In general, if one combines the results from machine experiments and

cosmic ray experiments (not forgeting the possible cause of discrepancy in some of the cosmic ray experiments in which deviation from theory is claimed), the result will favour the validity of the Q.E.D.

CHAPTER 8

CONCLUSIONS

The present experiment set out to investigate the interaction asymmetry of the cosmic ray muon and also to measure the absolute values of its interaction probability, and by doing so to resolve the possible cosmic ray - accelerator inconsistencies.

The present experiment covers muon energies up to 200 GeV and energy transfers up to 10 GeV. Consequently most of the events observed are due to the knock-on production process and therefore the present experiment may be considered as testing the theory of this interaction. Essentially two interaction experiments were carried out to investigate the electromagnetic interaction of cosmic ray muons. The results on the asymmetry measurements from the two experiments are in good agreement with each other and therefore increase confidence in the data. The combined results from these interaction experiments (I and II) on the asymmetry as a function of energy transfer are given in figure 6.9. No asymmetry was found for all ranges of energy transfer up to 10 GeV. However, the experimental point at 1 GeV is somewhat higher than unity suggesting that there could be an asymmetry of as high as 13%. Whether such an excess is real or due to statistical fluctuation is impossible to decide at this stage. If there is really an asymmetry in this region of energy transfer, then it is probably much lower than that quoted by Kotzer et al. (1965) and Allkofer et al. (1970) and the statistical accuracy needed to establish it is of the order of 1%. Apart from the results of Kotzer et al. and Allkofer et al., the general feature of the results from the other experiment is an agreement with theory.

As for the dependence of a possible asymmetry on muon energy, the results of the present experiment favour no dependence.

The present results on the asymmetry are supported by the absolute cross

section measurements given in Chapter 7 and also by results from accelerator experiments. Experiments with muons from accelerators seem to disprove the possibility of an asymmetry and such a results led Kotzer et al. (1967) to suggest that the asymmetry in cosmic ray experiments could come from muons arising from the decay of kaons since accelerator experiments use predominantly muons from the decay of pions. However, this suggestion must be weakened in view of the results from the present experiment and from the Mk II horizontal spectrograph.

The present measurements of the absolute values of the interaction probability are presented in figures 7.10, 7.11, 7.12 and 7.13. It can be seen that there is a satisfactory agreement with expectation, although it is not possible to guarantee that they are accurate to more than $\pm$ 30% in view of various approximations used. However, the relative probability is accurate and the measured experimental points give a consistent slope with theory. A more accurate measurement for the absolute probability was given by Backenstoss et al. (1963) who found excellent agreement with theory. The experiment of Deery and Neddermeyer (1961), which suggested a disagreement with knock-on theory is much less accurate than that of Backenstoss et al. and, as reported by the authors, it is not possible with any degree of certainty, to exclude the possibility that the deviation is due to a statistical fluctuation.

Combining our results on the asymmetry with a more accruate result on the absolute probabilities, we would arrive at the following conclusion: the electromagnetic interactions of positive and negative muons with energies up to 100 GeV and energy transfer up to 10 GeV show no definite anomalous effects. Such a result is in conflict with the results of Kotzer et al. (1965) and Allkofer et al. (1970). Our results do not show a conflict with the theoretical description of the muon interaction as calculated from Q.E.D. and they support the predictions of this theory.

ACKNOWLEDGEMENTS

The author wishes to thank Professor G. D. Rochester, F.R.S., for the provision of the facilities for this work, and for his interest and support.

The author would like to express his sincere appreciation to Professor A. W. Wolfendale for his generous guidance and invaluable help throught the work. Dr. M. G. Thompson is acknowledged with gratitude for his invaluable help and constant advice.

The author is very grateful to Dr. C. Grupen and Dr. E.C.M. Young for their assistance in analysing the data and to Mr. S. Hansen for his help in the film scanning.

The author is grateful to all members of MARS Group for their helpful discussion and interest. Mr. K. Tindale, the technician of the Group for his help at all stages of the work. Mrs. P. Russell is thanked for her ready assistance and for drawing the diagrams of this thesis.

The technical staff of the Physics Department are thanked for their willing help.

The assistance of the staff of the University Computer Unit, and the use of their facilities is acknowledged.

The author is very grateful to Mrs. J. Moore for her patient work in typing this thesis.

The financial support from the Gulbenkian Foundation and Basrah University is greatly appreciated.

At last, but by no means least, warm and sincere thanks to my wife for help and assistance in many ways.

REFERENCES

Alexander, D., Thompson, M.G., Turner, J.L., and Wolfendale, A.W., 1969, 11th Int. Conf. on Cosmic Rays, Budapest, 4, 215.

Allkofer, O.C., Grupen, C., and Stamm, W., 1971, Proc. 12th Int. Conf. on Cosmic Rays, Hobart, 4, 1452.

Allkofer, O.C., Grupen, C., and Stamm, W., 1971, Phys. Rev. D, 4, 3, 638.

Ashton, et al., 1965, Private communication, see Kelly, G.N., Mackeown, P.K., Said, S., and Wolfendale, A.W., 1968, Can. J. Phys., 46, S365.

Ashton, F., Coats, R.B., and Simpson, D.A., 1968, Can. J. Phys., 46, 363.

Ayre, C.A., Hamdan, M.A., Hume, C.J., Nandi, B.C., Thompson, M.G., Wells, S.C., Whalley, M.R., and Wolfendale, A.W., 1971, Proc. 12th Int. Conf. on Cosmic Rays, Hobart, 4, 1364.

Ayre, C.A., Grupen, C., Hamdan, M.A., Hume, C.J., Thompson, M.G., Wells, S.C., and Wolfendale, A.W., 1971, Proc. 12th Int. Conf. on Cosmic Rays, Hobart, 4, 1447.

Ayre, C.A., Hamdan, M.A., Hume, C.J., Nandi, B.C., Thompson, M.G., Wells, S.C., and Whalley, M.R., 1972, (in the press).

Ayre, C.A., Hamdan, M.A., Hume, C.J., Stubbs, F.W., Thompson, M.G., Wells, S.C., and Whalley, M.R., 1972, (in the press).

Ayre, C.A., Hume, C.J., Nandi, B.C., Thompson, M.G., Wells, S.C., Whalley, M.R., and Wolfendale, A.W., 1972, (in the press).

Backenstoss, G., Hyams, B.D., Knop, G., Marin, P.C., and Stierlin, U., 1963, Phys. Rev., 129, 2759.

Barton, J.C., Rogers, I.W., and Thompson, M.G., 1965, Proc. 9th Int. Conf. on Cosmic Rays, London, 2, 970.

Barret, P.H., Bollinger, L.M., Cocconi, G., Eisenberg, Y., and Greisen, K., 1952, Rev. Mod. Phys., 24, 133.

Bhabha, H.J., 1935, Proc. Roy. Soc., A152, 559.

Bhabha, H.J., 1938, Proc. Roy. Soc., A164, 257.

Bhabha, H. J., and Chakrabarty, S.K., 1948, Phys. Rev., 74, 1352.

Belenkii, S.Z., and Ivanenko, I.P., 1959, USP. Fiz. Nauk, 69, 591.

Block, M.M., King, D.T., and Wada, W.W., 1954, Phys. Rev., 96, 1627.

Buja, Z., 1963, Acta Physica Polonica, 24, 381.

Chaudhuri, N., and Sinha, M.S., 1964, Nuovo Cimento, 65A, 727.

Chin, S., Hanayama, Y., Hara, T., Higashi, S., Kitamura, T., Miono, S., Nakagawa, M., Ozaki, S., Takahashi, T., Tsuji, K., Watase, Y., Kobayakawa, K., and Shibata, H., 1969, Proc. 11th Int. Conf. on Cosmic Rays, Budapest, 4, 59.

Christy, R.F., and Kusaka, S., 1941, Phys. Rev., 59, 405.

Deery, R.F., and Neddermeyer, S.H., 1961, Phys. Rev., 121, 6, 1803.

Erlykin, A.D., 1965, Proc. 9th Int. Conf. on Cosmic Rays, London, 2, 999.

Fowler, G.N., and Wolfendale, A.W., 1958, Progress in elementary particles and cosmic ray physics, Vol. IV (North-Holland Pub. Co., Amsterdam), Chap. III.

Furry, W.H., 1937, Phys. Rev., 52, 569.

Gaebler, J.F., Hazen, W.E., and Hendel, A.Z., 1961, Nuovo Cimento, 19, 265.

Grawford, D.F., and Messel, H., 1962, Phys. Rev., 128, 2352.

Grupen, C., and Hamdan, M.A., 1971, Internal Report (unpublished)

Grupen, C., Hamdan, M.A., Hansen, S., Thompson, M.G., Wolfendale, A.W., and Young, E.C.M., 1972, J. Phys. A, (in the press).

Grupen, C., Hamdan, M.A., Hansen, S., Thompson, M.G., Wolfendale, A.W., and Young, E.C.M., 1972, J. Phys. A, (in the press).

Hayman, P.J., and Wolfendale, A.W., 1962, Proc. Phys. Soc., 80, 710.

Hazen, N.E., 1955, Phys. Rev., 99, 911.

Hazen, W.E., and Hendel, A.Z., (see Kearny and Hazen)

Hess, V.F., November 1912, 1084.

Ivanenko, I.P., and Samosudov, B.E., 1959, JETP, 8, 884.

Ivanenko, I.P., and Samosudov, B.E., 1967, Bull. Acad. Sci., U.S.S.R., (Phys. Ser.) 30, 10, 1722.

Jain, P.L., Wixon, N.J., Phillips, D.A., and Fecteau, J.T., 1970, Phys. Rev., D1, 3813.

Jakbaev, Zh.S., Lukin, Yu.T., and Emelyanov, Yu. A., 1965, Proc. 9th Int. Conf. on Cosmic Rays, London, 2, 967.

Kearney, P.D., and Hazen, W.E., 1965, Phys. Rev., 138, 173.

Kelner, S.R., and Kotov, Yu. D., 1968, Cand. J. Phys., 46, 387.

Kirk, T.B.W., and Neddermeyer, S.H., 1968, Phys. Rev., 171, 1412.

Kokoulin, R.P., and Petrukhin, A.A., 1971, Proc. 12th Int. Conf. on Cosmic Rays, Hobart, 4, 1446.

Kotzer, P., and Neddermeyer, S.H., 1965, Bull. Amer. Phys. Soc., 10, 80.

Kotzer, P., and Neddermeyer, S.H., 1967, Bull. Amer. Phys. Soc., 12, 916.

Lloyd, J.L., and Wolfendale, A.W., 1959, Proc. Phys. Soc., A73, 178.

Matano, M., Nagano, M., Shibata, S., Suga, K., Tanahashi, G., Kameda, T., Toyoda, Y., and Hasekawa, H., 1968, Cand. J. Phys., 46, 369.

McDiarmid, I.B., and Wilson, M.D., 1962, Canad. J. Phys., 40, 698.

Misaki, A., Mizutani, K., Ogata, T., Shirai, T., Akashi, M., Watanabe, Z., and Tsuneoka, Y., 1969, Proc. 11th Int. Conf. on Cosmic Rays, Budapest, 4, 157.

Murota, T., Ueada, A., and Tanaka, H., 1956, Prog. Theor. Phys., 16, 482.

Murzin, V.S., and Rapoport, I.D., 1965, JETP, 20, 1,

Nishina, Y., Tomonaga, S., and Kobayasi, M., 1935, Sci. Pap. Inst. Phys. Chem. Research, Japan, 27, 137.

Petrukhin, A.A., and Shestakov, S.S., 1968, Can. J. Phys., 46, 377.

Racah, G., 1937, Nuovo Cimento, 14, 93.

Roe, B.P., and Ozaki, S., 1959, Phys. Rev., 116, 1022.

Rogers, I.W., 1965, Ph.D. Thesis, University of Durham.

Said, S. S., 1966, Ph.D. Thesis, University of Durham.

Wilson, R. R., 1950, Phys. Rev., 79, 204.

Wilson, R. R., 1951, Phys. Rev., 84, 100.

Wilson, R. R., 1952, Phys. Rev., 86, 261.

Kiraly, P., Thompson, M.G. and Wolfendale, A.W., 1969, J. Phys. A., 4, 367.